Hochschule für Angewandte Wissenschaften Hamburg
Hamburg University of Applied Sciences

Characterization of a terpene synthase activity in *Castellaniella defragrans*

Master Thesis

Master of Science (M.Sc.)

Department Biotechnologie
der Hochschule für Angewandte Wissenschaften Hamburg

Submitted by
Elisabeth Engler-Hüsch

Hamburg, April 2017

This master thesis in the masters program “Pharmaceutical Biotechnology” at the University of Applied Sciences Hamburg was carried out in the department of microbiology at the Max-Planck-Institute for Marine Microbiology in Bremen under the supervision of Prof. Dr. Jens Harder between the 4th of October 2016 and the 4th of April 2017.

1st referee: Prof. Dr. Oliver Ullrich, Hochschule für Angewandte Wissenschaften Hamburg
2nd referee: Prof. Dr. Jens Harder, Max-Planck-Institut für Marine Mikrobiologie in Bremen

Abstract

Monoterpenes are hydrocarbons with multiple beneficial properties, for instance antimicrobial effects. The interest in monoterpenes for the pharmaceutical use has increased over the last decades. Monoterpenes synthases can catalyze the formation of various monoterpenes due to highly active carbocation intermediates.

The β-proteobacterium *Castellaniella defragrans* 65Phen is capable of using monoterpenes as sole carbon and energy source under anaerobic denitrifying conditions. A new degradation pathway for the acyclic monoterpenes β-myrcene and geraniol was ascertained, revealing a novel enzyme, the linalool dehydratase/isomerase. A deletion mutant lacking this enzyme did grow on (R,S)-linalool under formation of the two monocyclic monoterpenes α-terpinene and terpinolene as metabolites. This had led to the suggestion of another metabolism pathway in *Castellaniella defragrans* 65Phen, involving hitherto unknown enzymes.

In this thesis biomass of *Castellaniella defragrans* 65Phen Δ*ldi* from several multi-fed batch cultivations grown on linalool and nitrate was used to develop an improved purification approach by a combination of anion exchange chromatography and size exclusion chromatography. This combination yielded high enzyme purities with few protein bands observable on denaturing gels. The enzyme of interest was further characterized, revealing an optimal pH range from pH 6,0 to pH 9,0 and an optimal temperature of 37 °C for enzyme activity.

Previous studies did suggest a single enzyme to be involved in the transformation, while size exclusion chromatography during this study revealed two enzymes of different molecular sizes, a 114 kDa enzyme for synthesis of α-terpinene and a 72 kDa enzyme for synthesis of terpinolene. Furthermore, an increase in size up to 144 ± 11 kDa was observed for the partially purified terpinolene synthase, leading to the suggestion of a multi-enzyme complex formation during anion exchange chromatography.

A potential protein band at 55 kDa on a denaturing gel was hypothesized to be the one responsible for terpinolene synthase activity.

Table of contents

List of tables

List of figures

Abbreviations

APS	Ammonium persulfate
ATP	Adenosine triphosphate
Atu	Acyclic terpene utilization
BSA	Bovine serum albumin
BVOC	Biogenic volatile organic compounds
CV	Column volume
DEAE	Diethylaminoethyl
DMAPP	Dimethylallyl diphosphate
DTT	Dithiothreitol
EDTA	Ethylendiaminetetraacetic acid
FPP	Farnesyl diphosphate
GC	Gas chromatography
GeoA	Geraniol dehydrogenase
GeoB	Geranial dehydrogenase
GGP	Geranylgeranyl diphosphate
GPP	Geranyl diphosphate
HIC	Hydrophobic interaction chromatography
IEC	Ion exchange chromatography
IPP	Isopentenyl diphosphate
LC	Liquid chromatography
LDI	Linalool dehydratase/isomerase
Lis	Linalool isomerase
Liu	Leucine/isovalerate utilization
MALDI-ToF	Matrix-assisted laser desorption/ionization-time of flight
MEP	2-C-methyl-D-erythritol 4-phosphate

MVA	Mevalonate
NPP	Neryl diphosphate
PAGE	Polyacrylamide gel electrophoresis
pI	Isoelectric point
SDS	Sodium dodecyl sulfate
SEC	Size exclusion chromatography
TEMED	N, N, N', N'-tetramethylethylenediamine
Tris	Tris(hydroxymethyl)-aminomethane
Tween 20	Polyoxyethylene (20) sorbitan monolaurate

1 Introduction

1.1 Monoterpenes

Monoterpenes are part of a group of highly diverse hydrocarbons, found in nature mostly as components of the essential oils in plants. Their structural diversity can only be compared to the myriad of biological functions they fulfill. Besides pollinator attraction, monoterpenes act also as repellants for herbivores, insects, and microbial pathogens [Croteau, 1987]. Monoterpenes and other essential oil components have found their way in food, pharmaceutical, cosmetic, and agrochemical industry, where their antimicrobial and rodent-repellent properties are exploited [Diaz Carrasco *et al.*, 2016; Hansen *et al.*, 2016; Uma, Huang, and Kumar, 2017]. High-throughput mining for these natural compounds has become of particular interest for drug discovery over the last years [de Souza, 2007; Koehn and Carter, 2005; Pichersky, Noel, and Dudareva, 2006; Yin *et al.*, 2007]. A combination of terpenes and synthetic drugs has been shown to increase the activity of active compounds and decrease cytotoxicity [Theoduloz *et al.*, 2015].
Additionally to their effects on bacterial cells, these biogenic volatile organic compounds (BVOCs) also affect the climate and the plant kingdom. Global warming leads to increased emission of BVOCs [Kesselmeier and Staudt, 1999; Peñuelas, Rutishauser, and Filella, 2009], resulting in generation of physiological and ecological alterations. This can lead to a change in plant protection, plant defense, inter-plant communication, and pollination [Peñuelas and Staudt, 2010].

Although terpenes are mostly synthesized by plants, they can be produced by bacteria and fungi as well [Ebel, 2010; Effmert *et al.*, 2012; Heddergott, Calvo, and Latgé, 2014]. Terpene production is even known in the animal kingdom, particularly for insects like beetles and termites [Gershenzon and Dudareva, 2007]. Posttranslational modification of proteins in eukaryotic cells by addition of terpene residues, a progress named prenylation, plays an important role in regulation of these proteins [Hottman and Li, 2014; Wang and Casey, 2016]. All terpenes derive from two five-carbon (C_5) precursor units, the isopentenyl diphosphate (IPP) and its isomer dimethylallyl diphosphate (DMAPP) which are built via two different pathways, the mevalonate (MVA) pathway and the 2-C-methyl-D-erythritol 4-phosphate (MEP) pathway [Kirby and Keasling, 2009]. These pathways can

be found in different cellular compartments of the plant. While the MVA pathway is located in the cytosol, the MEP pathway is located in the plastids of plant cells [Cheng *et al.*, 2007]. Most bacteria use the MEP pathway and only a minority uses the MVA pathway [Rohmer *et al.*, 1993; Sangari *et al.*, 2010]. Condensation reactions of IPP and DMAPP catalyzed by prenyltransferases lead to the formation of several diphosphates, starting with the ten-carbon (C_{10}) geranyl diphosphate (GPP), followed by the fifteen-carbon (C_{15}) farnesyl diphosphate (FPP) and the twenty-carbon (C_{20}) geranylgeranyl diphosphate (GGP) [Boronat and Rodríquez-Concepción, 2015; Cheng *et al.*, 2007]. These diphosphates are the starting point for the synthesis of various terpene structures. According to the number of C_5 units the terpenes can be divided into monoterpenes (C_{10}), sesquiterpenes (C_{15}), diterpenes (C_{20}), and up to polyterpenes (>C_{40}) [Davis and Croteau, 2000]. Monoterpenes are mainly built in the plastids of plants and can be acyclic, monocyclic or bicyclic (Figure 1) [Kesselmeier and Staudt, 1999].

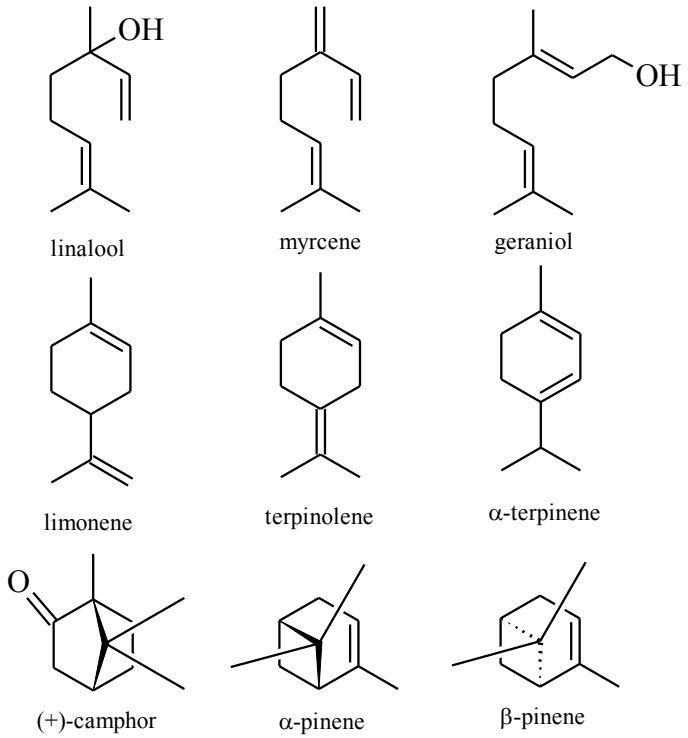

Figure 1: Selected structures of monoterpenes. The first row shows acyclic, the second row monocyclic and the third row bicyclic monoterpenes.

Monoterpene synthesis starts with GPP or its isomer neryl diphosphate (NPP) [Bohlmann and Gershenzon, 2009]. After subtraction of the diphosphate moiety, the geranyl cation recombines with the diphosphate anion to linalyl diphosphate [Davis and Croteau, 2000;

Marmulla, 2015]. An intramolecular shift of the positive charge to the primary position results in the linalyl cation. This cation is the precursor for all acyclic monoterpenes [Schilmiller *et al.*, 2009]. A ring-closure in the linalyl resp. the neryl cation leads to an α-terpinyl cation, the precursor of all cyclic monoterpenes (Figure 2) [Croteau, 1986].

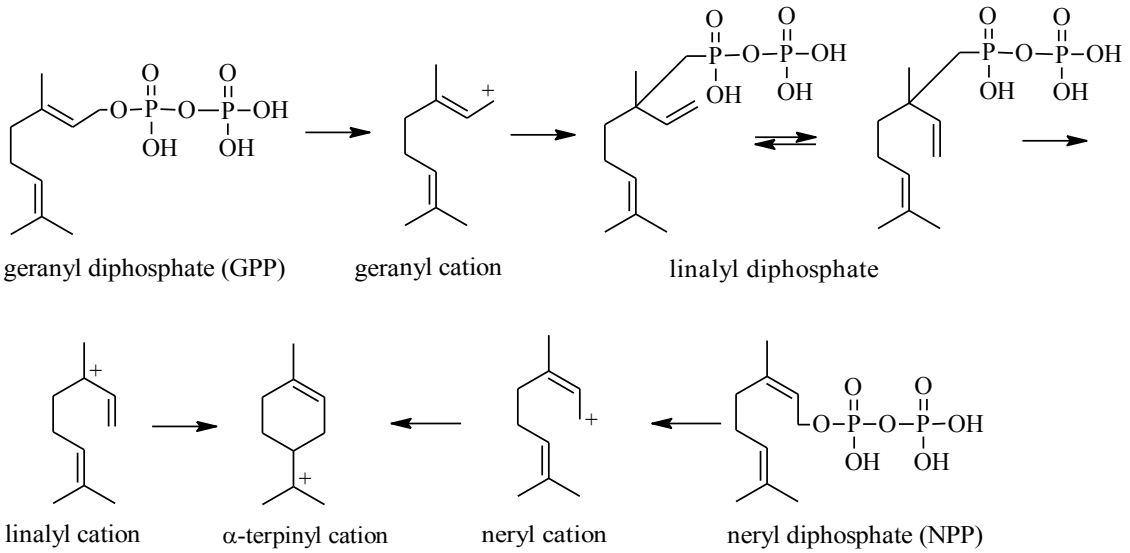

Figure 2: Initial monoterpene synthesis from GPP resp. NPP to the α-terpinyl cation. The intermediates geranyl cation, linalyl diphosphate and linalyl cation are necessary to allow cyclization to the α-terpinyl cation. Modified after Schilmiller *et al.* [2009] and Bohlmann, Meyer-Gauen, and Croteau [1998].

The ability of monoterpene synthases to form multiple products from one GPP may be due to the highly reactive carbocations which are formed as intermediates during the reaction. These carbocations can be stabilized either by deprotonation or by other chemical reactions [Davis and Croteau, 2000], like additions of double bonds, hydride shifts, and rearrangements with a subsequent deprotonation resp. an addition of a hydroxyl group [Bohlmann, Meyer-Gauen, and Croteau, 1998].

1.2 Microbial degradation of monoterpenes

The antibacterial effect of monoterpenes is caused by their lipophilicity, allowing them to interact with the cell membrane of microorganisms [Turina *et al.*, 2006]. A disturbance of the lipid fraction of the plasma membrane, followed by a change in membrane permeability was suggested [Trombetta *et al.*, 2005], causing a leakage of intracellular material. This leads to the loss of the cellular integrity and as a consequence to cell death [Andrews, Parks, and Spence, 1980]. Cell damage intensity depends on the properties of the cell wall, for instance permeability, composition, and net charge [Zengin and Baysal,

2014]. Bacteria can counteract the toxic effects by changing the membrane fluidity and by using efflux pumps in the cell membrane [Alcalde-Rico *et al.*, 2016; Melo *et al.*, 2015; Papadopoulos *et al.*, 2008].

Below toxic concentrations monoterpenes can be used as sole carbon and energy source by various microorganisms. The growth on monoterpenes under aerobic conditions was demonstrated for many *Pseudomonas* species. Examples for this growth are *P. citronellolis* on citronellol [Seubert, 1960], *Pseudomonas* sp. strain PIN on α- and β-pinene [Yoo and Day, 2002], *P. rhodesiae* on α-pinene and *P. fluorescens* on limonene [Bicas *et al.*, 2008]. The growth of *Rhodococcus erythropolis* on limonene was demonstrated as well [van der Werf, Swarts, and de Bont, 1999].

Besides the aerobic degradation, the anaerobic degradation of monoterpenes was investigated. *P. citronellolis* was shown to grow on citronellol and 3,7-dimethyl-1-octanol [Harder and Probian, 1995]. Several strains of *Thauera linaloolentis* and *Thauera terpenica* were isolated on menthol, linalool, and eucalyptol [Foss and Harder, 1998]. *P. fluorescens* grew on limonene [Bicas *et al.*, 2008], and *Castellaniella* (ex *Alcaligenes*) defragrans was shown to grow on α-phellandrene [Foss, Heyen, and Harder, 1998; Heyen and Harder, 2000].

The aerobic degradation of the acyclic monoterpenes citronellol and geraniol in *Pseudomonas* sp. is classified as the acyclic terpene utilization (Atu) and leucine/isovalerate utilization (Liu) pathway. *atu*ABCDEFGH and *liu*RABCDE are the genes involved in these pathways [Förster-Fromme and Jendrossek, 2006; Höschle, Gnau, and Jendrossek, 2005]. The anaerobic degradation of monoterpenes was mainly invested in *Thauera* and *Castellaniella* species revealing several enzymes involved in the degradation of linalool and limonene. In enrichment cultures the formation of geraniol and geranial from linalool was found [Harder and Probian, 1995]. In *Thauera linaloolentis* and *Thauera terpenica* the mineralization from monoterpenes to carbon dioxide was observed [Foss and Harder, 1998]. During the growth of *P. fluorescens* on limonene α-terpineol was produced [Bicas *et al.*, 2008]. *Castellaniella defragrans* formed geranic acid from the acyclic monoterpene β-myrcene [Heyen and Harder, 2000].

1.3 *Castellaniella defragrans* 65Phen

The β-proteobacterium *Castellaniella* (ex *Alcaligenes*) *defragrans* strain 65Phen was isolated from a ditch in a forest on α-phellandrene as sole carbon and energy source under denitrifying conditions. The Gram-negative rod-shaped bacteria were characterized as motile and mesophile [Foss, Heyen, and Harder, 1998]. Based on a phylogenetic and chemotaxonomic data analysis the strain *Alcaligenes defragrans* 65Phen was reclassified as *Castellaniella defragrans* 65Phen [Kämpfer *et al.*, 2006].

1.3.1 Enzymatic degradation of monoterpenes in *Castellaniella defragrans* 65Phen

C. defragrans 65Phen grows on acyclic monoterpenes under anaerobic conditions, using a degradation pathway alternative to the aforementioned Atu/Liu pathway from *Pseudomonas* sp.. Linalool dehydratase/isomerase (LDI) catalyzes the isomerization of geraniol to linalool and the dehydration of linalool to β-myrcene [Brodkorb *et al.*, 2010]. The bifunctional enzyme showed a native molecular size of 160 kDa via size exclusion chromatography, while in denaturing protein gels a band with a molecular size of 40 kDa was shown, leading to the suggestion that the native form of the enzyme is a homotetramer [Brodkorb *et al.*, 2010]. Crystal structures obtained by X-ray crystallography of the LDI revealed a homopentameric structure [Weidenweber *et al.*, 2016]. Dependency of the enzymatic reaction on dithiothreitol (DTT) as a reducing agent was ascertained as well as the reversibility of the enzymatic reaction [Brodkorb *et al.*, 2010]. Besides LDI, the enzymes geraniol dehydrogenase (GeoA) and geranial dehydrogenase (GeoB), involved in the β-myrcene degradation, were identified [Lüddeke *et al.*, 2012]. Figure 3 shows this reaction with the involved enzymes.

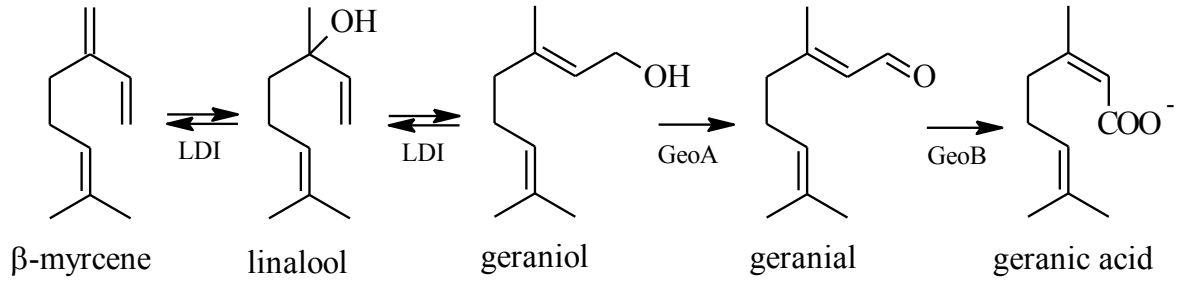

Figure 3: Anaerobic β-myrcene transformation in *C. defragrans* 65Phen. Linalool dehydratase/isomerase (LDI) is catalyzing the transformation of β-myrcene to linalool and further to geraniol. Geraniol dehydrogenase (GeoA) and geranial dehydrogenase (GeoB) are catalyzing the further transformation to geranial and geranic acid. Modified after Brodkorb *et al.* [2010].

Studies of the oxidation of the monocyclic monoterpene limonene to perillyl alcohol revealed an additional monoterpene degradation pathway in *C. defragrans*. The product perillyl alcohol was oxidized to perillic acid via perillyl aldehyde. GeoA and GeoB are catalyzing these reactions, revealing that acyclic and monocyclic alcohols are substrates of the same enzymes. A perillyl CoA thioester and a subsequent ring cleavage were hypothesized (Figure 4) [Petasch *et al.*, 2014].

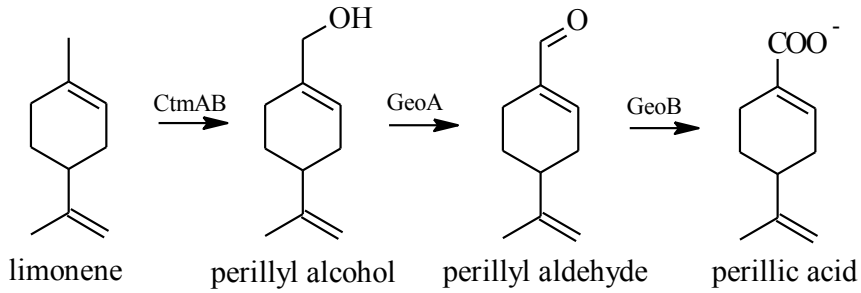

Figure 4: Anaerobic limonene degradation in *C. defragrans* 65Phen. Involved enzymes are the limonene dehydrogenase (CtmAB), the geraniol dehydrogenase (GeoA) and the geranial dehydrogenase (GeoB). Limonene is degraded via perillyl alcohol and perillyl aldehyde to perillic acid. Modified after Petasch *et al.* [2014].

1.3.2 Genomic island in *Castellaniella defragrans*

*C. defrag*rans has a genome of 3,95 Mb and contains a 70 kb genomic island coding for over 50 proteins, many of them proved to be involved in the monoterpene metabolism (i.e. LDI, GeoA, GeoB, etc.). The majority of the genes inside this island show high similarity to genes from β-proteobacteria other than *Alcaligenaceae*. Therefore, a possible event of horizontal gene transfer had been proposed [Petasch *et al.*, 2014].

1.4 Deletion mutants in *Castellaniella defragrans* and a novel linalool metabolism pathway

An in-frame deletion mutant *C. defragrans* 65Phen Δ*ldi* lacking the enzyme LDI was constructed via the introduction of deletion cassettes by conjugation and homologous recombination. It was proven that the LDI was essential for the growth on acyclic monoterpenes like β-myrcene, but not for the growth on cyclic monoterpenes like α-phellandrene and limonene [Lüddeke, Dikfidan, and Harder, 2012]. The latter had led to the suggestion of a novel metabolism pathway including hitherto unknown enzymes.

Growth of *C. defragrans* 65Phen Δ*ldi* on (R,S)-linalool led to formation of the monocyclic monoterpenes α-terpinene and terpinolene [Marmulla, 2015]. This novel linalool biotransformation was examined further and revealed an adenosine triphosphate (ATP) – dependency. An activation of linalool to a linalyl diphosphate intermediate prior to molecular cyclization had been suggested (Figure 5) [Marmulla, 2015]. This reaction bears a resemblance to the initial monoterpene synthesis described before (see Figure 2), resulting in an α-terpinyl cation as precursor for all cyclic monoterpenes.

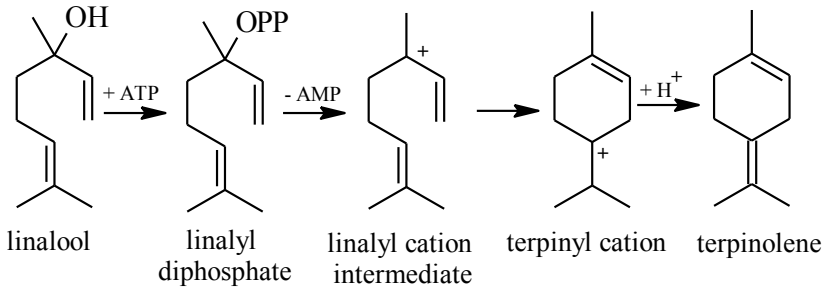

Figure 5: Proposed transformation from linalool to terpinolene. Linalool is activated to linalyl diphosphate followed by a cleavage of the phosphate moiety. The resulting linalyl cation intermediate undergoes a cyclization to the terpinyl cation, a precursor for cyclic monoterpenes. Modified after Marmulla [2015].

ATP is required as cosubstrate for the reaction with Mg^{2+} as its metal cofactor. Addition of DTT was shown to have a stimulating effect on the enzymatic reaction [Marmulla, 2015].

1.5 Monoterpene synthases

Terpene synthase (also referred to as terpene cyclase) genes encode for proteins of 550 – 850 amino acid residues with native molecular sizes of 50 – 100 kDa [Bohlmann, Meyer-Gauen, and Croteau, 1998].

Monoterpene synthases were shown to have a so-called βα structural organization, with a C-terminal α-helical bundle and a N-terminal β-domain [Gao, Honzatko, and Peters, 2012]. The active site is located in the C-terminal α-domain and contains three aspartate residues protruding into the upper part of the active site cavity of the enzyme. This aspartate-rich DDxxD motif is involved in the coordination of divalent cations for substrate binding [Cheng *et al.*, 2007]. Furthermore the cavity serves as a template for the correct conformation of the substrate for cyclization to a cyclic monoterpene causing the product diversity of the monoterpene synthases [Christianson, 2008; Lesburg *et al.*, 1997]. Next to the DDxxD motif the active site does also contain a less conserved NSE/DTE motif

[Srividya *et al.*, 2015]. In 2014, the active site of a terpene synthase was reprogrammed by Li *et al.* [2014] leading to the production of new terpenes with diverse structures.

Purification of several terpene synthases was performed in previous studies revealing the potential of liquid chromatography. With this method the monoterpene synthase pinene cyclase [Lewinsohn, Gijzen, and Croteau, 1992], the sesquiterpene cyclase (+)-δ-cadinene synthase [Davis *et al.*, 1996], and the monoterpene synthase linalool isomerase (Lis) [Marmulla *et al.*, 2016] were purified.

Aim of the thesis

This thesis had the objective to purify a novel monoterpene synthase from *Castellaniella defragrans* 65Phen by means of liquid chromatography. Denaturing protein gels were used to identify the purification success. An optimal purification will allow a better understanding of the enzyme's properties and biochemistry.

Temperature and pH values optimal for enzyme activity were defined in the course of this study. The findings of this thesis can be used for further purification and characterization of the enzyme leading to a better understanding of the anaerobic monoterpene degradation in *Castellaniella defragrans* 65Phen.

2 Material and Methods

All chemicals and biochemicals were purchased from AppliChem GmbH (Darmstadt, Germany), Bio-Rad Laboratories GmbH (Munich, Germany), Carl Roth GmbH + Co. KG (Karlsruhe, Germany), Merck KGaA (Darmstadt, Germany), Serva Electrophoresis GmbH (Heidelberg, Germany), Sigma-Aldrich Chemie GmbH (Taufkirchen, Germany). In all experiments ultrapure water was used (MilliQ, 0,22 µm filter, OPTILAB-Standard water system, USA).

2.1 Cell disintegration

After biomass resuspension in three parts (1:3 (v/v)) 25 mM Tris-HCl buffer, pH 7,5 and thawing at room temperature, the cells were disrupted using a One-Shot cell disrupter (Constant Systems Ltd., Daventry, GB). The cell suspension was filled into a metal cylinder. The disruption was initiated by a sudden pressure of 1,5 kbar which moved a piston upwards pushing the cell suspension through a hole of 0,18 mm in diameter (Figure 6). Decompression after the hole and shear forces disrupted the cells. Afterwards the disrupted cells were in the cap placed on top of the cylinder. This cycle was done twice to ensure cell disruption.

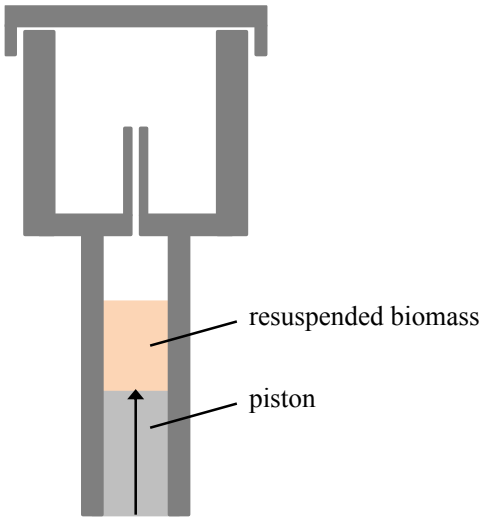

Figure 6: Scheme of the One-Shot cell disrupter.

2.2 Ultracentrifugation

The cell lysate obtained by cell disintegration was transferred to centrifuge tubes and centrifuged at 331000 x *g* and 4 °C for 40 minutes in a Beckman Coulter Optima L-70 Ultracentrifuge (Beckman Coulter Inc., Brea, USA) using a 70.1 Ti rotor. The soluble extract (supernatant) was transferred into Eppendorf vials, while the pellet was resuspended in 25 mM Tris-HCl buffer, pH 7,5, in a volume equal to the volume of obtained soluble extract. Afterwards the resuspended pellet was transferred to Eppendorf vials. The soluble extract was either used immediately for activity measurements and further processing or frozen fast in liquid nitrogen to prevent crystallization inside the sample during freezing, and subsequently stored at -80 °C.

2.3 Liquid chromatography

Protein purification was performed by liquid chromatography (LC). For all chromatographic procedures an ÄKTA purifier system (GE Healthcare Europe GmbH, Freiburg, Germany) was used at 8 °C. All buffers were prepared and pH values adjusted at room temperature. The buffers were vacuum filtered through a 0,2 µm filter unit before use. A detector measured the absorbance at 280 nm. All columns were re-equilibrated after each run with binding buffer. Size exclusion chromatography (SEC), ion exchange chromatography (IEC) and hydrophobic interaction chromatography (HIC) were investigated for enzyme purification. After each purification step, protein concentration and enzymatic activity were determined.

For chromatogram analysis consistent fraction names were required. The names were generated according to the elution volume of the fractions from the column. Eluted protein was collected as 1 mL fractions. Consequently, the first fraction of a chromatography is called F1 and is eluting from 0,01 – 1,00 mL and fraction F2 is eluting from 1,01 – 2,00 mL.

2.3.1 Size exclusion chromatography

SEC is based on the steric exclusion mechanism. Molecules with a size larger then the size of the cavities of the porous beads inside the column elute first, while molecules with a smaller size enter the cavities and elute in a delayed fashion. By this method, proteins can be separated according to their size. The resolution range of the column material is

determined by the cavity size. Small ions are retained the longest and their elution is observable as a change of conductivity at the end of the chromatographic run.

The binding buffer (25 mM Tris-HCl, 100 mM KCl, pH 7,5) was used for equilibration of a Superdex 75 prep grade column (dimensions 16 x 600 mm; CV 120 mL; HighLoad) at a flow of 0,5 mL/min.

Calibration of the SEC column was performed with a gel filtration standard (Bio-Rad Laboratories GmbH, Munich, Germany) containing molecular weight markers ranging from 1,35 kDa to 670 kDa. The determined resolution capacity is ranging from 1,35 kDa to 155 kDa and is broader than the one given by the manufacturer of the column (3 kDa – 70 kDa). For the calculation of the calibration curve the K_{av}-values of the marker proteins had to be determined using formula (1), with the elution volume V_e, the void volume of the column V_0 determined by the proteins eluting first (41,88 mL), and the column volume V_t (120 mL).

$$K_{av} = \frac{(V_e - V_0)}{(V_t - V_0)} \qquad (1)$$

2.3.2 Ion exchange chromatography

IEC was used to separate proteins according to their net surface charge. For this method, the pH of the buffer and of the whole chromatographic system is very important. With a pH below the isoelectric point (pI) of the protein, the net surface charge of the protein is positive and the protein will bind to a cation exchanger. If the pH is above the pI of the protein the net surface charge is negative and the protein will bind to an anion exchanger. During this study only anion exchangers were used. At pH 7,5 the enzyme activity of interest was binding to the anion exchanger.

Standard was a diethylaminoethyl (DEAE) column (dimension: 16 x 100 mm; CV 20 mL; packed with Sepharose FF; binding capacity 30 mg protein/mL). The column was equilibrated with the binding buffer (25 mM Tris-HCl, pH 7,5 resp. pH 8,0) at a flow rate of 1,0 mL/min. After elution of the flow-through, bound protein was eluted from the column by an increasing salt concentration in the elution buffer. For this purpose, a second buffer (25 mM Tris-HCl, 1 M KCl, pH 7,5 resp. pH 8,0) was used. The two buffers can be mixed by the ÄKTA purifier system to obtain a specific KCl concentration for elution. This procedure creates linear or step gradients. At the end of each run the column was

purged with 1 M KCl until the last peak eluted from the column comprising strongly bound protein or nucleic acids.

Alternative to the weak anion exchange column DEAE was a strong anion exchange column Resource Q (dimensions: 6,4 x N/A mm; CV 1 mL; packed with Source 15Q; binding capacity 25 mg protein/mL). The conditions during binding and elution were the same as for the weak anion exchanger. In theory, high pressure of up to 15 bar is applicable with this column. The DEAE column can only operate at pressures below 1,5 bar. Both columns can be operated in a pH range of pH 2 – pH 12 without significant change in function.

2.3.3 Hydrophobic interaction chromatography

HIC was used to separate proteins according to their hydrophobicity. The more hydrophobic a protein, the stronger it binds to the stationary phase of the separation column. Binding on a HIC column is dependent on amino acid residues at the protein surface and factors like the salt concentration and organic solvents in the liquid phase surrounding the protein. Interaction of a protein with the hydrophobic stationary phase is enhanced by high salt concentrations in the binding buffer (for example 1 M $(NH_4)_2SO_4$).

The samples were loaded on a Phenyl column (dimensions 16 x 100 mm; CV 20 mL; packed with Phenyl Sepharose FF). After washing of the column with binding buffer (25 mM Tris-HCl, 500 resp. 100 mM $(NH_4)_2SO_4$, pH 7,5) at a flow rate of 1 mL/min, bound protein was eluted from the column with a decreasing gradient of $(NH_4)_2SO_4$. Subsequently, a step gradient elution with another elution buffer (25 mM Tris-HCl, 0,1 % (v/v) Tween 20, pH 7,5) resp. 20 % (v/v) ethanol and water followed.

2.3.4 Combination of chromatographic methods

Different chromatographic runs were combined in several approaches to increase the purification success. The most active fractions of the first chromatographic step (e.g. an IEC) were pooled and in some cases concentrated on an Amicon filter unit (10 kDa cut-off; Merck Millipore, Danvers, USA). Afterwards the mixture was loaded on the next chromatographic column (e.g. a SEC).

2.4 Bradford protein assay

Protein content was determined for all samples by the Bradford protein assay. The dye Coomassie Brilliant Blue forms a complex with the proteins by binding to basic and aromatic amino acid residues. This binding leads to a shift of the absorption maximum from 470 nm to 595 nm which can be detected using a spectrophotometer (Eppendorf AG, Hamburg, Germany).

In a 1,5 mL semi-microcuvette sealed with parafilm 800 µL of Milli-Q water, 200 µL of Bradford reagent (Dye reagent concentrate, Bio-Rad laboratories GmbH, Munich, Germany) and 20 µL of (diluted) protein sample, protein standard or blank, respectively, were mixed. After 10 minutes of incubation at room temperature the absorbance at 595 nm was measured in triplicates with the spectrophotometer. For absorbance values higher than 0,8 the samples were further diluted to obtain a value in the linear range of the device. The protein concentration was identified by absorbance comparison to bovine serum albumin (BSA) standards (Figure 7). The R^2 of the calibration curve was 0,9906 and all determined values were inside the calculated confidence intervals at a 95 % significance level.

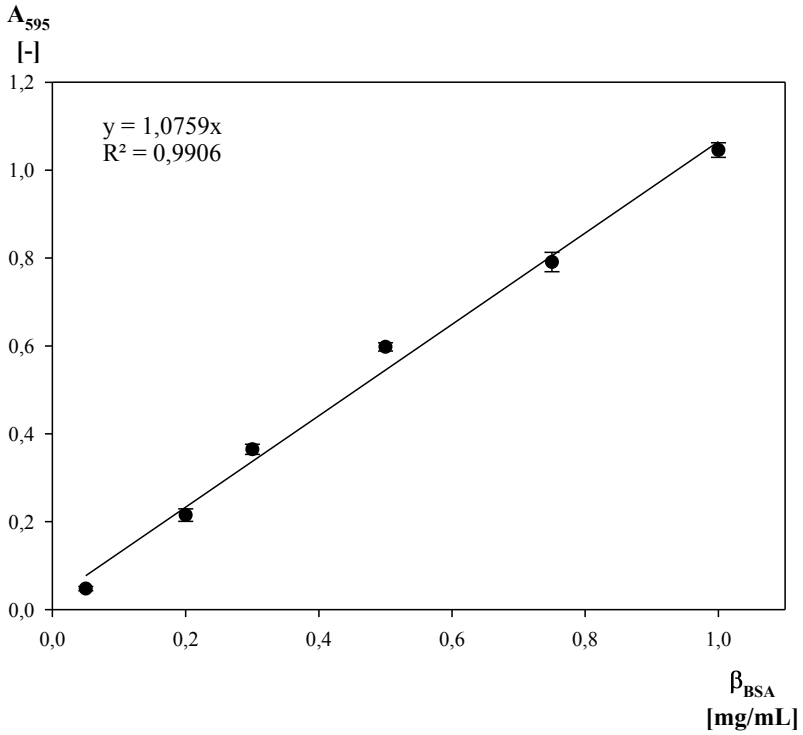

Figure 7: Calibration plot for BSA. BSA concentrations ranging from 0,05 mg/mL to 1,00 mg/mL in 20 µL sample volume. Samples were measured in triplicates after 10 minutes of incubation.

2.5 SDS-PAGE

A sodium dodecyl sulfate-polyacrylamide gel electrophoresis (SDS-PAGE) was implemented to analyze the protein purification progress. Additionally, the size of the protein of interest as well as its identity by additional mass spectrometry experiments can be determined. For the separation and the stacking gel Milli-Q water, separation resp. stacking buffer, acrylamide, ammonium persulfate (APS), and N, N, N', N' - tetramethylethylenediamine (TEMED) were mixed (Table 1).

Table 1: Composition of the separation and the stacking gel for SDS-PAGE. For separation 10 % polyacrylamide and for stacking 4 % polyacrylamide were chosen. Volumes are given for two gels.

Separation gel (10 % polyacrylamide)	**Stacking gel (4 % polyacrylamide)**
4,16 mL Milli-Q water	2,82 mL Milli-Q water
2,5 mL separation buffer	1,5 mL stacking buffer
3,34 mL 30 % (v/v) acrylamide	0,66 mL 30 % (v/v) acrylamide
100 µL 10 % (v/v) APS	60 µL 10 % (v/v) APS
10 µL 6,6 M TEMED	6 µL 6,6 M TEMED

The separation buffer consists of 1,5 M Tris-HCl and 0,4 % (v/v) SDS, pH 8,8. The stacking buffer consists of 0,5 M Tris-HCl and 0,4 % (v/v) SDS, pH 7,5. As soon as TEMED was added to the mixture it started to polymerize and was poured between glass plates to form a gel. First the separation gel was cast and after 20 – 30 minutes of polymerization the stacking gel was cast on top of it. A comb was stuck into the top of the gel to form wells for the samples. After polymerization of the second gel on the cast stand, the gel units were transferred into the separation chamber which was filled afterwards with running buffer comprising 25 mM Tris-HCl, 192 mM glycine and 0,025 mM SDS, pH 8,8.
A maximum of 20 µg protein per well were applied to avoid overloading of the gel lane. Small wells were used (15 µL volume per well) with protein samples in a concentration range from 0,7 to 0,9 mg/mL. Samples with higher concentrations were diluted with 25 mM Tris-HCl buffer, pH 7,5.
5 x loading buffer (0,2 M Tris-HCl, 10 % (v/v) SDS, 20 % (v/v) glycerol, 10 mM DTT, 0,05 % (v/v) Bromophenol blue, pH 6,8) was added to the samples which were heated in the Mastercycler gradient (Eppendorf AG, Hamburg, Germany) at 95 °C for 5 minutes. 7 µL of a PageRuler unstained protein ladder (Thermo Fisher Scientific, Bremen, Germany) and the prepared samples were loaded into the wells of the gel. Electrophoresis

was performed at 70 V for roughly 3 hours with a Bio-Rad Power Pac HC (Bio-Rad Laboratories, GmbH, Munich, Germany). Afterwards the gels were stained in staining solution comprising 0,1 % (v/v) Coomassie G250 Brilliant Blue, 10 % (v/v) acetic acid, and 40 % (v/v) ethanol. The gels were stained for 2 hours on a shaker. Afterwards the gels were destained overnight with destaining solution comprising 10 % (v/v) acetic acid and 20 % (v/v) ethanol. At the end of the procedure the gels were fixed with fixation solution (10 % (v/v) acetic acid) to prevent diffusion of the bands and scanned with an ImageScanner using the software *ImageMaster*. Afterwards the contrast of the picture was adjusted with *Adobe Photoshop CS5* and the pictures were cropped with *Microsoft PowerPoint 2010*. During the image editing the aspect ratio of the pictures was maintained constant.

2.6 Quantification of monoterpenes

Monoterpene synthesis was determined via an enzyme activity assay followed by quantification with gas chromatography (GC).

2.6.1 Monoterpene synthase activity assay

Enzyme activity assays were performed in 1,5 mL glass vials (WICOM Germany GmbH, Heppenheim, Germany) closed with a lid containing a Teflon-coated rubber septum preventing monoterpenes from dissolving into the rubber and escaping from the enzymatic reaction. The required supplements for the enzyme activity assay were mixed prior to the assay (Table 2). This mixture was filled up with 25 mM Tris-HCl, pH 7,5. To neutralize the acidic pH arising from ATP, Na_2CO_3 was added and the pH was determined via a pH strip to avoid protein precipitation during the assay. By this means, the final pH of the mixture was set to pH 7,0.

Due to the low stability of DTT and ATP in solution exposed to oxygen and light, respectively, stock solutions of 1 mL 200 mM ATP and 0,5 mL 1 M DTT were prepared once a week. Stock solutions of 5 mL 2 M $MgCl_2$ and 5 mL 2 M Na_2CO_3 were prepared at the beginning of the study. All stock solutions were stored at -20 °C.

Table 2: Concentrations of the three supplements required for the enzyme activity assay given as end concentrations in the stock solution and in the assay. Additionally 25 mM Tris-HCl buffer, pH 7,5 and Na_2CO_3 were added.

Supplement	Concentration in the mixture [mM]	Concentration in the assay [mM]
ATP	71,4	10,0
DTT	14,3	2,0
$MgCl_2$	107,1	15,0

70 µL of the supplement mixture per assay were added to a glass vial followed by 330 µL of either 25 mM Tris-HCl buffer, pH 7,5 (blank) or sample. The samples were diluted before with 25 mM Tris-HCl buffer, pH 7,5 to end concentrations in the assay of 5 mg/mL for soluble extract, 1 mg/mL for SEC fractions and 0,5 mg/mL for IEC fractions. Whenever these concentrations could not be obtained 330 µL of sample were used.

After the assay was prepared the glass vial was closed and the vials were flushed with nitrogen gas for at least 30 seconds through a needle to replace the air in the headspace of the vial with nitrogen. Thus, the reaction took place under anaerobic conditions. Addition of 100 µL of a linalool dilution containing Tween 20 and Tris-HCl, pH 7,5 (Table 3) via a 1 mL syringe started the reaction.

Table 3: Concentrations of the three components in the linalool dilution given as end concentrations in the dilution and in the assay.

Component	Concentration in the dilution	Concentration in the assay
Linalool	25 mM	5 mM
Tween 20	2,5 % (v/v)	0,5 % (v/v)
Tris-HCl	25 mM	25 mM

The assays were incubated for two hours at 28 °C and 60 rpm. Addition of 50 µL 0,5 M ethylendiaminetetraacetic acid (EDTA) stopped the enzymatic reaction via complex formation with Mg^{2+}. Samples were then transferred in 1,5 mL Eppendorf tubes filled with 200 µL n-hexane. After 20 minutes of incubation at 28 °C and 120 rpm the Eppendorf tubes were centrifuged for 10 minutes at 4 °C and 20800 x *g* to induce phase separation. 100 µL of the monoterpene containing organic top phase were transferred into a brown-glass GC vial which was closed afterwards with an aluminum crimp containing a Teflon-coated rubber septum. In an automated process 1 µL from this vial was measured by GC.

2.6.2 Gas chromatography

Monoterpenes were quantified by GC with flame ionization detection (PerkinElmer, Rodgau, Germany) on an Optima 5 column (50 m x 0,32 mm; 0,25 µm film thickness; Macherey-Nagel GmbH & Co. KG, Düren, Germany) with hydrogen as carrier gas at 65 cm/s. Sample injection was performed by an autosampler (CTC analytics AG, Zwingen, Switzerland) with a consistent sample amount of 1 µL. The optimized temperature program started with an initial column temperature of 80 °C. After 2 minutes the temperature was increasing to 120 °C at a rate of 4 °C/min. After 0,1 minutes at 120 °C the temperature was increasing further to 320 °C at a rate of 45 °C/min. This temperature was kept constant for another 2,9 minutes. During the whole program the injection port had a temperature of 250 °C and the detection port had a temperature of 350 °C.

Quantification of α-terpinene and terpinolene was performed by retention time comparison with monoterpene standards (90 – 95 % purity) measured in triplicates (Figure 8 and Figure 9). The R^2 was 0,9959 for α-terpinene and 0,9968 for terpinolene and all determined values were inside the calculated confidence intervals at a 95 % significance level.

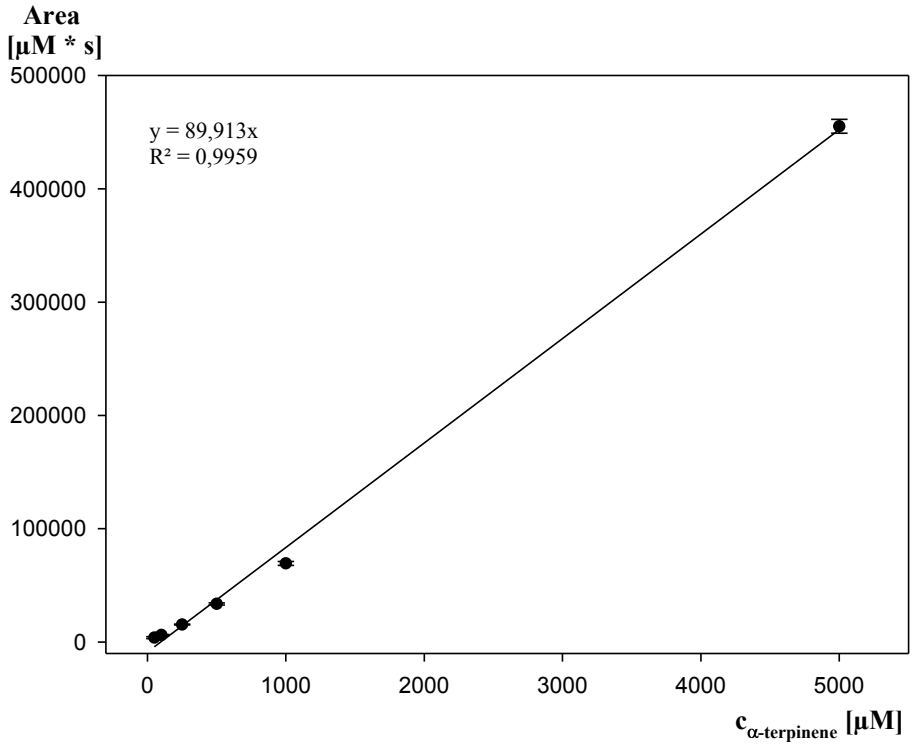

Figure 8: Calibration plot for α-terpinene. Monoterpene concentrations ranging from 50 µM to 5000 µM. Samples were measured in triplicates and injected by an autosampler.

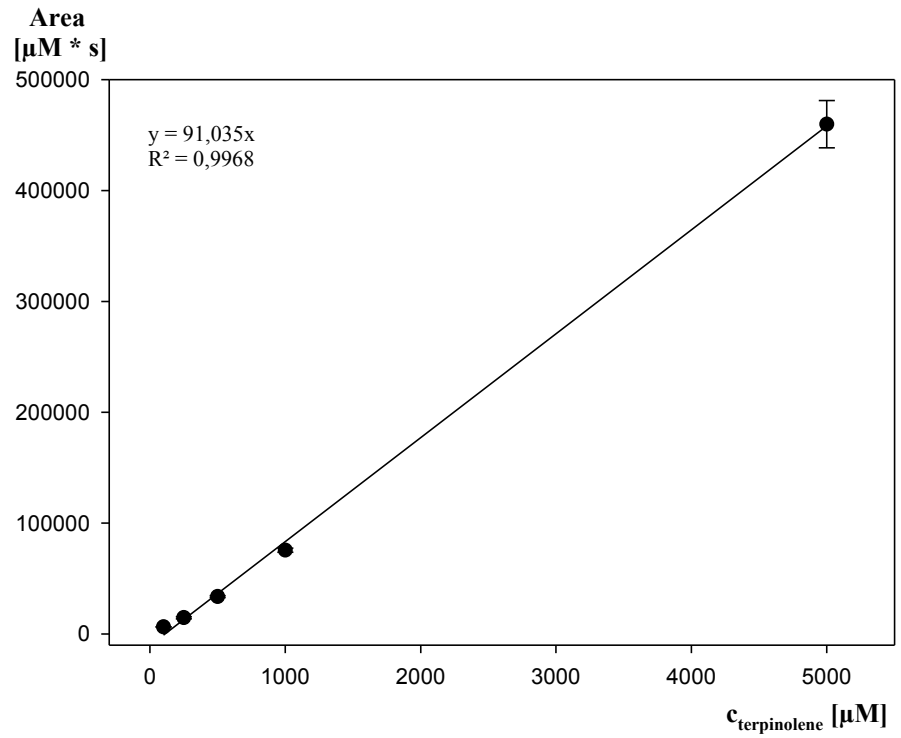

Figure 9: Calibration plot for terpinolene. Monoterpene concentrations ranging from 50 µM to 5000 µM. Samples were measured in triplicates and injected by an autosampler.

2.6.3 Data interpretation

To determine the success of the enzyme enrichment throughout the purification levels purification tables were made. These tables contain the different purification levels with the volume of each level next to the determined protein amount in mg and the total enzyme activity in pkat. By dividing the total enzyme activity by the protein amount the specific enzyme activity in pkat/mg can be calculated. The relative specific activity is calculated by division of the specific enzyme activity by the specific enzyme activity calculated for the first purification level while the protein yield is calculated by division of total protein by total protein of the first purification level and multiplication with 100 %. Not all fractions were tested for every chromatography. The values in between the tested fractions were determined by linear interpolation resulting in the values of the integrated peak. The last row of the purification table gives the results of these integrated peak values (Table 4) with the total protein amount and total enzyme activity as sums of the single values of the integrated peak. The specific activity, the relative specific activity, and the protein yield of the integrated peak were calculated from these values.

Table 4: Example for a purification table including the required calculations. The sums in the bottom row were obtained by a calculated integrated peak

Purification level	**Volume [mL]**	**Total protein [mg]**	**Total activity [pkat]**	**Specific activity [pkat/mg]**	**Relative specific activity**	**Protein yield [%]**
Soluble Extract		x_1	y_1	$z_1 = \frac{y_1}{x_1}$	1,0	100,0
Chromatographic fractions	volume of the fractions	x_2	y_2	$z_2 = \frac{y_2}{x_2}$	$\frac{z_2}{z_1}$	$\frac{x_2}{x_1} \cdot 100$
…	…	…	…	…	…	…
Integrated peak		$x_{int} = \Sigma(x_i)$	$y_{int} = \Sigma(y_i)$	$z_{int} = \frac{y_{int}}{x_{int}}$	$\frac{z_{int}}{z_1}$	$\frac{x_{int}}{x_1}$

3 Results

The identification of the proteins involved in the synthesis of α-terpinene and terpinolene from (R,S)-linalool was approached by purification of the enzyme activities on chromatography columns.

3.1 Enzyme activities in soluble extracts

Biomass of *Castellaniella defragrans* 65Phen Δ*ldi* was available for this study from several multi-fed batch cultivations grown on linalool and nitrate in a pH-controlled 10 L-fermenter. High pressure cell disruption and ultracentrifugation yielded soluble extracts that were assayed for α-terpinene and terpinolene synthase activities. Both activities were observed. Terpinolene activities were ranging from 0,64 to 4,40 pkat/mg referred to a sample volume of 1 mL, except for extracts from cells harvested on the 18th of March 2016 (Table 5).

Table 5: Extractions of biomasses of *C. defragrans* 65Phen Δ*ldi*. Protein concentration and enzyme activity in the soluble extracts were determined.

Extract no	Fermentation [date of harvest]	Protein concentration [mg/mL]	Specific α-terpinene activity [pkat/mg]	Specific terpinolene activity [pkat/mg]
1	19.02.2016	13,0	1,76	1,98
2	19.02.2016	13,3	1,62	3,11
3	19.02.2016	18,2	2,22	2,70
4	16.12.2015	19,5	0,95	4,40
5	18.03.2016	17,0	1,62	0,09
6	18.03.2016	19,1	1,25	0,06
7	18.03.2016	20,5	1,24	0,05
8	16.12.2015	19,6	1,71	0,64
9	16.12.2015	22,8	1,52	0,79
10	19.02.2016	9,77	2,56	1,75

3.2 Purification by anion exchange chromatography

Enzyme activity was retained on a DEAE-Sepharose column and eluted with an increasing KCl gradient. The soluble extract was loaded on the weak anion exchanger followed by purification in one chromatographic run. Afterwards protein concentrations and specific monoterpene synthase activities for α-terpinene and terpinolene were determined in fractions.

3.2.1 Purification on a weak ion exchanger with a 5 column volume gradient

The binding capacity of the 20 mL-column was considered and only 11 mL of soluble extract 2 (Table 5) comprising 146 mg of protein were diluted with 30 mL of binding buffer (25 mM Tris-HCl, pH 7,5). After the unbound protein had been eluted, a linear gradient from 0 mM KCl to 300 mM KCl over 5 CV was applied for protein elution. The column was cleaned with a step gradient from 300 mM KCl to 1 M KCl. Figure 10 and Figure 11 show detected protein, α-terpinene and terpinolene synthase activities, respectively.

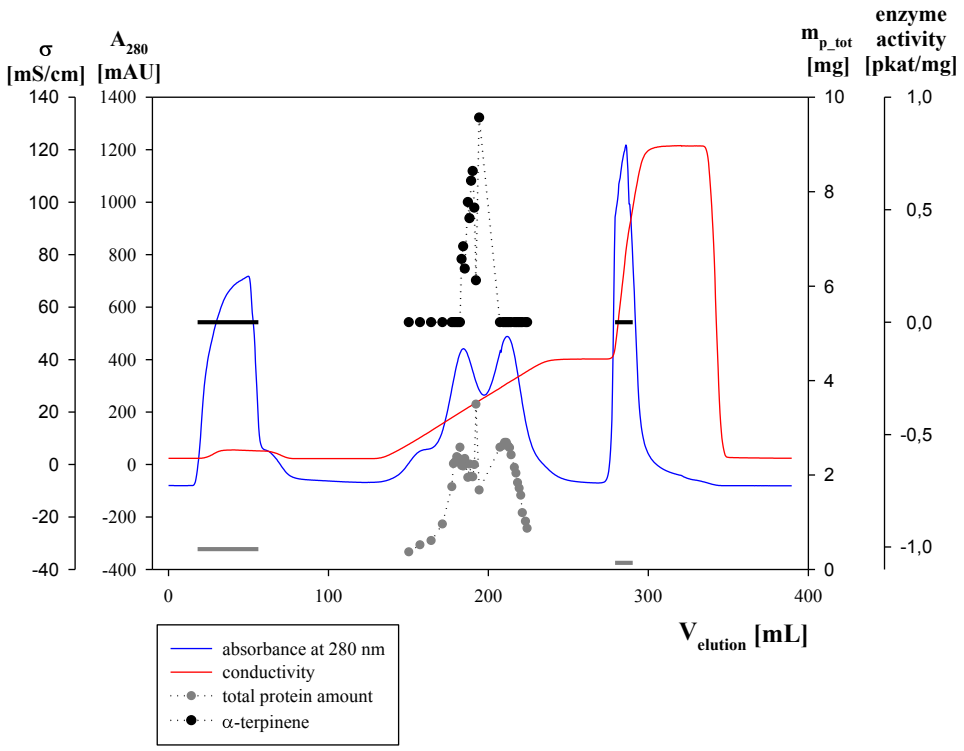

Figure 10: Protein separation and α-terpinene synthase activity on DEAE-Sepharose using a linear gradient from 0 to 300 mL KCl over 5 CV (100 mL). The IEC was performed with 146 mg protein in 25 mM Tris-HCl, pH 7,5 (binding buffer) at a flow rate of 1 mL/min. Blue line: Inline measured absorbance at 280 nm; red line: Inline measured conductivity. The protein amount was determined offline in triplicates. Enzyme activity was determined offline in a single test and reached a maximum of 0,91 pkat/mg.

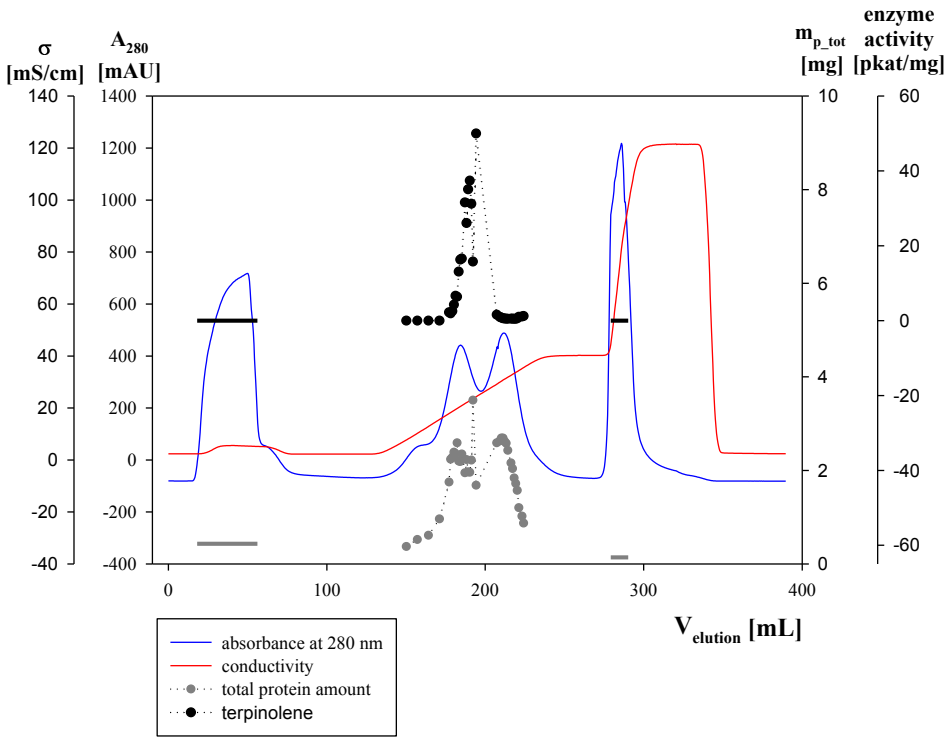

Figure 11: Protein separation and terpinolene synthase activity on DEAE-Sepharose using a linear gradient from 0 to 300 mL KCl over 5 CV (100 mL). The IEC was performed with 146 mg protein in 25 mM Tris-HCl, pH 7,5 (binding buffer) at a flow rate of 1 mL/min. Blue line: Inline measured absorbance at 280 nm; red line: Inline measured conductivity. The protein amount was determined offline in triplicates. Enzyme activity was determined offline in a single test and reached a maximum of 50 pkat/mg.

Synthase activities for α-terpinene and terpinolene were detected in several fractions starting at a salt concentration of 142 mM KCl and reaching a maximum at 181 mM KCl. Both synthase activities started to elute in the second peak detected by UV absorbance and reached maxima between the second and the third peak. The specific synthase activity for α-terpinene was lower than the one for terpinolene (Table 6 and Table 7).

Table 6: Purification of α-terpinene synthase activity by IEC from soluble extract obtained from biomass of *C. defragrans*. Integrated peak from F184 to F207.

c_{KCl_calc} [mM]	Purification level	Volume [mL]	Total protein [mg]	Total activity [pkat]	Specific activity [pkat/mg]	Relative specific activity	Protein yield [%]
-	Soluble Extract 2	11	146	21,5	0,15	1,0	100,0
	IEC						
138	Fraction 183	1	2,59	0,00	0,00	0,0	1,8
142	Fraction 184	1	2,20	0,62	0,28	1,9	1,5
144	Fraction 185	1	2,19	0,74	0,34	2,3	1,5
148	Fraction 186	1	2,35	0,56	0,24	1,6	1,6
154	Fraction 188	1	1,95	1,04	0,53	3,6	1,3
156	Fraction 189	1	2,23	1,03	0,46	3,1	1,5
160	Fraction 190	1	1,97	1,24	0,63	4,3	1,3
162	Fraction 191	1	1,96	1,32	0,67	4,6	1,3
166	Fraction 192	1	2,22	1,13	0,51	3,5	1,5
168	Fraction 193	1	3,50	0,65	0,19	1,3	2,4
174	Fraction 195	1	1,68	1,53	0,91	6,2	1,2
213	Fraction 208	1	2,59	0,00	0,00	0,0	1,8
	Integrated peak		52,6	20,9	0,40	2,7	36,0

Table 7: Purification of terpinolene synthase activity by IEC from soluble extract obtained from biomass of *C. defragrans*. Integrated peak from F173 to F225.

c_{KCl_calc} [mM]	Purification level	Volume [mL]	Total protein [mg]	Total activity [pkat]	Specific activity [pkat/mg]	Relative specific activity	Protein yield [%]
-	Soluble Extract 2	11	146	41,3	0,28	1,0	100,0
	IEC						
106	Fraction 172	1	0,96	0,00	0,00	0,0	0,7
124	Fraction 178	1	1,75	3,89	2,22	7,9	1,2
126	Fraction 179	1	2,24	4,35	1,94	6,9	1,5
130	Fraction 180	1	2,28	5,80	2,55	9,0	1,6
132	Fraction 181	1	2,39	10,2	4,28	15,2	1,6
136	Fraction 182	1	2,36	15,7	6,65	23,5	1,6
138	Fraction 183	1	2,59	16,6	6,39	22,6	1,8
142	Fraction 184	1	2,20	28,8	13,1	46,3	1,5
144	Fraction 185	1	2,19	35,7	16,3	57,7	1,5
148	Fraction 186	1	2,35	39,0	16,6	58,7	1,6

Table 7: Purification of terpinolene synthase activity by IEC from soluble extract obtained from biomass of *C. defragrans*. Integrated peak from F173 to F225. ***(Continued)***

c_{KCl_calc} [mM]	Purification level	Volume [mL]	Total protein [mg]	Total activity [pkat]	Specific activity [pkat/mg]	Relative specific activity	Protein yield [%]
154	Fraction 188	1	1,95	61,6	31,6	112	1,3
156	Fraction 189	1	2,23	58,1	26,1	92,2	1,5
160	Fraction 190	1	1,97	69,1	35,1	124	1,3
162	Fraction 191	1	1,96	73,3	37,4	132	1,3
166	Fraction 192	1	2,22	69,3	31,2	110	1,5
168	Fraction 193	1	3,50	55,2	15,8	55,8	2,4
174	Fraction 195	1	1,68	84,0	50,0	177	1,2
213	Fraction 208	1	2,59	4,14	1,60	5,7	1,8
219	Fraction 210	1	2,63	2,61	0,99	3,5	1,8
222	Fraction 211	1	2,69	2,20	0,82	2,9	1,8
226	Fraction 212	1	2,69	1,76	0,65	2,3	1,8
228	Fraction 213	1	2,62	1,52	0,58	2,1	1,8
232	Fraction 214	1	2,58	1,39	0,54	1,9	1,8
234	Fraction 215	1	2,43	1,19	0,49	1,7	1,7
240	Fraction 217	1	2,16	1,14	0,53	1,9	1,5
243	Fraction 218	1	2,04	1,11	0,54	1,9	1,4
246	Fraction 219	1	1,84	0,89	0,49	1,7	1,3
249	Fraction 220	1	1,72	0,87	0,51	1,8	1,2
251	Fraction 221	1	1,57	0,94	0,60	2,1	1,1
255	Fraction 222	1	1,20	1,22	1,02	3,6	0,8
261	Fraction 224	1	1,02	1,14	1,12	3,9	0,7
264	Fraction 225	1	0,87	1,09	1,26	4,4	0,6
	Integrated peak		107	1318	12,3	43,5	73,4

The integrated α-terpinene synthase peak consisted of fractions F184 – F207 and had a total amount of 52,6 mg protein (36,0 % of initial protein) and a total synthase activity of 20,9 pkat, while the integrated terpinolene synthase peak consisted of fractions F173 – F225 and had a total amount of 107 mg protein (73,4 % of initial protein) and a total synthase activity of 1318 pkat. Total α-terpinene synthase activity did slightly decrease from 21,5 to 20,9 pkat. This is also reflected in the relative specific activity (2,7 x). Total terpinolene synthase activity did increase from 41,3 to 1318 pkat, indicating the presence of inhibitory substances in the soluble extract. This is also reflected in the relative specific

activity (43,5 x). A variable increase of activities during purification indicates that both activities respond individually to IEC.

After one purification step the active fractions on the SDS-PAGE showed prominent bands at 38 kDa, 60 kDa, 70 kDa, 85 kDa and 100 kDa with one exception in the middle of the fraction range from F196 – F207 (Figure 12). Most of these protein bands were also visible in inactive fractions thus giving no clear result regarding the protein bands responsible for enzyme activity. Fractions F196 – F207 were lost due to a failure of the fraction collector.

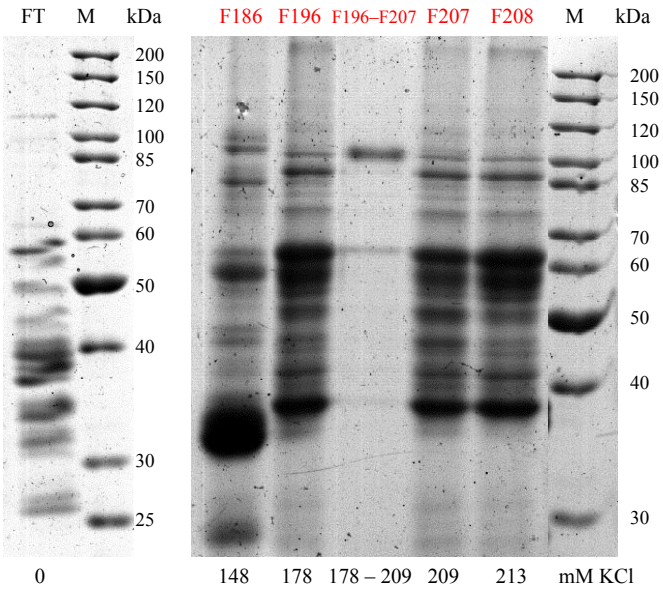

Figure 12: SDS-PAGE of single step IEC fractions with a 5 CV gradient. Samples were applied on a polyacrylamide gel with 10 % acrylamide in the separation gel. Electrophoresis was carried out at 70 V for 3 hours. The gel was stained with Coomassie Blue staining solution. (FT) flow-through and five active (red) fractions. Due to a failure of the fractionator the fractions F196 – F207 were lost. At the bottom of the gel the calculated KCl concentration in the fractions is given.

3.2.2 Purification on a weak ion exchanger with a 15 column volume gradient

After dilution of 7 mL of soluble extract 7 (Table 5) comprising 144 mg of protein with 3,5 mL of binding buffer (25 mM Tris-HCl, pH 7,5), the sample was loaded onto the weak anion exchanger. After the unbound protein had been eluted, a linear gradient from 0 mM KCl to 300 mM KCl over 15 CV was applied for protein elution. The column was cleaned with a step gradient from 300 mM KCl to 1 M KCl. Figure 13 shows detected protein and terpinolene synthase activity.

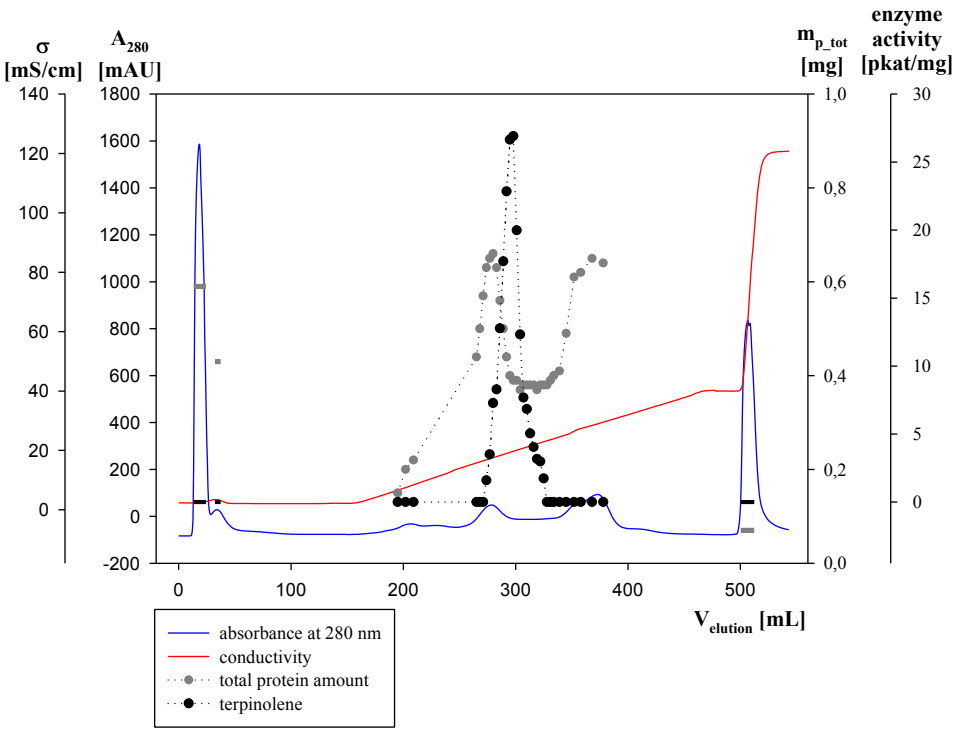

Figure 13: Protein separation and terpinolene synthase activity on DEAE-Sepharose using a linear gradient from 0 to 300 mL KCl over 15 CV (300 mL). The IEC was performed with 144 mg protein in 25 mM Tris-HCl, pH 7,5 (binding buffer) at a flow rate of 1 mL/min. Flow rate during gradient elution: 0,3 mL/min. Blue line: Inline measured absorbance at 280 nm; red line: Inline measured conductivity. The protein amount was determined offline in triplicates. Enzyme activity was determined offline in a single test and reached a maximum of 26,9 pkat/mg.

A specific synthase activity for α-terpinene was not detected. Synthase activity for terpinolene was detected in several fractions starting at a salt concentration of 117 mM KCl and reaching a maximum at 141 mM KCl. Due to the smooth gradient with a higher resolution, more peaks detected by UV absorbance are visible in the chromatogram than in the 5 CV-gradient experiment. The terpinolene synthase activity started to elute in the third peak and reached a maximum between the third and the fourth peak (Table 8 and Table 9).

Table 8: Purification of α-terpinene synthase activity by IEC from soluble extract obtained from biomass of *C. defragrans*.

Purification level	Volume [mL]	Total protein [mg]	Total activity [pkat]	Specific activity [pkat/mg]	Relative specific activity	Protein yield [%]
Soluble Extract 7	7	144	25,2	0,18	1,0	100,0
IEC						
Fraction 271 - 329	1 each	0,37 - 0,66	0,00	0,00	0,0	17,9

Table 9: Purification of terpinolene synthase activity by IEC from soluble extract obtained from biomass of *C. defragrans*. Integrated peak from F273 to F328.

c_{KCl_calc} [mM]	Purification level	Volume [mL]	Total protein [mg]	Total activity [pkat]	Specific activity [pkat/mg]	Relative specific activity	Protein yield [%]
-	Soluble Extract 7	7	144	1,05	0,01	1,0	100,0
	IEC						
114	Fraction 271	1	0,57	0,00	0,00	0,0	0,4
117	Fraction 275	1	0,63	1,01	1,60	219	0,4
120	Fraction 278	1	0,65	2,28	3,51	479	0,5
123	Fraction 281	1	0,66	4,81	7,29	996	0,5
126	Fraction 284	1	0,63	5,23	8,29	1134	0,4
129	Fraction 287	1	0,56	7,16	12,8	1748	0,4
132	Fraction 290	1	0,50	8,85	17,7	2421	0,3
135	Fraction 293	1	0,44	10,1	22,9	3125	0,3
138	Fraction 296	1	0,40	10,7	26,6	3643	0,3
141	Fraction 299	1	0,39	10,5	26,9	3679	0,3
144	Fraction 302	1	0,39	7,79	20,0	2733	0,3
147	Fraction 305	1	0,37	4,56	12,3	1686	0,3
150	Fraction 308	1	0,38	2,92	7,69	1051	0,3
153	Fraction 311	1	0,38	2,60	6,84	935	0,3
156	Fraction 314	1	0,38	1,92	5,04	690	0,3
159	Fraction 317	1	0,38	1,54	4,05	553	0,3
162	Fraction 320	1	0,37	1,17	3,17	433	0,3
165	Fraction 323	1	0,38	1,13	2,98	408	0,3
168	Fraction 326	1	0,38	0,66	1,73	237	0,3
171	Fraction 329	1	0,38	0,00	0,00	0,0	0,3
	Integrated peak		25,8	254	9,88	1350	17,9

Although α-terpinene synthase activity was detected in the soluble extract no activity was detected in IEC fractions. The integrated terpinolene synthase peak consisted of fractions F273 – F328 and had a total amount of 25,8 mg protein (17,9 % of initial protein) and a total synthase activity of 254 pkat. Total terpinolene synthase activity did increase from 1,05 to 254 pkat, reflected in a high relative specific activity (1350 x).

The SDS-PAGE gel of active and inactive fractions showed a distribution of individual protein bands over several fractions (Figure 14). A band at 35 kDa visible in fraction F196

is distinct from fraction F269 to F287 before it vanishes until fraction F317. The same distribution effect is visible for other bands like the one at 100 kDa. This indicates either that the fraction collector has a higher resolution than the column or that the protein is interacting with other proteins and has slightly changing binding characteristics. The gel showed the requirement for additional purification steps in order to obtain protein bands assignable to enzyme activity.

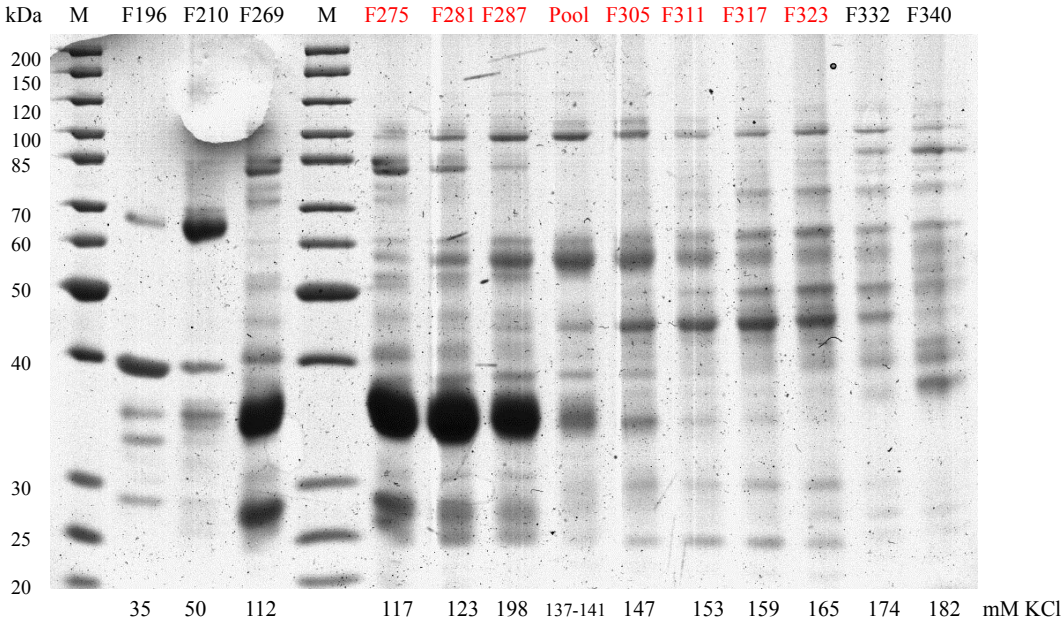

Figure 14: SDS-PAGE of single step IEC fractions with a 15 CV gradient. Samples were applied on a polyacrylamide gel with 10 % acrylamide in the separation gel. Electrophoresis was carried out at 70 V for 3 hours. The gel was stained with Coomassie Blue staining solution. Inactive and active (red) fractions. At the bottom of the gel the calculated KCl concentration in the fractions is given. Pool: F295 – F299.

3.2.3 Purification on a weak ion exchanger with a step gradient

In order to reduce the time required for one purification step a combination of linear gradient and step gradient was tested. 5 mL of soluble extract 8 (Table 5) comprising 98 mg of protein were diluted with 2,5 mL of binding buffer (25 mM Tris-HCl, pH 7,5). The sample was loaded onto the weak anion exchanger. After the unbound protein had been eluted, a first step up to 100 mM KCl was performed. As soon as the conductivity reached a plateau a linear gradient from 100 mM KCl to 200 mM KCl over 2 CV was applied for protein elution followed by a second step from 200 mM KCl to 300 mM KCl. The column was cleaned with a step gradient from 300 mM KCl to 1 M KCl. Figure 15 and Figure 16 show detected protein, α-terpinene and terpinolene synthase activities, respectively.

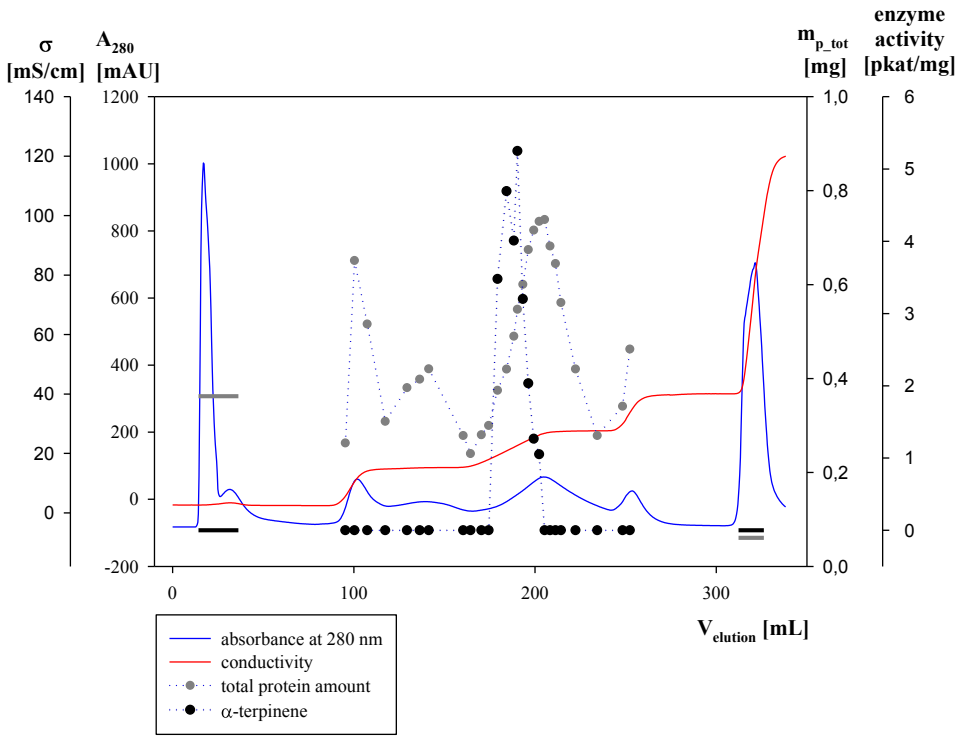

Figure 15: Protein separation and α-terpinene synthase activity on DEAE-Sepharose using a step gradient. The IEC was performed with 98 mg protein in 25 mM Tris-HCl, pH 7,5 (binding buffer) at a flow rate of 1 mL/min. Blue line: Inline measured absorbance at 280 nm; red line: Inline measured conductivity. The protein amount was determined offline in triplicates. Enzyme activity was determined offline in a single test and reached a maximum of 5,25 pkat/mg.

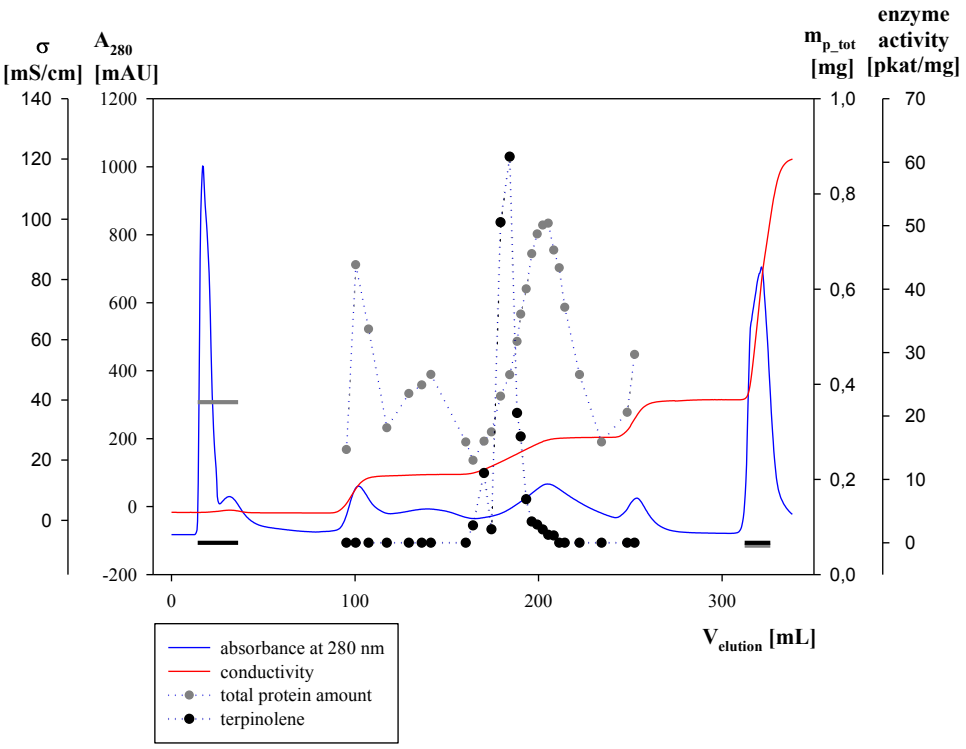

Figure 16: Protein separation and terpinolene synthase activity on DEAE-Sepharose using a step gradient. The IEC was performed with 98 mg protein in 25 mM Tris-HCl, pH 7,5 (binding buffer) at a flow rate of 1 mL/min. Blue line: Inline measured absorbance at 280 nm; red line: Inline measured conductivity. The protein amount was determined offline in triplicates. Enzyme activity was determined offline in a single test and reached a maximum of 60,9 pkat/mg.

Synthase activities for α-terpinene and terpinolene were detected in several fractions starting at a salt concentration of 106 mM KCl and reaching maxima at 161 mM KCl for α-terpinene and 146 mM KCl for terpinolene. Compared to the 15 CV-gradient experiment this approach was less time consuming and comparable to the 5 CV-gradient experiment but with a better peak resolution (Table 10 and Table 11).

Table 10: Purification of α-terpinene synthase activity by IEC from soluble extract obtained from biomass of *C. defragrans*. Integrated peak from F176 to F205.

c_{KCl_calc} [mM]	Purification level	Volume [mL]	Total protein [mg]	Total activity [pkat]	Specific activity [pkat/mg]	Relative specific activity	Protein yield [%]
-	Soluble Extract 8	5	97,8	33,4	0,34	1,0	100,0
	IEC						
123	Fraction 175	1	2,98	0,00	0,00	0,0	3,0
135	Fraction 180	1	0,38	1,30	3,48	10,2	0,4
146	Fraction 185	1	0,42	1,98	4,69	13,7	0,4
156	Fraction 189	1	0,49	1,97	4,01	11,7	0,5
161	Fraction 191	1	0,55	2,87	5,25	15,4	0,6
169	Fraction 194	1	0,60	1,92	3,20	9,4	0,6
178	Fraction 198	1	0,67	1,37	2,03	6,0	0,7
183	Fraction 200	1	0,72	0,91	1,27	3,7	0,7
190	Fraction 203	1	0,73	0,77	1,05	3,1	0,8
194	Fraction 206	1	0,74	0,00	0,00	0,0	0,8
	Integrated peak		16,1	43,9	2,73	8,0	16,4

Table 11: Purification of terpinolene synthase activity by IEC from soluble extract obtained from biomass of *C. defragrans*. Integrated peak from F162 to F210.

c_{KCl_calc} [mM]	Purification level	Volume [mL]	Total protein [mg]	Total activity [pkat]	Specific activity [pkat/mg]	Relative specific activity	Protein yield [%]
-	Soluble Extract 8	5	97,8	12,4	0,13	1,0	100,0
	IEC						
103	Fraction 161	1	0,28	0,00	0,00	0,0	0,3
106	Fraction 165	1	0,24	0,67	2,73	21,5	0,2
115	Fraction 171	1	0,28	3,06	11,0	86,3	0,3
123	Fraction 175	1	2,98	6,33	2,13	16,7	3,0
135	Fraction 180	1	0,38	19,0	50,5	397	0,4
146	Fraction 185	1	0,42	25,6	60,9	478	0,4
156	Fraction 189	1	0,49	10,1	20,5	161	0,5
161	Fraction 191	1	0,55	9,19	16,8	132	0,6
169	Fraction 194	1	0,60	4,12	6,87	54,0	0,6
178	Fraction 198	1	0,67	2,26	3,35	26,3	0,7
183	Fraction 200	1	0,72	2,05	2,86	22,4	0,7
190	Fraction 203	1	0,73	1,54	2,09	16,4	0,8
194	Fraction 206	1	0,74	0,92	1,25	9,8	0,8
197	Fraction 209	1	0,68	0,79	1,16	9,1	0,7
198	Fraction 211	1	0,64	0,00	0,00	0,0	0,7
	Integrated peak		36,1	347	9,61	75,5	36,9

The integrated α-terpinene synthase peak consisted of fractions F176 – F205 and had a total amount of 16,1 mg protein (16,4 % of initial protein) and a total synthase activity of 43,9 pkat, while the integrated terpinolene synthase peak consisted of fractions F162 – F210 and had a total amount of 36,1 mg protein (36,9 % of initial protein) and a total synthase activity of 347 pkat. Total α-terpinene synthase activity did slightly increase from 33,4 to 43,9 pkat and total terpinolene synthase activity did increase from 12,4 to 347 pkat, reflected in the relative specific activities for α-terpinene (8,0 x) and for terpinolene (75,5 x).

The SDS-PAGE gel of active and inactive fractions showed a distribution of individual protein bands over several fractions, with prominent bands at 35 kDa, 60 kDa, 70 kDa, and 100 kDa (Figure 17). This can have one of the aforementioned reasons (section 3.2.2). The

gel revealed, as well as the gels before, the requirement for additional purification steps in order to obtain protein bands assignable to enzyme activity.

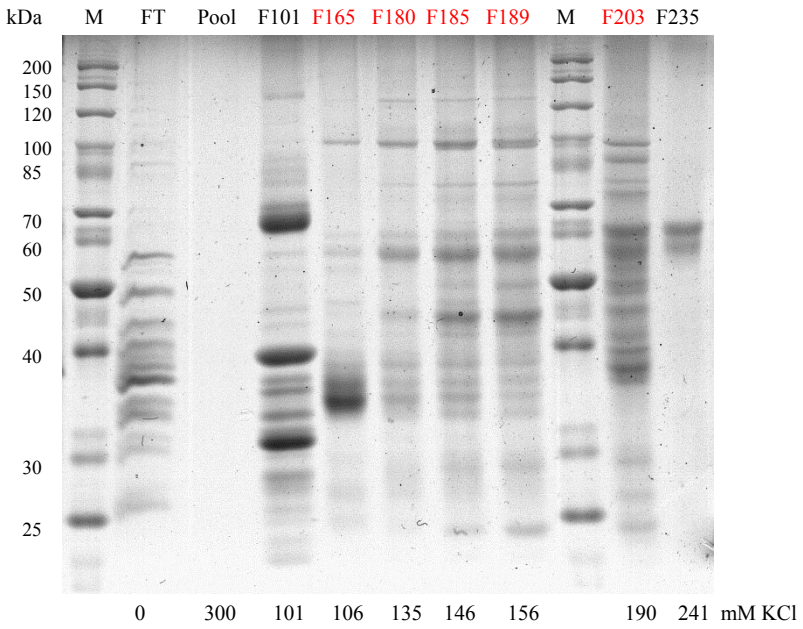

Figure 17: SDS-PAGE of single step IEC fractions with a step gradient. Samples were applied on a polyacrylamide gel with 10 % acrylamide in the separation gel. Electrophoresis was carried out at 70 V for 3 hours. The gel was stained with Coomassie Blue staining solution. (FT) flow-through, inactive and active (red) fractions. At the bottom of the gel the calculated KCl concentration in the fractions is given. FT: F15 – F37; Pool: F316 – F327. F185 is the most active fraction of this chromatographic run.

3.3 Purification by hydrophobic interaction chromatography

A strong binding to hydrophobic columns has been observed for other monoterpene metabolizing enzymes like the LDI [Brodkorb *et al.*, 2010]. To eliminate the possibility of protein precipitation during binding to the Phenyl-Sepharose column due to high salinity in the binding buffer (25 mM Tris-HCl, 500 respectively 100 mM $(NH_4)_2SO_4$, pH 7,5) the stability of the soluble proteins was tested before the chromatographic separation. The soluble extract 3 (Table 5) was mixed with 25 mM Tris-HCl including 5 M $(NH_4)_2SO_4$, pH 7,5 to final concentrations of 250, 500 and 1000 mM $(NH_4)_2SO_4$. After 10 minutes at room temperature no precipitation was observable and the enzyme activity assay did not reveal any activity losses due to high salt concentrations.

Soluble extract was filtered prior to the injection on the HIC column. The enzyme activity was retained on the column followed by a gradual elution of bound protein by applying buffers with decreasing hydrophobicity. Afterwards protein concentration and specific monoterpene synthase activities for α-terpinene and terpinolene were determined.

3.3.1 Hydrophobic interaction chromatography with a 10 column volume gradient and additional elution with water

After addition of 5 mL 25 mM Tris-HCl including 1 M $(NH_4)_2SO_4$, pH 7,5 to 5 mL of soluble extract 3 (Table 5) comprising 91 mg of protein, the sample was loaded onto a 20 mL-Phenyl-Sepharose column. After the unbound protein had been eluted, a linear gradient from 500 mM $(NH_4)_2SO_4$ to 0 mM $(NH_4)_2SO_4$ over 10 CV was applied for protein elution. Afterwards an additional elution with water was performed. Figure 18 shows detected protein and terpinolene synthase activity.

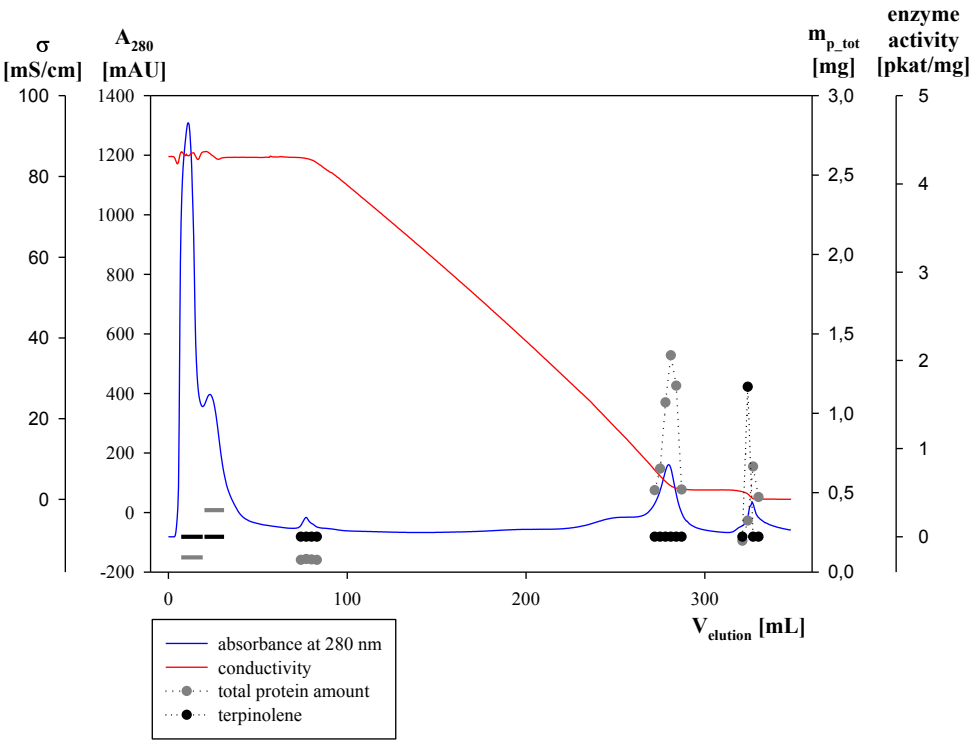

Figure 18: Protein separation and terpinolene synthase activity on Phenyl-Sepharose using a linear gradient from 500 to 0 mM $(NH_4)_2SO_4$ over 10 CV (200 mL) followed by elution with water. The HIC was performed with 91 mg protein in 25 mM Tris-HCl including 500 mM $(NH_4)_2SO_4$, pH 7,5 (binding buffer) at a flow rate of 1 mL/min. Blue line: Inline measured absorbance at 280 nm; red line: Inline measured conductivity. The protein amount was determined offline in triplicates. Enzyme activity was determined offline in a single test and reached a maximum of 1,70 pkat/mg.

α-terpinene synthase activity was not detected at all. Due to this result no purification table is shown. Synthase activity for terpinolene was detected in one fraction during the elution with water. This activity did reach a very low value of 1,70 pkat/mg.

The SDS-PAGE gel of some of the fractions revealed a 55 kDa and a 100 kDa protein band as prominent bands of the active fraction while large bands at 35 kDa and 60 kDa in fraction F279 (Figure 19) do not seem to be responsible for enzyme activity as it might

have been suggested after the SDS-PAGE gels from the IECs (Figure 12, Figure 14 and Figure 17).

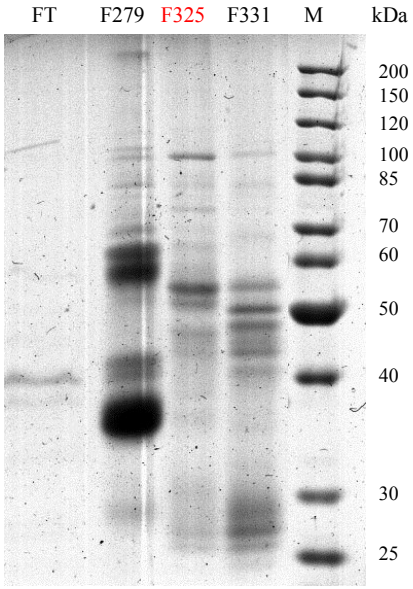

Figure 19: SDS-PAGE of single step HIC fractions with a 10 CV gradient and subsequent elution with water. Samples were applied on a polyacrylamide gel with 10 % acrylamide in the separation gel. Electrophoresis was carried out at 70 V for 3 hours. The gel was stained with Coomassie Blue staining solution. (FT) flow-through, inactive and active (red) fractions. FT: F8 – F20.

3.3.2 Hydrophobic interaction chromatography with a 1 column volume gradient and additional elution with 0,1 % (v/v) Tween 20, water, and ethanol

The result shown in section 3.3.1 led to the suggestion of a strong protein binding to the column due to a high hydrophobicity of the monoterpene synthase. Therefore, another HIC was performed starting with a lower salt concentration in the binding buffer (25 mM Tris-HCl including 100 mM $(NH_4)_2SO_4$, pH 7,5) and additional elution steps with 0,1 % (v/v) Tween 20 in the elution buffer (25 mM Tris-HCl, pH 7,5), water, and ethanol. 4 mL of mixed soluble extract (1 mL soluble extract 1, 2 mL soluble extract 2, 1 mL soluble extract 3 (Table 5)) comprising 58 mg protein were mixed with 0,5 mL 25 mM Tris-HCl including 1 M $(NH_4)_2SO_4$, pH 7,5 to obtain an end concentration of 100 mM $(NH_4)_2SO_4$. After sample application and elution of the unbound protein a linear gradient from 100 mM $(NH_4)_2SO_4$ to 0 mM $(NH_4)_2SO_4$ over 1 CV was applied for protein elution, followed by the aforementioned additional elution steps: 0,1 % (v/v) Tween 20 in 25 mM Tris-HCl, pH 7,5, water, and ethanol. Figure 20 shows detected protein and terpinolene synthase activity.

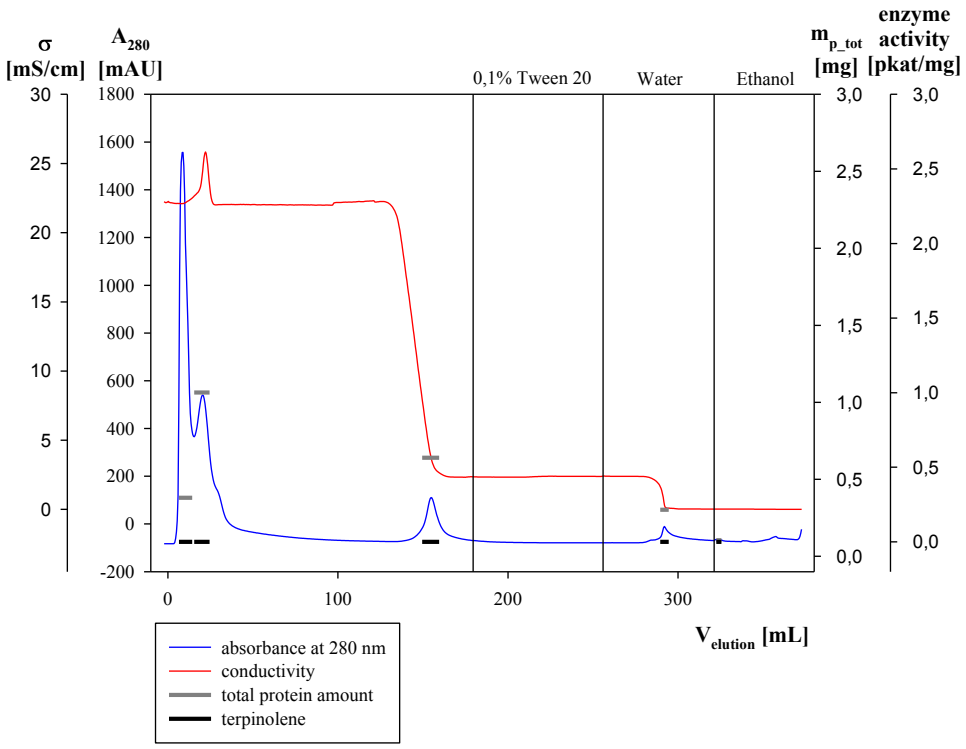

Figure 20: Protein separation and terpinolene synthase activity on Phenyl-Sepharose using a linear gradient from 500 to 0 mM $(NH_4)_2SO_4$ over 10 CV (200 mL) and subsequent elution with 0,1 % (v/v) Tween 20, water, and ethanol. The HIC was performed with 58 mg protein in 25 mM Tris-HCl including 100 mM $(NH_4)_2SO_4$, pH 7,5 (binding buffer) at a flow rate of 1 mL/min. Blue line: Inline measured absorbance at 280 nm; red line: Inline measured conductivity. The protein amount was determined offline in triplicates. Enzyme activity was determined offline in a single test of pooled fractions.

No synthase activity was detected in any of the fractions. The fractions during elution with 0,1 % (v/v) Tween 20 in the elution buffer (25 mM Tris-HCl, pH 7,5) were not tested, because no UV absorbance was detected during this elution step. Due to this result no purification table is shown.

The SDS-PAGE gel of some of the fractions revealed large protein bands at 35 kDa and 60 kDa in pool 2 without any detected specific enzyme activity (Figure 21). This pool was mixed of fractions collected at 0 mM $(NH_4)_2SO_4$ and showed the same protein bands as the 0 mM $(NH_4)_2SO_4$ fraction from the previous HIC (section 3.3.1).

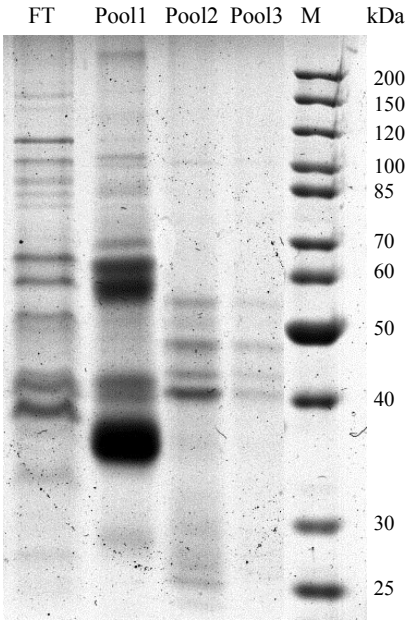

Figure 21: SDS-PAGE of single step HIC fractions with a 1 CV gradient and subsequent elution with 0,1 % (v/v) Tween 20, water, and ethanol. Samples were applied on a polyacrylamide gel with 10 % acrylamide in the separation gel. Electrophoresis was carried out at 70 V for 3 hours. The gel was stained with Coomassie Blue staining solution. (FT) flow-through and three inactive pools. FT: F8 – F15; Pool1: F151 – F161; Pool2: F291 – F296; Pool3: F324 – F327.

3.4 Purification by size exclusion chromatography

The enzyme activities were size fractionated on a Superdex 75 column. This method allows a size determination of the eluted monoterpene synthase. In a single step approach, soluble extract was loaded onto the column followed by elution in one chromatographic run. Afterwards protein concentration and specific monoterpene synthase activities for α-terpinene and terpinolene were determined.

3 mL of soluble extract 1 (Table 5) in binding buffer (25 mM Tris-HCl including 100 mM KCl, pH 7,5) comprising 39 mg of protein were loaded onto the column and eluted within 120 mL. Figure 22 and Figure 23 show detected protein, α-terpinene and terpinolene synthase activities, respectively.

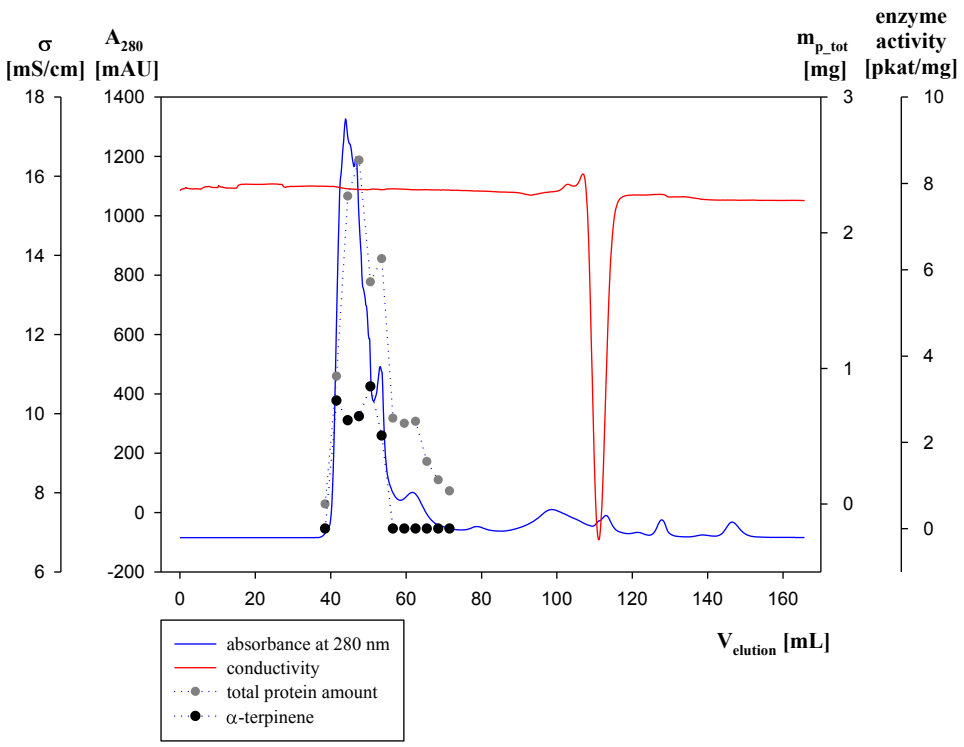

Figure 22: Protein separation and α-terpinene synthase activity on Superdex 75. The SEC was performed with 39 mg protein in 25 mM Tris-HCl including 100 mM KCl, pH 7,5 (running buffer) at a flow rate of 0,5 mL/min. Blue line: Inline measured absorbance at 280 nm; red line: Inline measured conductivity. The protein amount was determined offline in triplicates. Enzyme activity was determined offline in a single test and reached a maximum of 3,30 pkat/mg at an elution volume of 51 mL.

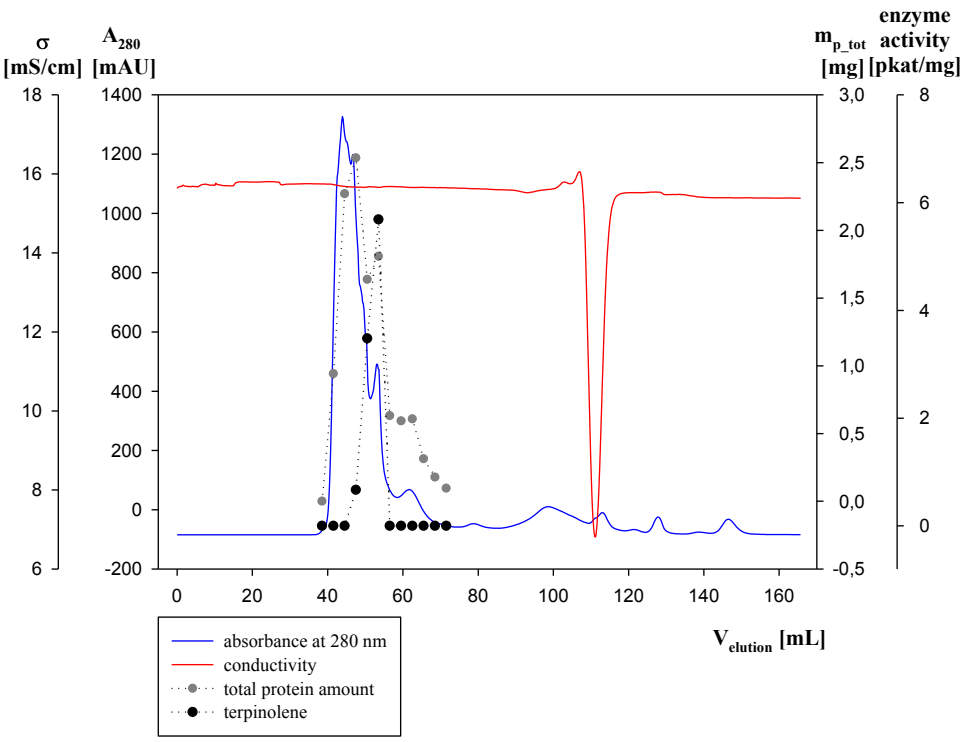

Figure 23: Protein separation and terpinolene synthase activity on Superdex 75. The SEC was performed with 39 mg protein in 25 mM Tris-HCl including 100 mM KCl, pH 7,5 (running buffer) at a flow rate of 0,5 mL/min. Blue line: Inline measured absorbance at 280 nm; red line: Inline measured conductivity. The protein amount was determined offline in triplicates. Enzyme activity was determined offline in a single test and reached a maximum of 5,69 pkat/mg at an elution volume of 53 mL.

Synthase activity for α-terpinene and terpinolene was detected in several fractions with maxima in fraction F51 for α-terpinene and fraction F53 for terpinolene. The values of the specific enzyme activity are comparable for both. For α-terpinene the maximum was 3,30 pkat/mg while the terpinolene synthase had a maximum of 5,69 pkat/mg (Table 12 and Table 13).

Table 12: Purification of α-terpinene synthase activity by SEC from soluble extract obtained from biomass of *C. defragrans*. Integrated peak from F40 to F56.

Purification level	Volume [mL]	Total protein [mg]	Total activity [pkat]	Specific activity [pkat/mg]	Relative specific activity	Protein yield [%]
Soluble Extract 1	3	38,9	22,8	0,59	1,0	100,0
SEC						
Fraction 39	1	0,00	0,00	0,00	0,0	0,0
Fraction 42	1	0,94	2,80	2,97	5,1	2,4
Fraction 45	1	2,27	5,70	2,51	4,3	5,8
Fraction 48	1	2,53	6,60	2,60	4,4	6,5
Fraction 51	1	1,64	5,40	3,30	5,6	4,2
Fraction 54	1	1,81	3,90	2,16	3,7	4,7
Fraction 57	1	0,63	0,00	0,00	0,0	1,6
Integrated peak		28,0	73,2	2,61	4,5	72,1

Table 13: Purification of terpinolene synthase activity by SEC from soluble extract obtained from biomass of *C. defragrans*. Integrated peak from F46 to F56.

Purification level	Volume [mL]	Total protein [mg]	Total activity [pkat]	Specific activity [pkat/mg]	Relative specific activity	Protein yield [%]
Soluble Extract 1	3	38,9	25,7	0,66	1,0	100,0
SEC						
Fraction 45	1	2,27	0,00	0,00	0,0	5,8
Fraction 48	1	2,53	1,70	0,67	1,0	6,5
Fraction 51	1	1,64	5,70	3,48	5,3	4,2
Fraction 54	1	1,81	10,3	5,69	8,6	4,7
Fraction 57	1	0,63	0,00	0,00	0,0	1,6
Integrated peak		20,6	53,1	2,57	3,9	53,1

The α-terpinene synthase integrated peak consisted of fractions F40 – F56 and had a total amount of 28,0 mg protein (72,1 % of initial protein) and a total synthase activity of 73,2 pkat, while the integrated terpinolene synthase peak consisted of fractions F46 – F56 and had a total amount of 20,6 mg protein (53,1 % of initial protein) and a total synthase activity of 53,1 pkat. Total α-terpinene synthase activity increased from 22,8 to 73,2 pkat and total terpinolene synthase activity increased from 25,7 to 53,1 pkat. This is also reflected in the relative specific activities for α-terpinene (4,5 x) and for terpinolene (3,9 x).

The SDS-PAGE gel of active and inactive fractions showed again the distinct protein bands at 35 kDa, 55 kDa and 60 kDa (Figure 24). The protein band pattern of the two fractions F45 and F48 appeared very much alike although fraction F45 had only α-terpinene synthase activity while fraction F48 had a synthase activity for both α-terpinene and terpinolene.

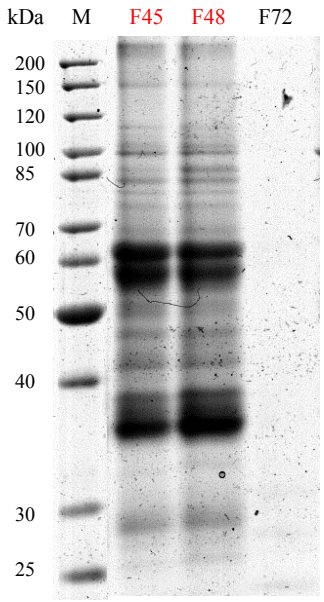

Figure 24: SDS-PAGE of single step SEC fractions. Samples were applied on a polyacrylamide gel with 10 % acrylamide in the separation gel. Electrophoresis was carried out at 70 V for 3 hours. The gel was stained with Coomassie Blue staining solution. Inactive and active (red) fractions.

3.5 Purification by anion exchange chromatography followed by hydrophobic interaction chromatography

IEC and HIC were combined to increase protein purification. 7 mL soluble extract 6 (Table 5) comprising 133 mg of protein were diluted with 3,5 mL of binding buffer (25 mM Tris-HCl, pH 7,5). The linear KCl gradient from 0 mM KCl to 300 mM KCl was performed over 15 CV (Figure 25). The most active fractions F293 – F297 (126 mM KCl – 129 mM KCl) were mixed and 3,5 mL comprising 1,68 mg of protein were loaded onto the HIC column. After the unbound protein had been eluted a linear gradient from 100 mM $(NH_4)_2SO_4$ to 0 mM $(NH_4)_2SO_4$ over 1 CV was applied for protein elution. Afterwards an additional elution with water was performed (Figure 26).

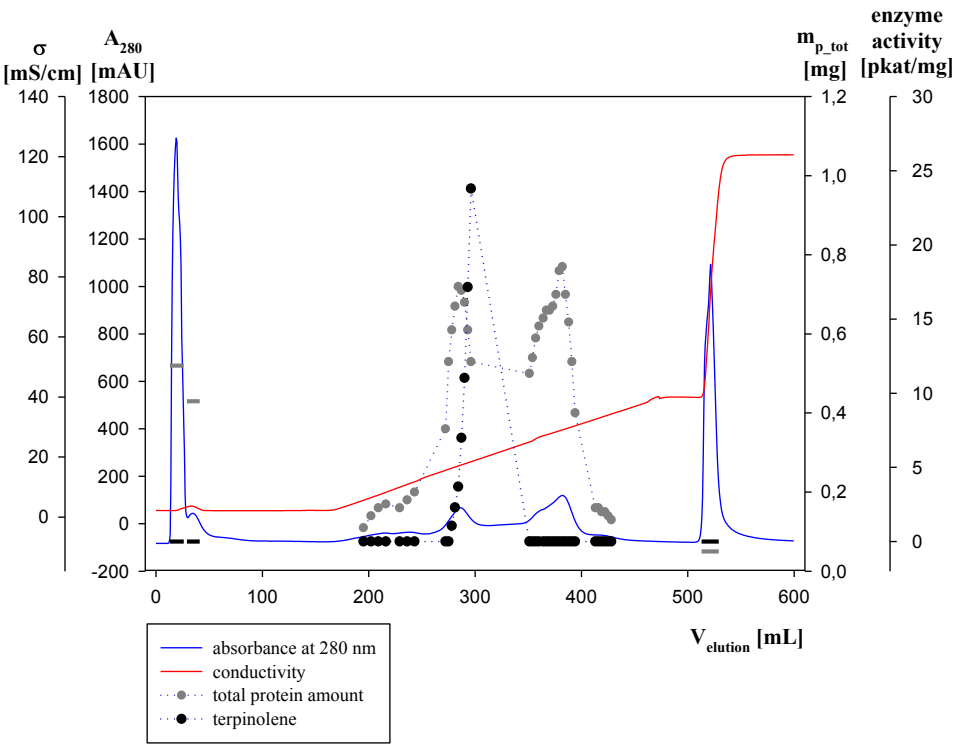

Figure 25: Protein separation and terpinolene synthase activity on DEAE-Sepharose using a linear gradient from 0 to 300 mL KCl over 15 CV (300 mL). The IEC was performed with 133 mg protein in 25 mM Tris-HCl, pH 7,5 (binding buffer) at a flow rate of 1 mL/min. Flow rate during gradient elution: 0,3 mL/min. Blue line: Inline measured absorbance at 280 nm; red line: Inline measured conductivity. The protein amount was determined offline in triplicates. Enzyme activity was determined offline in a single test and reached a maximum of 23,8 pkat/mg.

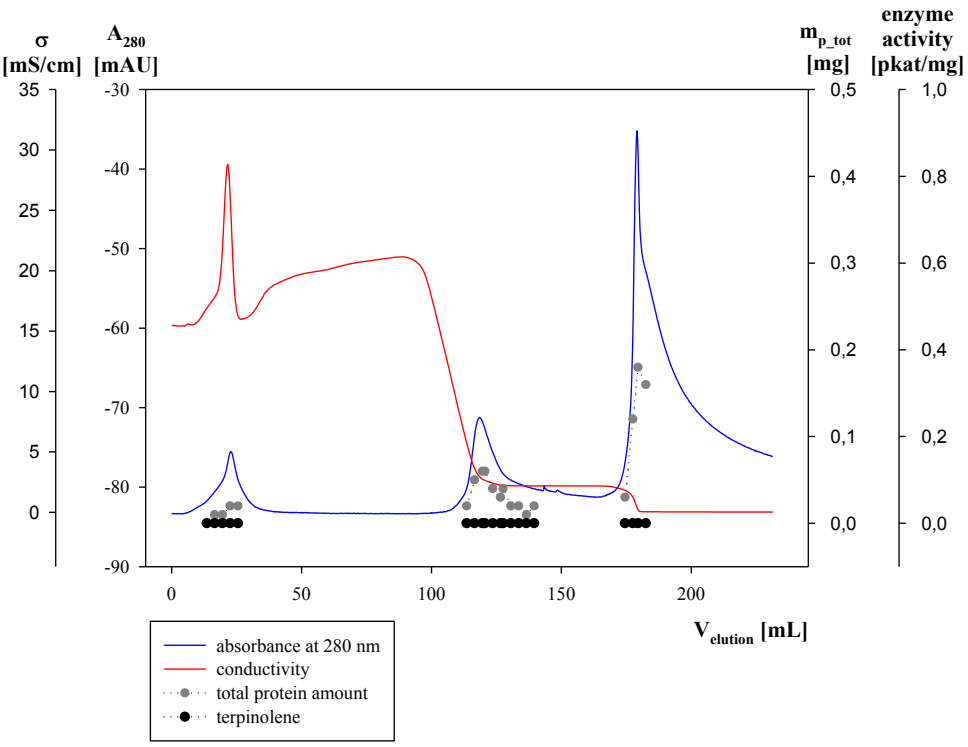

Figure 26: Protein separation and terpinolene synthase activity on Phenyl-Sepharose using a linear gradient from 500 to 0 mM $(NH_4)_2SO_4$ over 10 CV (200 mL) followed by elution with water. The HIC was performed with 1,68 mg protein in 25 mM Tris-HCl including 100 mM $(NH_4)_2SO_4$, pH 7,5 (binding buffer) at a flow rate of 1 mL/min. Blue line: Inline measured absorbance at 280 nm; red line: Inline measured conductivity. The protein amount was determined offline in triplicates. Enzyme activity was determined offline in a single test.

No enzyme activity was detected in the HIC fractions. The increase in conductivity at the beginning of the HIC is caused by the KCl concentration in the mixed fractions from the IEC. Protein concentrations between 0,00 and 0,16 mg/mL were determined in the HIC fractions (Table 14 and Table 15).

Table 14: Purification of α-terpinene synthase activity by a multiple step purification with IEC and HIC from soluble extract obtained from biomass of *C. defragrans*.

Purification level	Volume [mL]	Total protein [mg]	Total activity [pkat]	Specific activity [pkat/mg]	Relative specific activity	Protein yield [%]
Soluble Extract 6	7	133	23,8	0,18	1,0	100,0
IEC						
Pool (Fraction 293 - 297)	3,5	1,68	0,00	0,00	0,0	1,3
HIC						
Fraction 14 - 184	1 each	0,00 - 0,16	0,00	0,00	0,0	0,7

Table 15: Purification of terpinolene synthase activity by a multiple step purification with IEC and HIC from soluble extract obtained from biomass of *C. defragrans*.

Purification level	Volume [mL]	Total protein [mg]	Total activity [pkat]	Specific activity [pkat/mg]	Relative specific activity	Protein yield [%]
Soluble Extract 6	7	133	1,05	0,01	1,0	100,0
IEC						
Pool (Fraction 293 - 297)	3,5	1,68	0,63	0,38	48,0	1,3
HIC						
Fraction 14 - 184	1 each	0,00 - 0,16	0,00	0,00	0,0	0,7

Although both enzyme activities were detected in soluble extract (23,8 pkat for α-terpinene and 1,05 pkat for terpinolene) only terpinolene synthase activity was detected in IEC fractions with 0,63 pkat and no enzyme activity was detected in the subsequent purification.

The SDS-PAGE gel of active and inactive fractions showed the protein bands of the soluble extract, the pool of the IEC applied onto HIC column as well as some of the inactive fractions of the HIC (Figure 27). In the active pool prominent bands at 35 kDa, 55 kDa and 100 kDa are visible, while in the inactive HIC fractions no clear bands are observable.

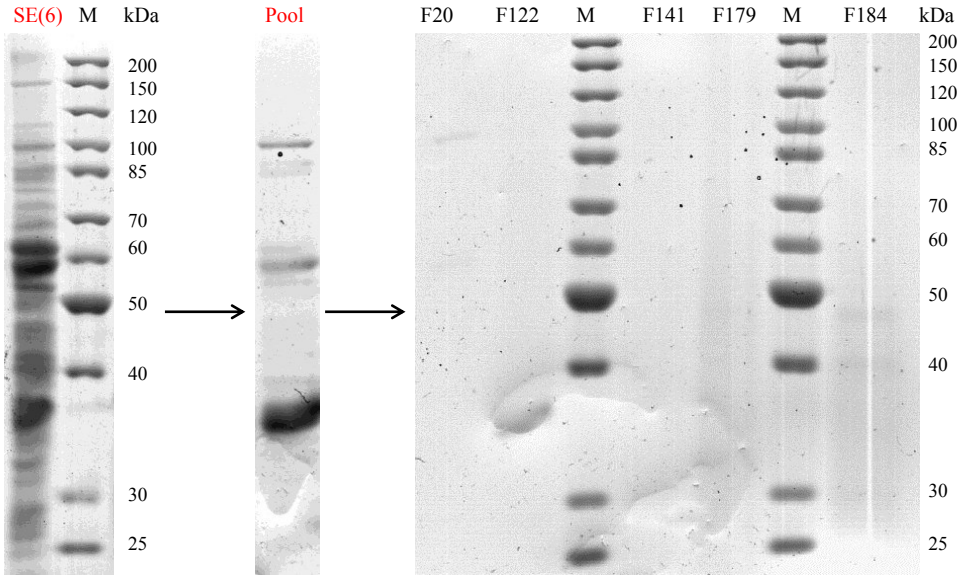

Figure 27: SDS-PAGE of two step purification fractions after IEC and HIC. Samples were applied on polyacrylamide gels with 10 % acrylamide in the separation gel. Electrophoresis was carried out at 70 V for 3 hours. The gels were stained with Coomassie Blue staining solution. Soluble extract (SE), the active (red) IEC pool and some HIC fractions. Pool: F293 – F297.

3.6 Purification by anion exchange chromatography followed by size exclusion chromatography

A combination of IEC and SEC was tested for the purification. 9 mL soluble extract 9 (Table 5) comprising 205 mg of protein were diluted with 4,5 mL of binding buffer (25 mM Tris-HCl, pH 7,5). The linear KCl gradient from 0 mM KCl to 300 mM KCl was performed over 15 CV (Figure 28 and Figure 29). The most active fractions of the flanking regions of the peak (F283 – F287 and F295 – F298 eluting at salt concentrations of 130 mM KCl – 134 mM KCl and 141 mM KCl – 144 mM KCl) were mixed, concentrated with an Amicon filter unit from 5 mL to 0,5 mL, and 0,8 mL comprising 1,89 mg of protein were loaded onto the SEC column. At this time, the SEC column contained a buffer with a higher ionic strength (Figure 30).

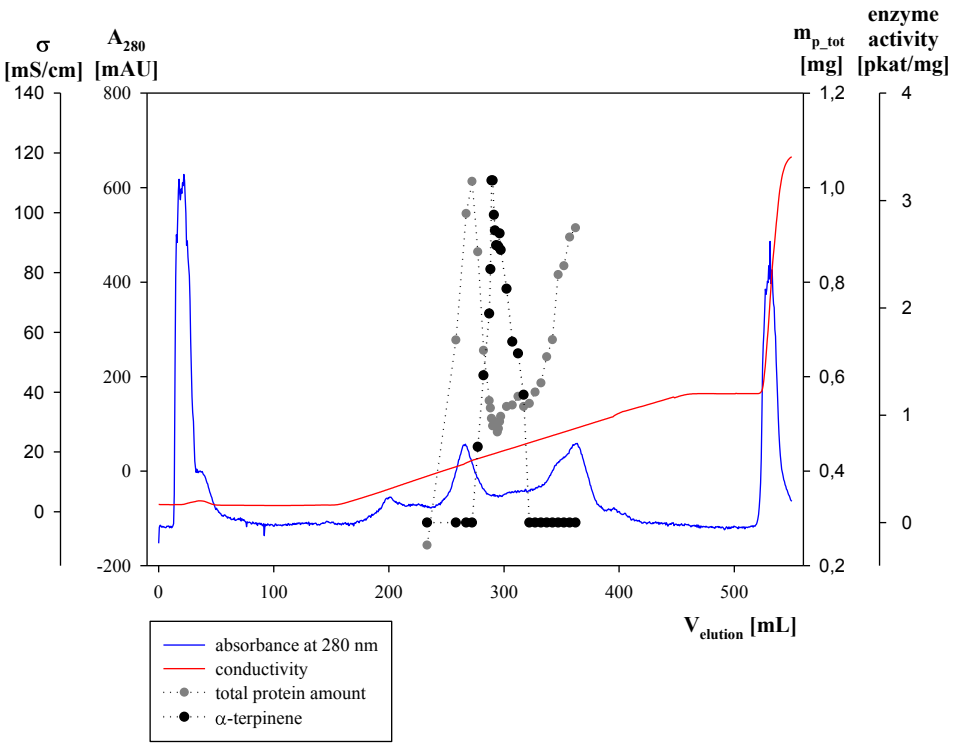

Figure 28: Protein separation and α-terpinene synthase activity on DEAE-Sepharose using a linear gradient from 0 to 300 mL KCl over 15 CV (300 mL). The IEC was performed with 205 mg protein in 25 mM Tris-HCl, pH 7,5 (binding buffer) at a flow rate of 1 mL/min. Flow rate during gradient elution: 0,36 mL/min. Blue line: Inline measured absorbance at 280 nm; red line: Inline measured conductivity. The protein amount was determined offline in triplicates. Enzyme activity was determined offline in a single test and reached a maximum of 3,19 pkat/mg.

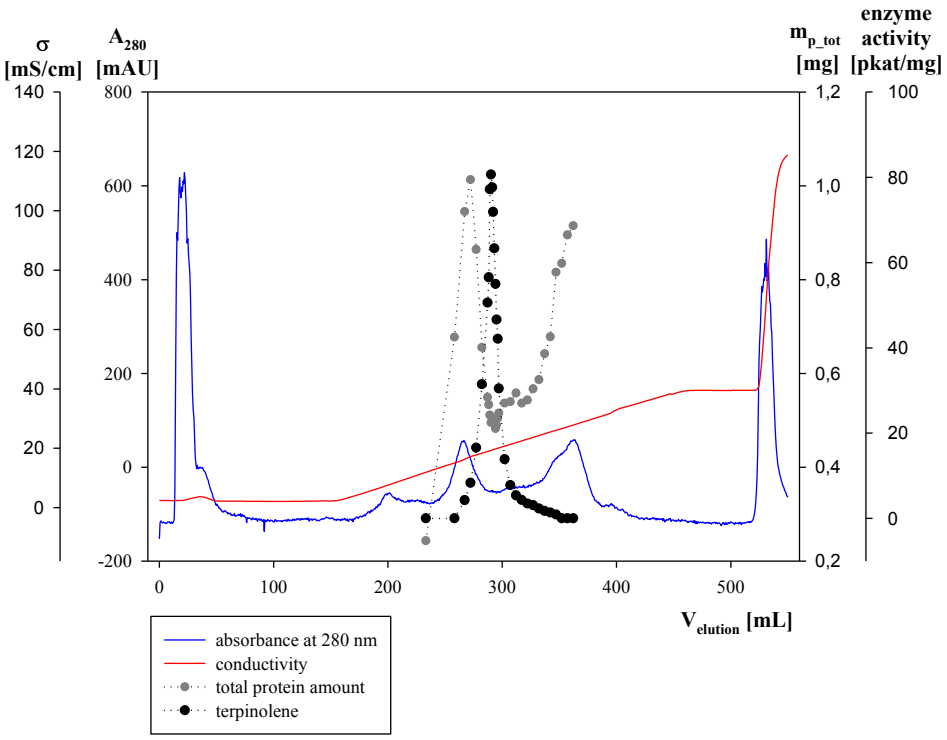

Figure 29: Protein separation and terpinolene synthase activity on DEAE-Sepharose using a linear gradient from 0 to 300 mL KCl over 15 CV (300 mL). The IEC was performed with 205 mg protein in 25 mM Tris-HCl, pH 7,5 (binding buffer) at a flow rate of 1 mL/min. Flow rate during gradient elution: 0,36 mL/min. Blue line: Inline measured absorbance at 280 nm; red line: Inline measured conductivity. The protein amount was determined offline in triplicates. Enzyme activity was determined offline in a single test and reached a maximum of 80,7 pkat/mg.

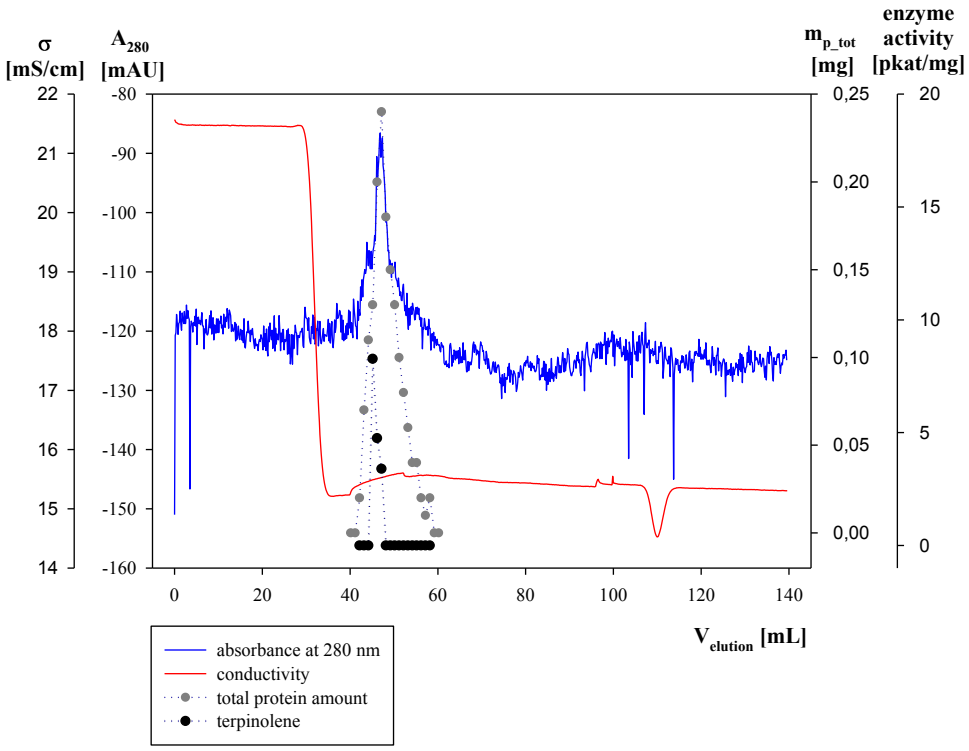

Figure 30: Protein separation and terpinolene synthase activity on Superdex 75. The SEC was performed with 1,89 mg protein in 25 mM Tris-HCl including 100 mM KCl, pH 7,5 (running buffer) at a flow rate of 0,5 mL/min. Due to a failure of the UV detector the obtained absorbance signal (blue) is noisy. A dropdown of the conductivity (red) at an elution volume of around 35 mL is due to an insufficient equilibration. The protein amount was determined offline in triplicates. Enzyme activity was determined offline in a single test and reached a maximum of 8,27 pkat/mg at an elution volume of 45 mL.

Although α-terpinene synthase activity was found in the pooled IEC fractions no α-terpinene activity was detected in SEC fractions. Nevertheless, terpinolene synthase activity was found in the fractions F46 – F48 with a maximum in fraction F46 (Table 16 and Table 17). The elution volume of this fraction is 45 mL and thus differs from the elution volume of terpinolene synthase activity during the first SEC (53 mL).

Table 16: Purification of α-terpinene synthase activity by a multiple step purification with IEC and SEC from soluble extract obtained from biomass of *C. defragrans*.

Purification level	Volume [mL]	Total protein [mg]	Total activity [pkat]	Specific activity [pkat/mg]	Relative specific activity	Protein yield [%]
Soluble Extract 9	9	205	34,8	0,17	1,0	100,0
IEC						
Pool (Fraction 283 - 287, 295 - 298, conc.)	0,8	1,89	0,58	0,31	1,8	0,9
SEC						
Fraction 43 - 59	1 each	0,01 - 0,24	0,00	0,00	0,0	0,8

Table 17: Purification of terpinolene synthase activity by a multiple step purification with IEC and SEC from soluble extract obtained from biomass of *C. defragrans*. Integrated peak from F46 to F48.

Purification level	Volume [mL]	Total protein [mg]	Total activity [pkat]	Specific activity [pkat/mg]	Relative specific activity	Protein yield [%]
Soluble Extract 9	9	205	18,1	0,09	1,0	100,0
IEC						
Pool (Fraction 283 - 287, 295 - 298, conc.)	0,8	1,89	19,6	10,4	118	0,9
SEC						
Fraction 45	1	0,11	0,00	0,00	0,0	0,1
Fraction 46	1	0,13	1,07	8,27	94,1	0,1
Fraction 47	1	0,20	0,94	4,75	54,0	0,1
Fraction 48	1	0,24	0,80	3,40	38,6	0,1
Fraction 49	1	0,18	0,00	0,00	0,0	0,1
Integrated peak		0,56	2,81	5,00	56,8	0,3

The integrated SEC peak consisted of fractions F46 – F48 and had a total amount of 0,56 mg protein (0,3 % of initial protein) and a total terpinolene synthase activity of 2,81 pkat. Total terpinolene synthase activity did increase from 18,1 pkat in the soluble extract to 19,6 pkat in the IEC pool. It decreased to 2,81 pkat during the subsequent SEC. This is also reflected in the relative specific activities for terpinolene (124 x after IEC and 56,8 x after SEC).

The SDS-PAGE gel of active and inactive fractions showed the protein bands of the soluble extract, the pool of the IEC applied onto the SEC column as well as some of the SEC fractions (Figure 31). There were many protein bands visible in the IEC pool, while the SEC fractions contained only some single bands. In the active fractions protein bands at around 35 kDa, 55 kDa and 60 kDa are observable. Nevertheless, these bands were also observed in several fractions without activity.

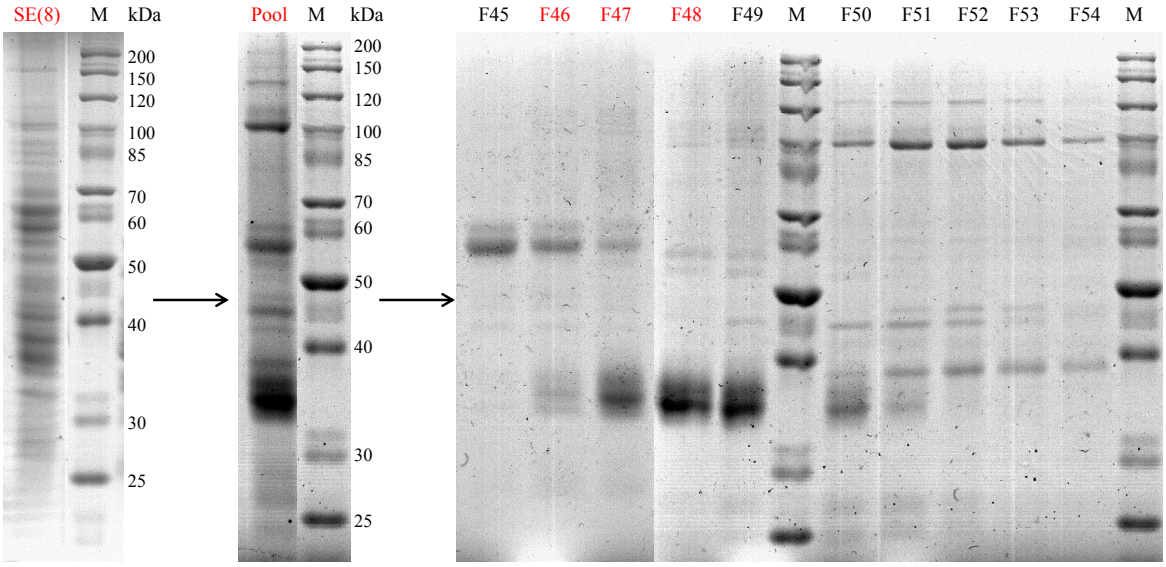

Figure 31: SDS-PAGE of two step purification fractions after IEC and SEC. Samples were applied on polyacrylamide gels with 10 % acrylamide in the separation gel. Electrophoresis was carried out at 70 V for 3 hours. The gels were stained with Coomassie Blue staining solution. Soluble extract (SE), the active (red) pool obtained from fractions of the IEC and inactive and active SEC fractions. Pool: F283 – F287 and F295 – F298. F46 is the most active fraction of this chromatographic run.

In a second experiment, active fractions obtained from another DEAE-IEC were mixed, concentrated with an Amicon filter unit from 15 mL to 1,2 mL, and loaded onto the SEC column. This procedure was performed with two of the UV peaks of the DEAE-IEC leading to the following result graphs which reveal a more typical chromatogram for a SEC (Figure 32).

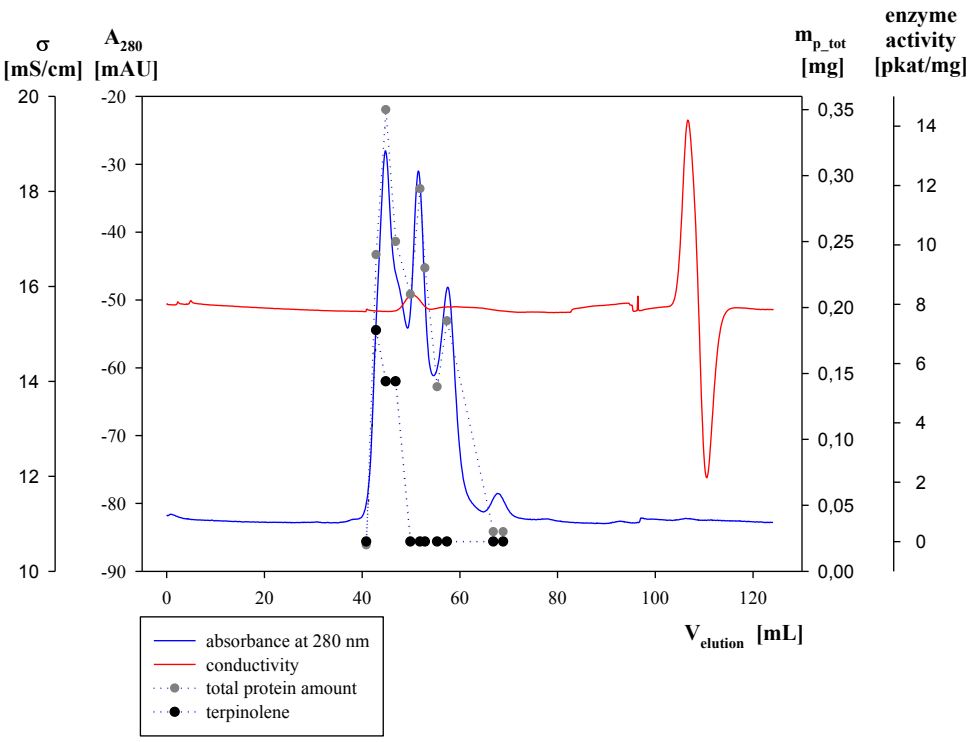

Figure 32: Protein separation and terpinolene synthase activity on Superdex 75. The SEC was performed with 6,15 mg protein in 25 mM Tris-HCl including 100 mM KCl, pH 7,5 (running buffer) at a flow rate of 0,5 mL/min. Blue line: Inline measured absorbance at 280 nm; red line: Inline measured conductivity. The protein amount was determined offline in triplicates. Enzyme activity was determined offline in a single test and reached a maximum of 7,13 pkat/mg at an elution volume of 43 mL.

α-terpinene formation was not detected during SEC. Terpinolene synthase activity was found in the first peak detected by UV absorbance (Table 18). The elution volume of the fraction with terpinolene synthase activity is 43 mL and is by this similar to the elution volume of terpinolene synthase activity during the SEC shown before (45 mL) and further away from the elution volume during the single SEC purification (53 mL).

Table 18: Purification of terpinolene synthase activity by a multiple step purification with IEC and SEC from soluble extract obtained from biomass of *C. defragrans*. Integrated peak from F43 to F49.

Purification level	Volume [mL]	Total protein [mg]	Total activity [pkat]	Specific activity [pkat/mg]	Relative specific activity	Protein yield [%]
Soluble Extract 4	6	117	86,0	0,73	1,0	100,0
IEC						
Pool (Fraction 181 - 199, conc.)	1,2	6,15	6,12	1,00	1,4	5,3
SEC						
Fraction 42	1	0,02	0,00	0,00	0,0	0,0
Fraction 44	1	0,24	1,71	7,13	9,7	0,2
Fraction 46	1	0,35	1,89	5,40	7,3	0,3
Fraction 48	1	0,25	1,35	5,40	7,3	0,2
Fraction 51	1	0,21	0,00	0,00	0,0	0,2
Integrated peak		1,80	9,90	5,52	7,5	1,5

The integrated SEC peak consisted of fractions F43 – F49 and had a total amount of 1,80 mg protein (1,5 % of initial protein) and a total terpinolene synthase activity of 9,90 pkat. Total terpinolene synthase activity did decrease from 86,0 pkat in the soluble extract to 6,12 pkat in the IEC pool. It increased to 9,90 pkat during the subsequent SEC. This is also reflected in the relative specific activities for terpinolene (1,4 x after IEC and 7,5 x after SEC).

The SDS-PAGE gel of active and inactive fractions showed the protein bands of the soluble extract, the pool of the IEC that was loaded onto the SEC column as well as some of the SEC fractions (Figure 33). The SEC fractions contained only some single bands.

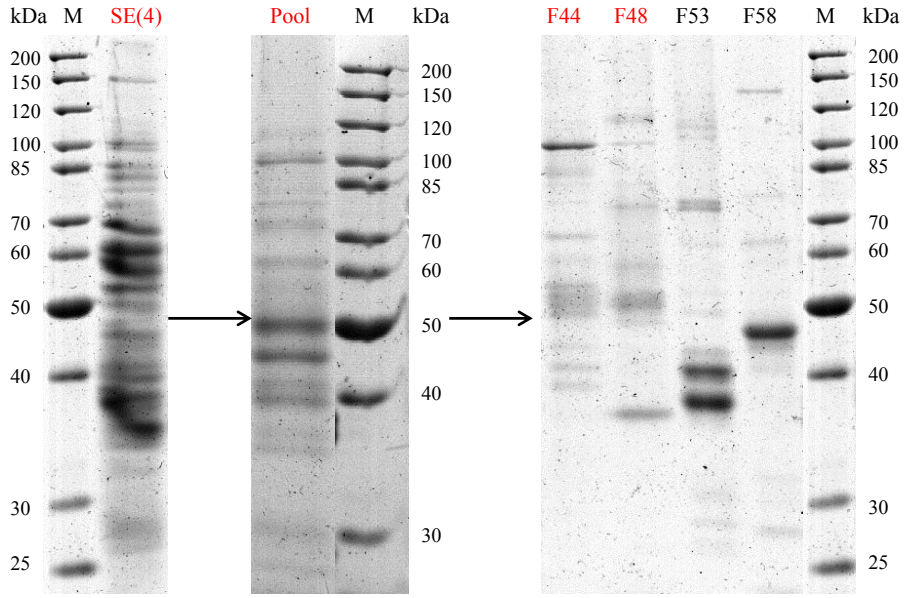

Figure 33: SDS-PAGE of two step purification fractions after IEC and SEC. Samples were applied on polyacrylamide gels with 10 % acrylamide in the separation gel. Electrophoresis was carried out at 70 V for 3 hours. The gels were stained with Coomassie Blue staining solution. Soluble extract (SE), the active (red) pool obtained from fractions of the IEC and inactive and active SEC fractions. Pool: F181 – F191. F44 is the most active fraction of this chromatographic run.

IEC peak two detected by UV absorbance was pooled, concentrated with an Amicon filter unit from 10 mL to 1,2 mL and loaded onto the SEC as well, leading to another chromatogram (Figure 34).

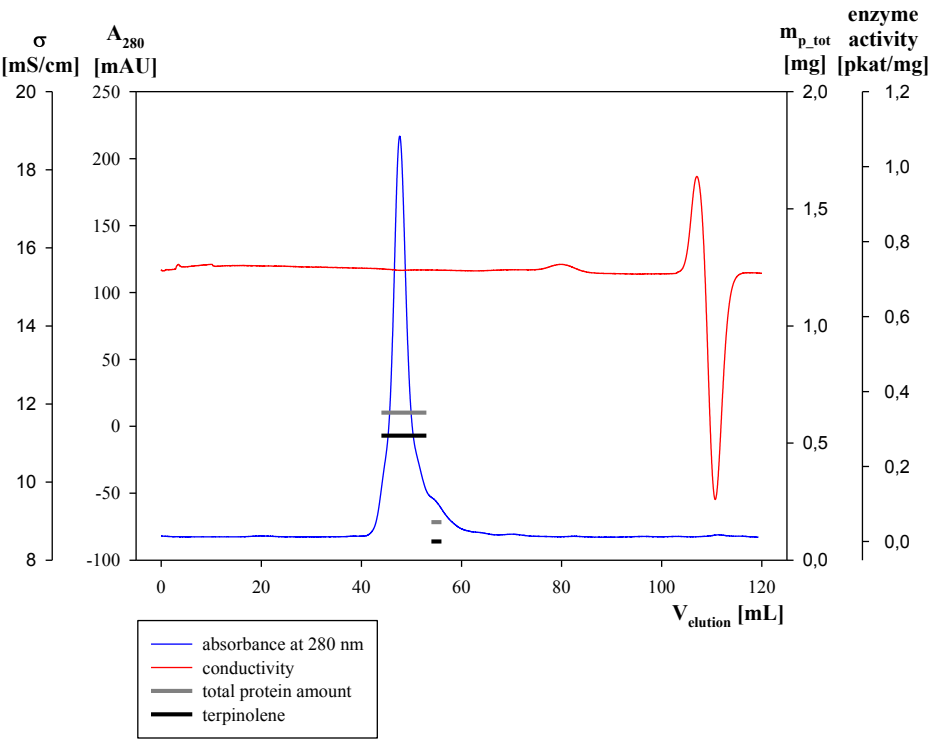

Figure 34: Protein separation and terpinolene synthase activity on Superdex 75. The SEC was performed with 12,7 mg protein in 25 mM Tris-HCl including 100 mM KCl, pH 7,5 (running buffer) at a flow rate of 0,5 mL/min. Blue line: Inline measured absorbance at 280 nm; red line: Inline measured conductivity. The protein amount was determined offline in triplicates. Enzyme activity was determined offline in a single test and reached a maximum of 0,28 pkat/mg at an elution volume of 44 mL.

SEC fractions contained only terpinolene synthase activity. Fractions were combined in two pools. The first and active pool started at an elution volume of 44 mL which is comparable to the elution volumes of terpinolene synthase activity observed in other two-step purifications (43 mL, 45 mL). The relative specific activity of 0,4 fold purification from this IEC SEC combination (Table 19) is below the relative specific activity of 7,5 fold purification from the IEC SEC combination shown before (Table 18). The highest relative specific activity of 56,8 fold purification was obtained in the IEC SEC combination shown first (Table 17).

Table 19: Purification of terpinolene synthase activity by a multiple step purification with IEC and SEC from soluble extract obtained from biomass of *C. defragrans*. 1.Pool of the SEC is composed of fractions F45 – F54 and 2.Pool is composed of fractions F55 – F57 (see Figure 34). Integrated peak from F45 to F57.

Purification level	Volume [mL]	Total protein [mg]	Total activity [pkat]	Specific activity [pkat/mg]	Relative specific activity	Protein yield [%]
Soluble Extract 4	6	117	86,0	0,73	1,00	100,0
IEC						
Pool (Fraction 142 - 154, conc.)	1,2	12,7	23,0	1,81	2,5	10,9
SEC						
1.Pool	10	6,30	1,78	0,28	0,4	5,4
2.Pool	3	0,48	0,00	0,00	0,0	0,4
Integrated peak		6,78	1,78	0,26	0,4	5,8

The integrated SEC peak consisted of two pools with fractions F45 – F57 and had a total amount of 6,78 mg protein (5,8 % of initial protein) and a total terpinolene synthase activity of 1,78 pkat. The total activity did decrease from 86,0 pkat in the soluble extract to 23,0 pkat in the IEC pool. It decreased further to 1,78 pkat during the subsequent SEC. This is also reflected in the relative specific activities for terpinolene (2,5 x after IEC and 0,4 x after SEC).

The SDS-PAGE gel of active and inactive fractions showed protein bands of the soluble extract, one IEC fraction applied onto the SEC column as well as both SEC pools (Figure 35). Many protein bands were visible in the IEC fraction, while in the SEC fraction only some protein bands were detected. Although the SDS-PAGE gel of the SEC looks rather blurry, there is a distinct protein band at around 35 kDa visible in the active pool. Nevertheless, this protein band was not visible in active fractions of other separations.

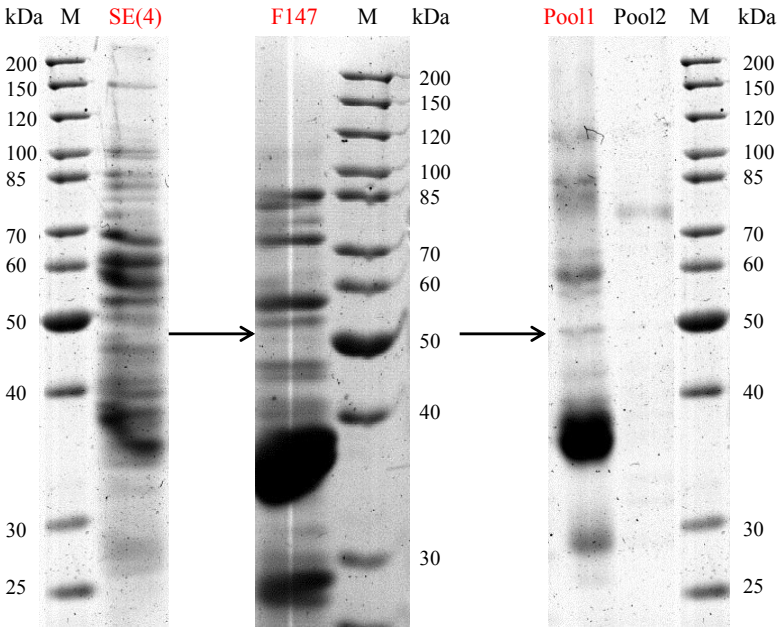

Figure 35: SDS-PAGE of two step purification fractions after IEC and SEC. Samples were applied on polyacrylamide gels with 10 % acrylamide in the separation gel. Electrophoresis was carried out at 70 V for 3 hours. The gels were stained with Coomassie Blue staining solution. Soluble extract (SE), one active (red) fraction of the IEC pool and the inactive and active SEC pools. Pool: F142 – F154; Pool1: F45 – F55; Pool2: F55 – F58.

3.7 Purification by anion exchange chromatography at pH 7,5 followed by anion exchange chromatography at pH 8,0

IEC at pH 7,5 was combined with IEC at pH 8,0. By a shift of the pH to 8,0 more negative charges on the surface of the protein are induced. With this approach, proteins forming supramolecular complexes might repel each other leading to a better separation of the involved proteins. Due to the increased negative net charge of the proteins the elution of the column might be shifted to higher KCl concentrations.

9 mL soluble extract 9 (Table 5) comprising 205 mg of protein were diluted with 4,5 mL of binding buffer (25 mM Tris-HCl, pH 7,5). A linear KCl gradient from 0 mM KCl to 300 mM KCl was performed over 15 CV (see Appendix A, Figure 52 and Figure 53). The flanking region fractions of the activity peak (F267 – F268 and F274 – F276 eluting at salt concentrations of 133 mM KCl – 134 mM KCl and 140 mM KCl – 142 mM KCl) were mixed obtaining 1,8 mL comprising 0,94 mg of protein. 0,18 mL of 100 mM Tris-base were added in order to obtain a pH of 8,0. Afterwards 15 mL binding buffer (25 mM Tris-HCl, pH 8,0) were added to dilute the sample, before it was subsequently loaded onto the IEC column. A linear KCl gradient from 0 mM KCl to 500 mM KCl was performed over 15 CV (see Appendix A, Figure 54).

Although α-terpinene as well as terpinolene synthase activities were found in the IEC pool loaded onto the second IEC, no enzyme activity was found in any of the fractions examined after the IEC at pH 8,0 (Table 20 and Table 21). Consequently, this purification approach was not further used.

Table 20: Purification of α-terpinene synthase activity by a multiple step purification with IEC at pH 7,5 and IEC at pH 8,0 from soluble extract obtained from biomass of *C. defragrans*.

Purification level	Volume [mL]	Total protein [mg]	Total activity [pkat]	Specific activity [pkat/mg]	Relative specific activity	Protein yield [%]
Soluble Extract 9	9	205	34,8	0,17	1,0	100,0
IEC pH 7,5						
Pool (Fraction 267, 268, 274 - 276)	1,8	0,94	0,61	0,65	3,9	0,5
IEC pH 8						
Fraction 255 - 504	1 each	0,00 - 0,17	0,00	0,00	0,0	0,1

Table 21: Purification of terpinolene synthase activity by a multiple step purification with IEC at pH 7,5 and IEC at pH 8,0 from soluble extract obtained from biomass of *C. defragrans*.

Purification level	Volume [mL]	Total protein [mg]	Total activity [pkat]	Specific activity [pkat/mg]	Relative specific activity	Protein yield [%]
Soluble Extract 9	9	205	18,1	0,09	1,0	100,0
IEC pH 7,5						
Pool (Fraction 267, 268, 274 - 276)	1,8	0,94	19,0	20,3	230	0,5
IEC pH 8						
Fraction 255 - 504	1 each	0,00 - 0,17	0,00	0,00	0,0	0,1

3.8 Purification by anion exchange chromatography using a weak anion exchanger followed by a strong anion exchanger

IEC with the weak anion exchanger DEAE-Sepharose was combined with IEC with the strong anion exchanger Resource-Q.

9 mL soluble extract 9 (Table 5) comprising 205 mg of protein were diluted with 4,5 mL of binding buffer (25 mM Tris-HCl, pH 7,5). The linear KCl gradient from 0 mM KCl to 300 mM KCl was performed over 15 CV (Figure 36 and Figure 37). The most active fractions of the peak F288 – F294 (135 mM KCl – 140 mM KCl) were mixed, concentrated with an Amicon filter unit from 3,5 mL to 0,1 mL, and diluted 1:10 (v/v) with binding buffer (25 mM Tris-HCl, pH 7,5). 0,5 mL of this pool comprising 2,39 mg of protein were loaded onto the Resource-Q column. The linear KCl gradient from 0 mM KCl to 300 mM KCl was performed over 20 CV (Figure 38).

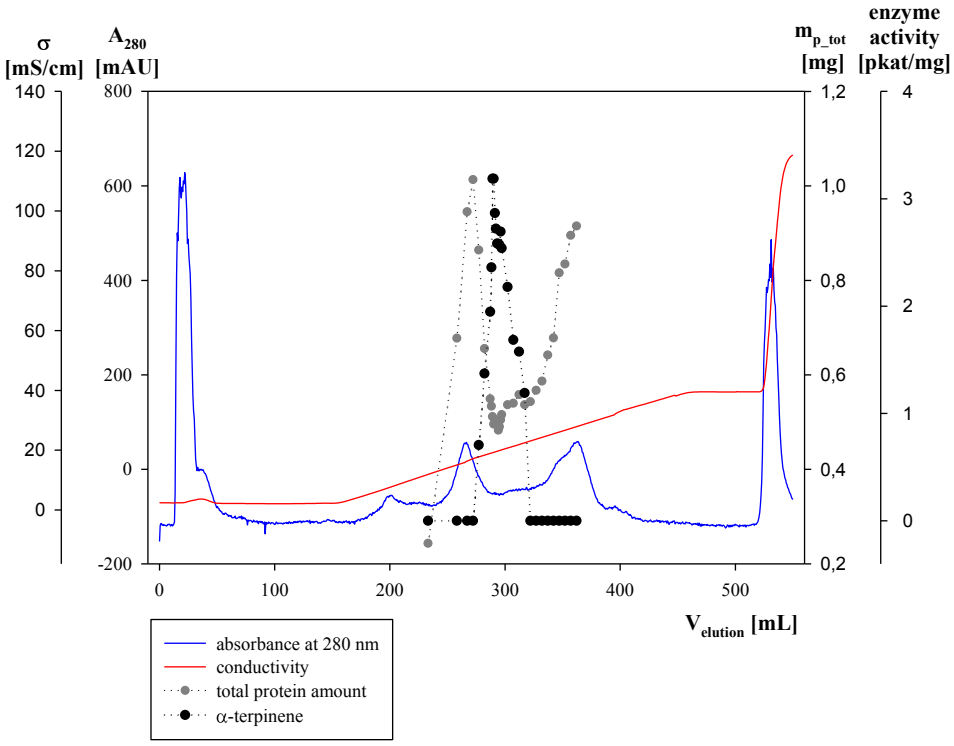

Figure 36: Protein separation and α-terpinene synthase activity on DEAE-Sepharose using a linear gradient from 0 to 300 mL KCl over 15 CV (300 mL). The IEC was performed with 205 mg protein in 25 mM Tris-HCl, pH 7,5 (binding buffer) at a flow rate of 1 mL/min. Flow rate during gradient elution: 0,36 mL/min. Blue line: Inline measured absorbance at 280 nm; red line: Inline measured conductivity. The protein amount was determined offline in triplicates. Enzyme activity was determined offline in a single test and reached a maximum of 3,19 pkat/mg.

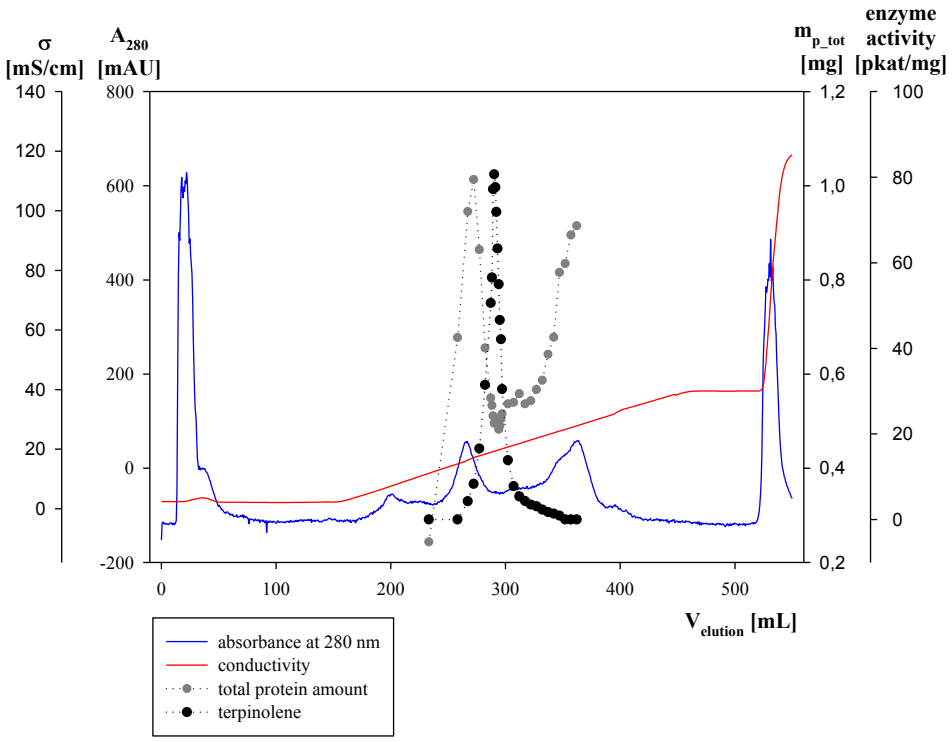

Figure 37: Protein separation and terpinolene synthase activity on DEAE-Sepharose using a linear gradient from 0 to 300 mL KCl over 15 CV (300 mL). The IEC was performed with 205 mg protein in 25 mM Tris-HCl, pH 7,5 (binding buffer) at a flow rate of 1 mL/min. Flow rate during gradient elution: 0,36 mL/min. Blue line: Inline measured absorbance at 280 nm; red line: Inline measured conductivity. The protein amount was determined offline in triplicates. Enzyme activity was determined offline in a single test and reached a maximum of 80,7 pkat/mg.

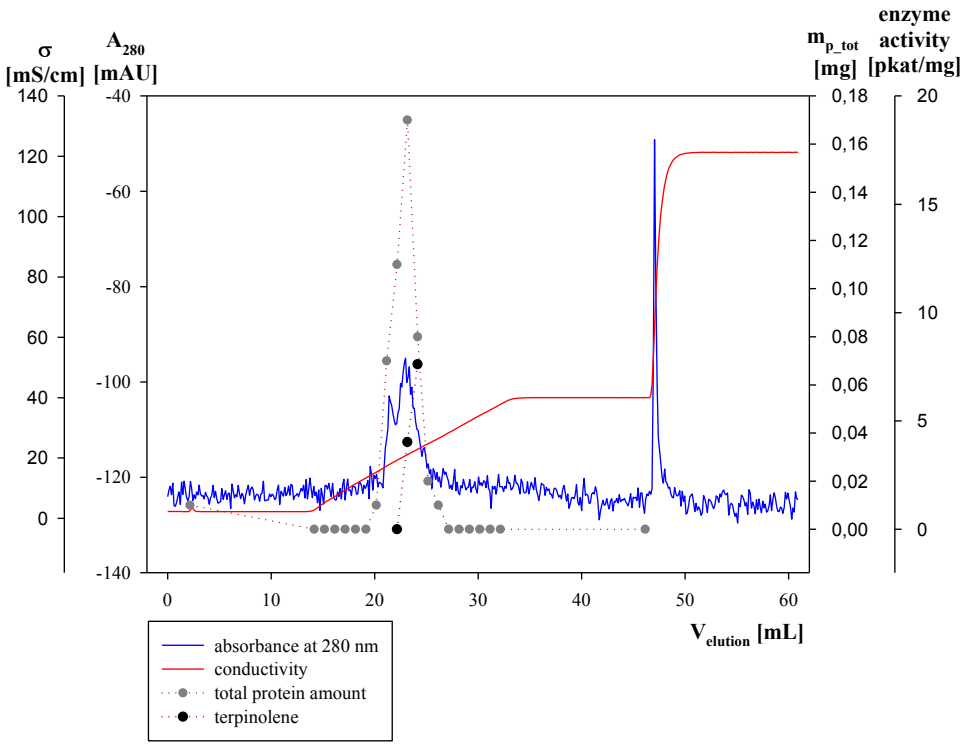

Figure 38: Protein separation and terpinolene synthase activity on Resource-Q using a linear gradient from 0 to 300 mL KCl over 20 CV (20 mL). The IEC was performed with 2,39 mg protein in 25 mM Tris-HCl, pH 7,5 (binding buffer) at a flow rate of 0,5 mL/min. Flow rate during gradient elution: 1 mL/min. Due to a failure of the UV detector the obtained absorbance signal (blue) is noisy. Red line: Inline measured conductivity. The protein amount was determined offline in triplicates. Enzyme activity was determined offline in a single test and reached a maximum of 7,62 pkat/mg.

No α-terpinene synthase activity was detected. Terpinolene synthase activity was detected in two fractions obtained from the strong IEC. In this approach only those fractions of the second IEC were tested for enzyme activity that did show protein bands on the SDS-PAGE gel. Therefore, only the fractions F23 – F25 (110 mM KCl – 135 mM KCl) were examined (Table 22 and Table 23).

Table 22: Purification of α-terpinene synthase activity by a multiple step purification with IEC using a weak and a strong anion exchanger from soluble extract obtained from biomass of *C. defragrans*.

Purification level	Volume [mL]	Total protein [mg]	Total activity [pkat]	Specific activity [pkat/mg]	Relative specific activity	Protein yield [%]
Soluble Extract 9	9	205	34,8	0,17	1,0	100,0
IEC weak						
Pool (Fraction 288 - 294, conc.)	0,5	2,39	0,00	0,00	0,0	1,2
IEC strong						
Fraction 23 - 25	1	0,08 – 0,17	0,00	0,00	0,0	0,2

Table 23: Purification of terpinolene synthase activity by a multiple step purification with IEC using a weak and a strong anion exchanger from soluble extract obtained from biomass of *C. defragrans*. Integrated peak from F24 to F25.

Purification level	Volume [mL]	Total protein [mg]	Total activity [pkat]	Specific activity [pkat/mg]	Relative specific activity	Protein yield [%]
Soluble Extract 9	9	205	18,1	0,09	1,0	100,0
IEC weak						
Pool (Fraction 288 - 294, conc.)	0,5	2,39	21,3	8,90	101	1,2
IEC strong						
Fraction 23	1	0,11	0,00	0,00	0,0	0,1
Fraction 24	1	0,17	0,68	4,03	45,8	0,1
Fraction 25	1	0,08	0,61	7,62	86,6	0,0
Integrated peak		0,25	1,29	5,18	58,9	0,1

The integrated peak obtained by IEC using a strong anion exchange column consisted of fractions F24 – F25 and had a total amount of 0,25 mg protein (0,1 % of initial protein) and a total terpinolene synthase activity of 1,29 pkat. Total terpinolene synthase activity did increase from 18,1 pkat in the soluble extract to 21,3 pkat in the fractions obtained by IEC using a weak anion exchanger. It decreased to 1,29 pkat during the subsequent IEC. This is also reflected in the relative specific activities for terpinolene (101 x after first IEC and 58,9 x after second IEC).

The first SDS-PAGE gel showed the protein bands of the weak IEC that were combined to a pool (Figure 39). The second SDS-PAGE gel showed the protein bands of the soluble extract, the pool of the weak IEC that was loaded onto the strong IEC column as well as some of the fractions of the strong IEC (Figure 40). The pooled fractions of the weak IEC show a similar protein band pattern. After the strong IEC only the fractions F22 – F25 show protein bands (other fractions tested and not shown). Therefore, only the fractions F23 – F25 were tested for activity revealing an enzyme activity in the fractions F24 and F25. This enzyme activity can be linked to protein bands at 45 kDa, 55 kDa and 100 kDa, with the protein band at 45 kDa being the only one not observable in the inactive fraction F23.

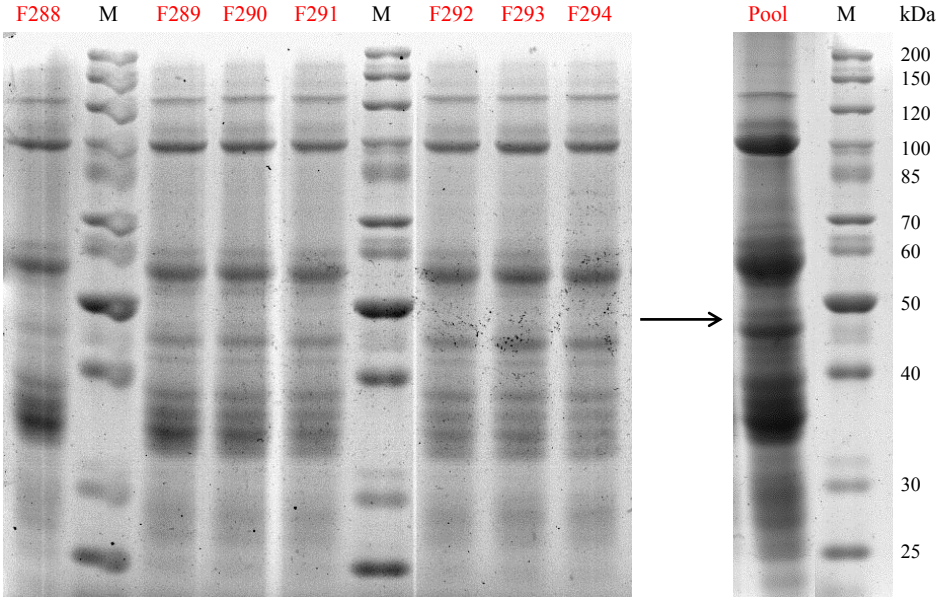

Figure 39: SDS-PAGE of fractions from an IEC using a weak anion exchanger that were pooled. Samples were applied on polyacrylamide gels with 10 % acrylamide in the separation gel. Electrophoresis was carried out at 70 V for 3 hours. The gels were stained with Coomassie Blue staining solution. Only fractions with enzyme activity (red) were pooled.

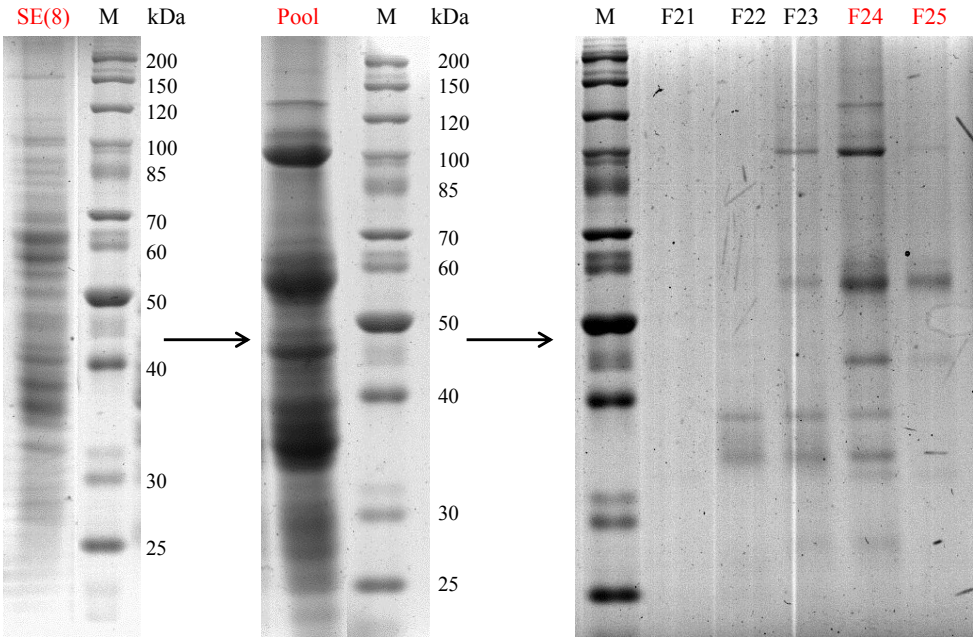

Figure 40: SDS-PAGE of two step purification fractions after IEC using a weak anion exchanger followed by a strong anion exchanger. Samples were applied on polyacrylamide gels with 10 % acrylamide in the separation gel. Electrophoresis was carried out at 70 V for 3 hours. The gels were stained with Coomassie Blue staining solution. Soluble extract (SE), the active (red) IEC pool using a weak anion exchanger and inactive and active IEC fractions using a strong anion exchanger. Due to bands in the fractions F23, F24 and F25 these fractions were tested for enzyme activity. Pool: F288 – F294. F25 is the most active fraction of this chromatographic run.

The same experiment performed a second time (see Appendix B, Figure 55, Figure 56 and Figure 57) with the same soluble extract did obtain a specific terpinolene synthase activity of 17,6 pkat/mg in the pool obtained from the weak IEC. This activity was completely lost after the strong IEC (see Appendix B, Table 26 and Table 27). A reason for this could be the low protein concentration (0,54 mg/mL) of the pool in this experiment. With a protein concentration of 4,78 mg/mL the strong IEC did succeed (see Table 23).

3.9 Purification by anion exchange chromatography using a weak anion exchanger followed by a strong anion exchanger and size exclusion chromatography

IEC on the weak anion exchanger DEAE-Sepharose was combined with IEC on the strong anion exchanger Resource-Q and a subsequent SEC on Superdex 75. By this purification approach an increase in specific activity was expected.

7 mL soluble extract 5 (Table 5) comprising 119 mg of protein were diluted with 7 mL of binding buffer (25 mM Tris-HCl, pH 7,5) and loaded onto the 20 mL weak anion exchange column. A linear KCl gradient from 0 mM KCl to 300 mM KCl was performed over

15 CV (Figure 41). The most active fractions of the peak F244 – F272 (119 mM KCl – 148 mM KCl) were mixed, concentrated with an Amicon filter unit from 6 mL to 0,4 mL, and diluted 1:10 (v/v) with binding buffer (25 mM Tris-HCl, pH 7,5). 4 mL of this pool comprising 3,68 mg of protein were loaded onto the 1 mL Resource-Q column. A linear KCl gradient from 0 mM KCl to 300 mM KCl was performed over 20 CV (Figure 42). The active pool (F25 – F26 eluting at salt concentrations of 94 mM KCl – 109 mM KCl) was mixed. 1,5 mL comprising 0,93 mg protein were loaded onto the Superdex 75 column (Figure 43).

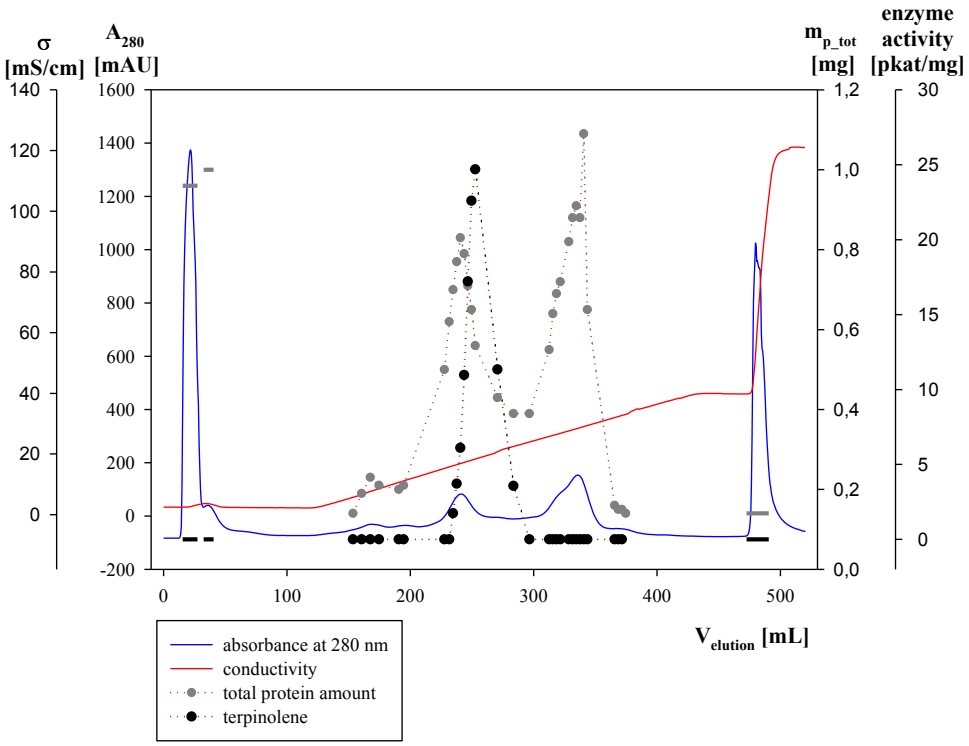

Figure 41: Protein separation and terpinolene synthase activity on DEAE-Sepharose using a linear gradient from 0 to 300 mL KCl over 15 CV (300 mL). The IEC was performed with 119 mg protein in 25 mM Tris-HCl, pH 7,5 (binding buffer) at a flow rate of 1 mL/min. Flow rate during gradient elution: 0,3 mL/min. Blue line: Inline measured absorbance at 280 nm; red line: Inline measured conductivity. The protein amount was determined offline in triplicates. Enzyme activity was determined offline in a single test and reached a maximum of 24,7 pkat/mg.

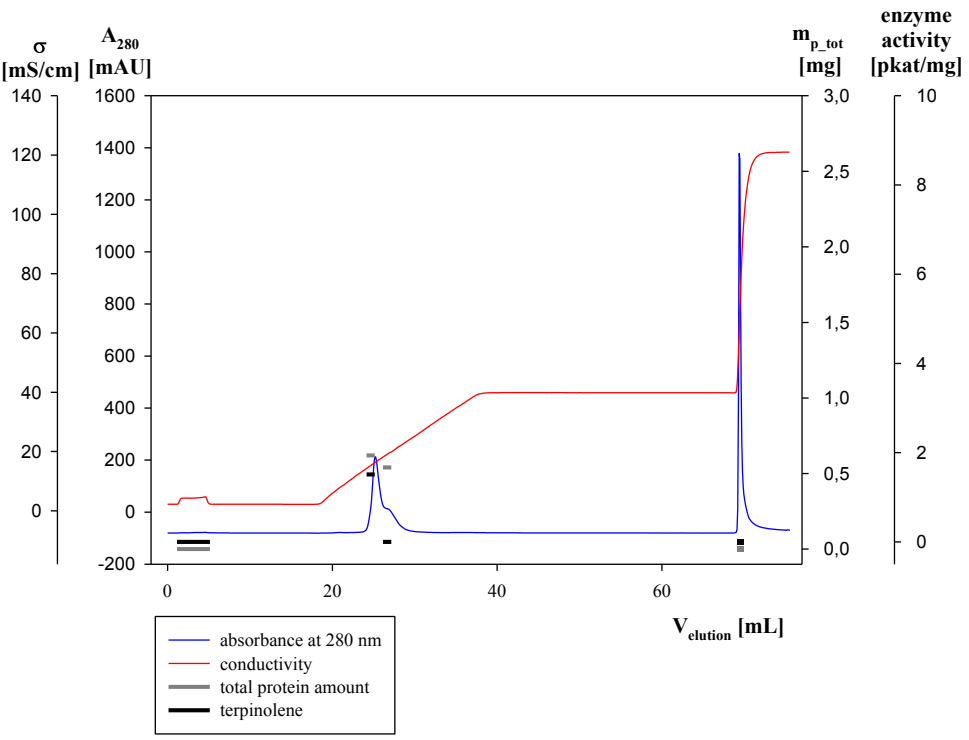

Figure 42: Protein separation and terpinolene synthase activity on Resource-Q using a linear gradient from 0 to 300 mL KCl over 20 CV (20 mL). The IEC was performed with 3,68 mg protein in 25 mM Tris-HCl, pH 7,5 (binding buffer) at a flow rate of 0,5 mL/min. Flow rate during gradient elution: 1 mL/min. Blue line: Inline measured absorbance at 280 nm; red line: Inline measured conductivity. The protein amount was determined offline in triplicates. Enzyme activity was determined offline in a single test and reached a maximum of 2,02 pkat/mg.

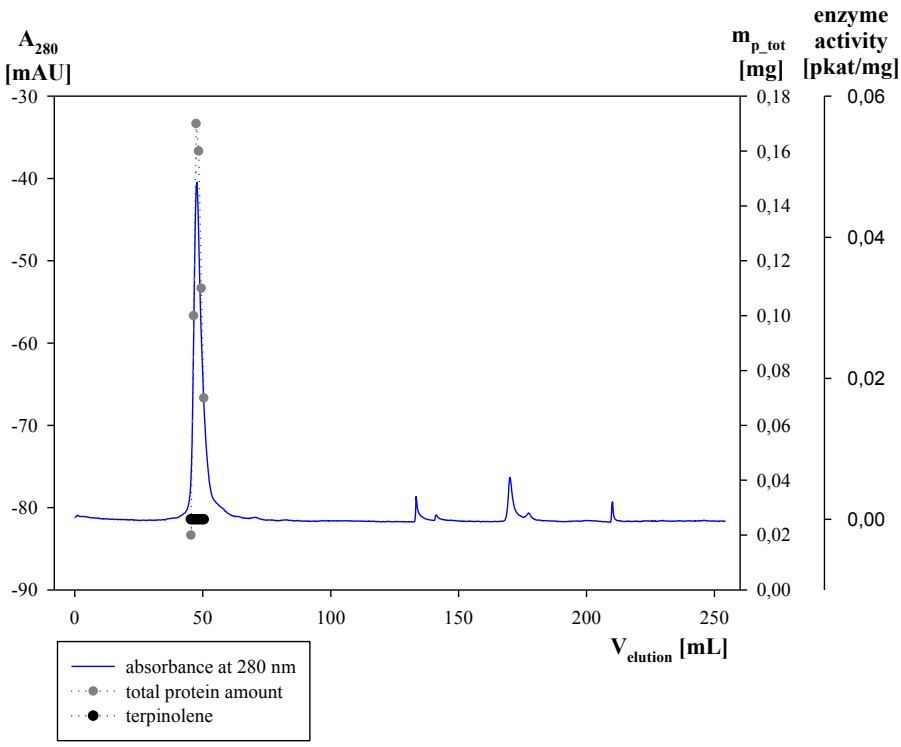

Figure 43: Protein separation and terpinolene synthase activity on Superdex 75. The SEC was performed with 0,93 mg protein in 25 mM Tris-HCl including 100 mM KCl, pH 7,5 (running buffer) at a flow rate of 0,5 mL/min. Blue line: Inline measured absorbance at 280 nm; red line: Inline measured conductivity. The protein amount was determined offline in triplicates. Enzyme activity was determined offline in a single test.

Although terpinolene synthase activity was found in the pooled IEC fractions, no activity was detected after SEC. The determined protein concentration did fit the peak detected by UV absorbance (Table 24 and Table 25). The elution volume of these fractions is around 48 mL and thus between the elution volumes of terpinolene synthase activity during aforementioned SECs (single step: 53 mL, multiple step: 45 mL, 43 mL, 44 mL).

Table 24: Purification of α-terpinene synthase activity by a multiple step purification with IEC using a weak and a strong anion exchanger and SEC from soluble extract obtained from biomass of *C. defragrans*.

Purification level	Volume [mL]	Total protein [mg]	Total activity [pkat]	Specific activity [pkat/mg]	Relative specific activity	Protein yield [%]
Soluble Extract 5	7	119	27,7	0,23	1,0	100,0
IEC weak						
Pool (Fraction 244 - 272, conc.)	4	3,68	0,00	0,00	0,0	3,1
IEC strong						
Pool (Fraction 25-26)	1,5	0,93	0,00	0,00	0,0	0,8
SEC						
Fraction 46 - 51	1 each	0,02-0,17	0,00	0,00	0,0	0,5

Table 25: Purification of terpinolene synthase activity by a multiple step purification with IEC using a weak and a strong anion exchanger and SEC from soluble extract obtained from biomass of *C. defragrans*.

Purification level	Volume [mL]	Total protein [mg]	Total activity [pkat]	Specific activity [pkat/mg]	Relative specific activity	Protein yield [%]
Soluble Extract 5	7	119	1,53	0,01	1,0	100,0
IEC weak						
Pool (Fraction 244 - 272, conc.)	4	3,68	4,99	1,36	106	3,1
IEC strong						
Pool (Fraction 25-26)	1,5	0,93	1,88	2,02	157	0,8
SEC						
Fraction 46 - 51	1 each	0,02 - 0,17	0,00	0,00	0,0	0,5

The SDS-PAGE gel showed the protein bands of the soluble extract, the pool of the weak IEC used for the strong IEC column, the pool of the strong IEC applied onto the SEC as well as some of the fractions of the SEC (Figure 44). Two prominent protein bands were in the pool of the strong IEC, at 35 to 40 kDa and at 85 kDa. The first one may consist of multiple protein bands. The latter band was not observable in the inactive fractions of the SEC. Enzyme activity was found in none of the fractions of the SEC.

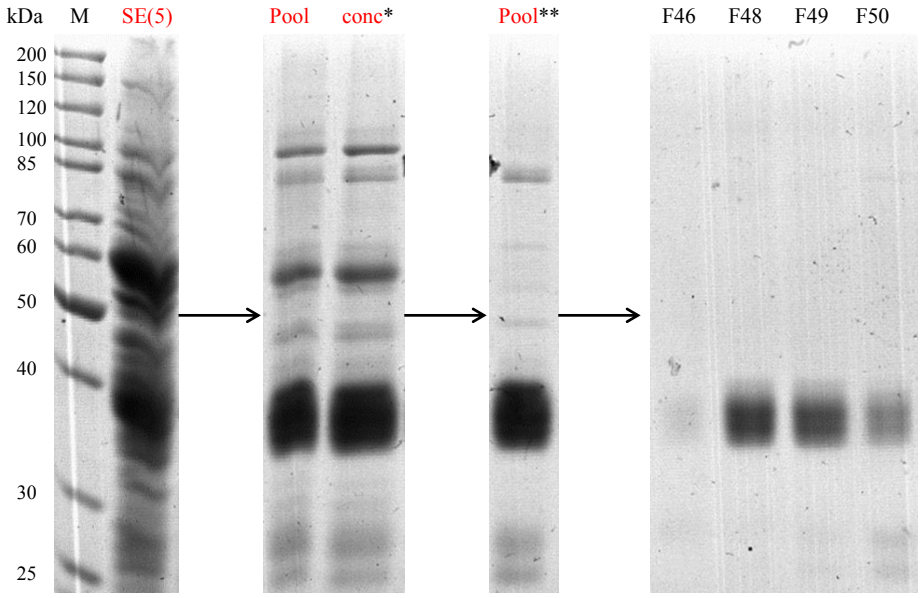

Figure 44: SDS-PAGE of three step purification fractions. Samples were applied on polyacrylamide gels with 10 % acrylamide in the separation gel. Electrophoresis was carried out at 70 V for 3 hours. The gels were stained with Coomassie Blue staining solution. Soluble extract (SE), the active (red) IEC pool using a weak anion exchanger, the active IEC pool using a strong anion exchanger and inactive SEC fractions. Pool(*): F244 – F272; Pool(**): F25 – F26.

3.10 Characterization of monoterpene synthase activity

The enzyme characteristics were tested over a time of 120 minutes which is within the linear range of incubation time for the enzyme activity assay [Scilipoti, 2016].

3.10.1 Determination of the optimal pH for enzyme activity

For the determination of the optimal pH an IEC (section 3.2.2) was performed with soluble extract and the most active fractions (F295 – F299 eluting at salt concentrations of 136 mM KCl – 140 mM KCl) were pooled and tested for activity at different pH at 28 °C. Enzyme activity was observed between pH 6,0 and pH 9,0 with an broad optimal range between pH 6,0 and pH 8,5 (Figure 45).

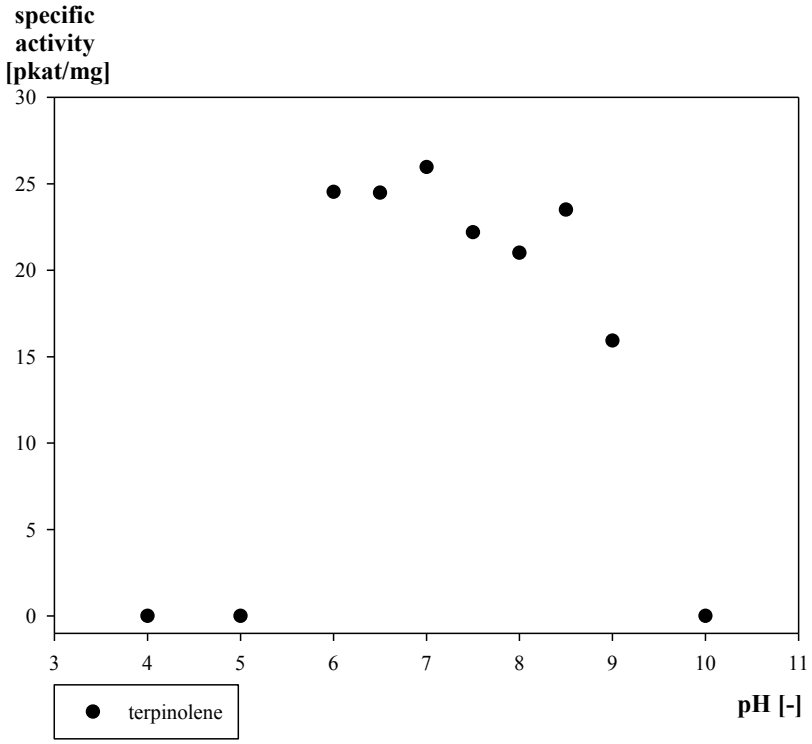

Figure 45: pH dependency of terpinolene synthase activity. A pool of active IEC fractions was tested in single assays. Each test contained 58 µg of protein.

3.10.2 Determination of the optimal temperature for enzyme activity

For the determination of the optimal temperature an IEC (section 3.2.2) was performed with soluble extract and the most active fractions in the flanking regions of the peak (F291 – F294 and F300 – F301 eluting at salt concentrations of 132 mM KCl – 135 mM KCl and 141 mM KCl – 142 mM KCl) were pooled and tested for activity at different temperatures at pH 7,5. Enzyme activity was observed between 12 °C and 60 °C with an optimum at 37 °C (Figure 46).

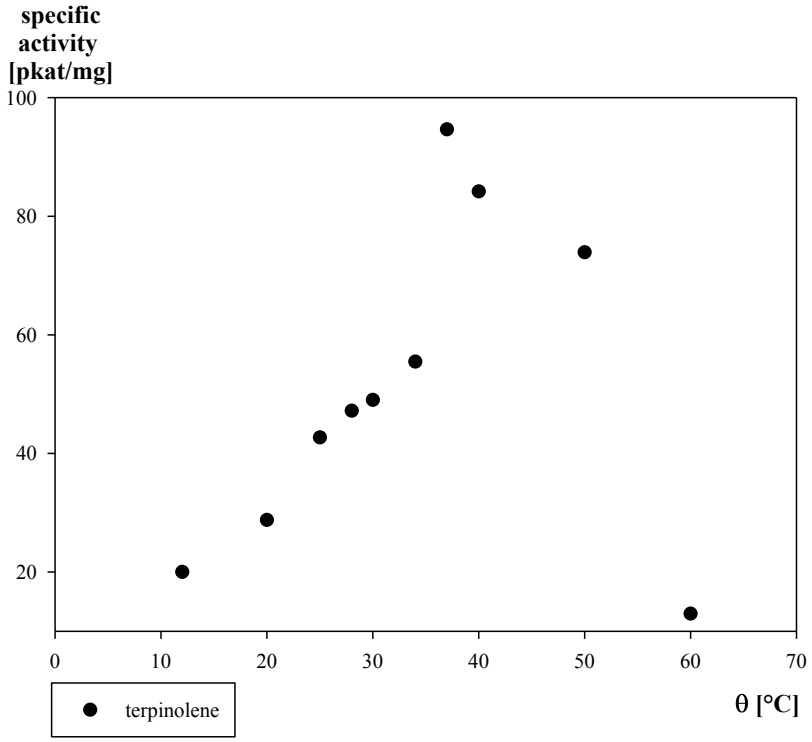

Figure 46: Temperature dependency of terpinolene synthase activity. A pool of active IEC fractions was tested in single assays. Each test contained 109 µg of protein.

3.10.3 Molecular size of the monoterpene synthase

The size of the enzyme responsible for the formation of α-terpinene and terpinolene from (R,S)-linalool was determined by SEC. A calibration curve with proteins of known size was applied to determine the size of the enzyme in the fraction with maximum enzyme activity (Figure 47). The apparent molecular size was dependent on the purification level or the sample buffer. Analysis of soluble fractions in a single experiment revealed the maximum α-terpinene synthase activity eluting at 51 mL, corresponding to an apparent molecular size of 114 kDa. Maximum terpinolene synthase activity was observed in the 53 mL fraction which corresponds to 72 kDa. The partially purified terpinolene synthase eluted in three SEC runs after averagely 44 mL with an apparent molecular size of 144 ± 11 kDa.

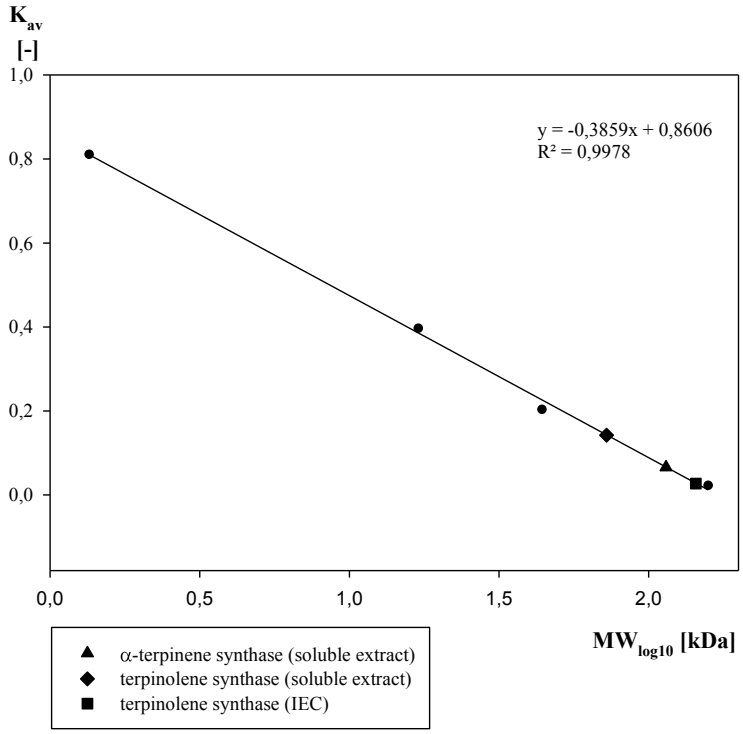

Figure 47: SEC calibration curve with standard proteins (●) and enzyme activities. α-terpinene synthase (▲); and terpinolene synthase (◆): soluble extract; terpinolene synthase (■): after partial purification.

4 Discussion

4.1 Purification approach for successful enrichment of terpinolene synthase activity

In the course of this study several purification approaches were tested for the purification of α-terpinene and terpinolene synthase activities in *C. defragrans* 65Phen. Single purification runs applying soluble protein extracts to a weak anion exchanger (DEAE) resulted in an increase in the relative specific terpinolene synthase activity to 43,5 fold purification after IEC with 5 CV gradient (see Table 7), 1350 fold purification after IEC with 15 CV gradient (see Table 9), and 75,5 fold purification after IEC with step gradient (see Table 11). This variation may result from different biomasses as starting points. For the single step SEC a relative specific terpinolene synthase activity of 3,9 fold purification and a protein yield of 53,1 % were found (see Table 13). The increase of total terpinolene synthase activity for all single step purifications indicates the presence of inhibitory substances in the soluble extract which are removed by the chromatographic procedures. Additionally, proteins competing with the monoterpene synthases for the added ATP in the soluble extract could have been removed by the purification. Despite the observed enrichment, the enzyme activity was not unequivocally assigned to any of the protein bands observed on denaturing protein gels. Therefore, the combination of several column materials was implemented.

The combination of a weak and a strong anion exchanger yielded a relative specific terpinolene synthase activity of 58,9 fold purification, a protein yield of 0,1 % and a decrease in total terpinolene activity (7 % of initial total enzyme activity) (see Table 23). This combination provided a more successful purification of terpinolene synthase activity than the single chromatographies aforementioned. The SDS-PAGE gel showed in accordance with this only few protein bands.

Even fewer protein bands were observable on the SDS-PAGE after the combination of IEC and SEC. The relative specific terpinolene synthase activity of this combination was 56,8 fold purification, with a protein yield of 0,3 % and a decrease in total terpinolene activity (16 % of initial total enzyme activity) (see Table 17).

Most monoterpenes have a hydrophobic character [Turina *et al.*, 2006] and a strong binding of monoterpene metabolizing enzymes to HIC columns has been observed in the past [Brodkorb *et al.*, 2010; Lüddeke *et al.*, 2012]. This hydrophobic behavior can be used to isolate the target enzyme from bulk proteins. Hence, this chromatographic method was included in the present study. Although enzyme activity was detected after a single HIC (see Figure 18), no enzyme activity was detected after another single HIC (see Figure 20) or a combination of IEC and HIC (see Table 15). A loss of monoterpene synthase activity during HIC has been reported before by Shelton *et al.* [2004]. The reason for this might be an unstable enzyme activity. Although the stability was tested prior to the chromatographic run with different salt concentrations and no precipitation was observable in the test solutions, soluble aggregates might have been formed due to high salt concentrations. Soluble aggregates are not visible as particles and cannot be removed by a 0,2 µm filter unit [Cromwell, Hilaro, and Jacobson, 2006], as it was used before HIC. An aggregation of the enzyme prior chromatography could have led to a loss of enzyme activity. Conformational changes during adsorption to the phenyl resin as well as aggregation during HIC could be further explanations for the loss of enzyme activity [Chen and Cramer, 2007].

Additionally, the phenyl resin could be to hydrophobic, resulting in irreversible attachment of the protein to the column, even after application of water, alcohol and detergents. Less hydrophobic materials like methyl, butyl and octyl have been successfully used before for terpene synthase purification [Alonso *et al.*, 1992; Brodkorb *et al.*, 2010; Hohn and Vanmiddlesworth, 1986] and might be used in future experiments.

Another reason might be the low protein amounts applied onto HIC. For the first HIC yielding an enzymatic activity a protein amount of 91 mg was applied, while for the other two HICs lower protein amounts were applied (58 mg for the single HIC and 1,68 mg for the multistep HIC).

The lack of protein bands on the SDS-PAGE gel of the multistep HIC (see Figure 27) might be due to the low protein amounts applied to the wells (0,1 – 1,8 µg). The wells of the SDS-PAGE gels of the single HICs showing protein bands (see Figure 19 and Figure 21) were loaded with 3,0 – 7,0 µg protein. Depending on the thickness of the gel, wells should be loaded with 0,5 – 4,0 µg if the proteins are purified and 40 – 60 µg if crude extracts shall be investigated [Kurien and Scofield, 2012]. In the laboratory protein amounts of maximal 20 µg are used for 1 mm thick gels. Concentration of the samples before SDS-PAGE could lead to more distinct protein bands. Furthermore, another staining

method for the gel could be used to detect protein bands. Silver staining was shown to have a higher sensitivity than Coomassie dyes, detecting proteins at a nanogram range [Switzer, Merril, and Shifrin, 1979].

During this study, a combination of IEC and SEC was ascertained to be the most successful purification approach for the enzyme responsible for formation of terpinolene from (R,S)-linalool. In further experiments, SEC could be run first followed by a subsequent IEC. Thus, small proteins could be separated from the enzyme of interest in a first step before continuing with a further enrichment of the enzyme. To increase the purification success, only the two or three most active fractions from the first SEC could be used for the subsequent purification by IEC using a weak anion exchanger followed by another SEC. Multiple SECs might be performed in a first step. Most active fractions of these SECs could be combined and loaded on an IEC column followed by the second SEC. Thereby, only fractions with the highest activity would be purified.

4.2 Importance of nitrate for enzyme activity

For the different cell extractions various enzyme activities were determined. The extractions of cells obtained from the cultivations harvested on the 18th of March 2016 show in particular low values of 0,05 – 0,09 pkat/mg for terpinolene. This result might be due to an insufficient nitrate supply during the cultivation process of *C. defragrans*. At the end of this cultivation batch nitrite and nitrate were not detectable anymore. Without nitrate as electron acceptor denitrification was not possible, ultimately reducing the physiological activity. This result shows the dependency of the metabolism of *C. defragrans* on a sufficient nitrate supply during cultivation as it was shown before [Heyen and Harder, 2000; Petasch *et al.*, 2014]. In spite of this, the total enzyme activity of α-terpinene was not affected in these extractions.

4.3 Loss of α-terpinene synthase activity throughout the chromatographic process

α-terpinene was not detected in any of the last steps of the multistep purifications. Assuming that one enzyme is responsible for the formation of both monoterpenes from one substrate, which is known for most monoterpene synthases [Christianson, 2008], this indicates a thermodynamically favorable formation of terpinolene from (R,S)-linalool.

Alterations in product formation could be due to interaction with the column material, leading to a decrease of α-terpinene production and an increase of terpinolene production. Formation of terpinolene from the α-terpinyl cation only requires a deprotonation (see Figure 5) while the formation of α-terpinene might require an additional enzyme which might have gone lost during purification.

Another reason could be linked to the amount of α-terpinene in the pellets obtained by cell disintegration. While no terpinolene activity was detected in the pellets, except for two extractions, α-terpinene activity was detected in the pellets of all extractions yielding specific activities of 50 – 70 % of total detected activity. This could indicate the presence of two enzymes instead of the previously assumed one enzyme, reflected also in the SEC of the soluble extract (see Figure 47). These enzymes synthesizing both α-terpinene and terpinolene might be located on two subunits of a protein or on two proteins forming a dimer. The hypothesis of two subunits is supported by the two enzyme activities necessary for synthesis of terpinolene from linalool which could be located on different subunits. First, a linalool kinase is needed which catalyzes the transfer of a phosphate group to linalool and by this the formation of linalyl diphosphate. The latter is required by the second enzyme, a monoterpene synthase, to form terpinolene (see Figure 5). α-terpinene formation might be catalyzed by a third enzyme. This enzyme might be (partly) located on a protein at the inner cell membrane like it was shown before for the linalool isomerase [Marmulla *et al.*, 2016]. During the extraction this enzyme could have been separated from the soluble extract resulting in low α-terpinene yields in the soluble extract and all subsequent purification steps. To confirm this hypothesis, differential centrifugation could be applied to determine the precise location of the enzyme activity in the cell [Livshts *et al.*, 2015]. An insoluble enzyme would require a different purification approach unlike the one described in this thesis.

4.4 Formation of multiprotein complexes during purification

After a SEC run from a soluble extract, an elution volume of 53 mL was determined for terpinolene synthase activity (Figure 48). This elution volume is equivalent to an apparent molecular size of 72 kDa.

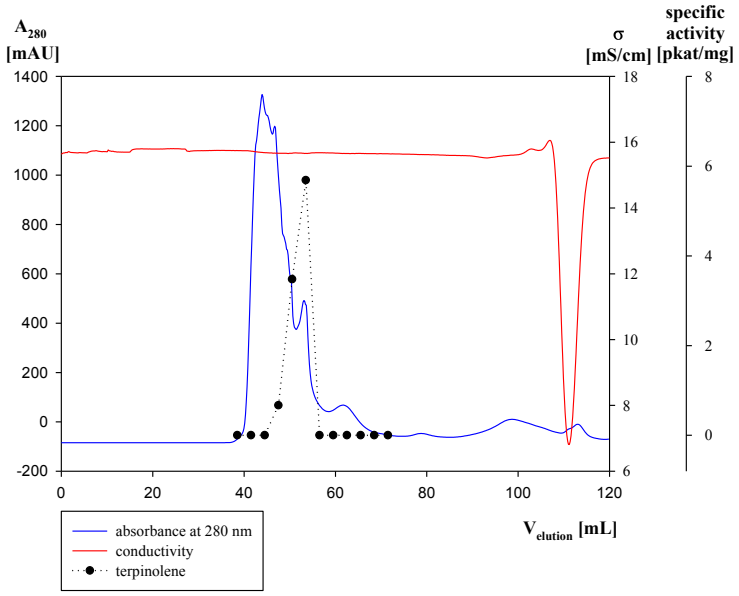

Figure 48: Chromatogram from SEC of terpinolene synthase activity purification with SEC as single purification step. The SEC was performed with 39 mg protein in 25 mM Tris-HCl including 100 mM KCl, pH 7,5 (running buffer) at a flow rate of 0,5 mL/min. Enzyme activity reached a maximum at an elution volume of 53 mL (Figure 23, modified).

In a previous experiment, using a Superdex 200 column, another running buffer (50 mM HEPES, pH 7,2), a flow of 0,75 mL/min and a different mixture of molecular weight markers, an elution volume of 62 mL, equivalent to a molecular size of 205 kDa, was determined for both, α-terpinene and terpinolene [Scilipoti, 2016]. This result had led to the hypothesis of one enzyme forming both monoterpenes from linalool as substrate.

In later experiments, the retention volumes of the fractions with terpinolene synthase activity of three IECs suggested an apparent molecular size of 144 ± 11 kDa (Figure 49).

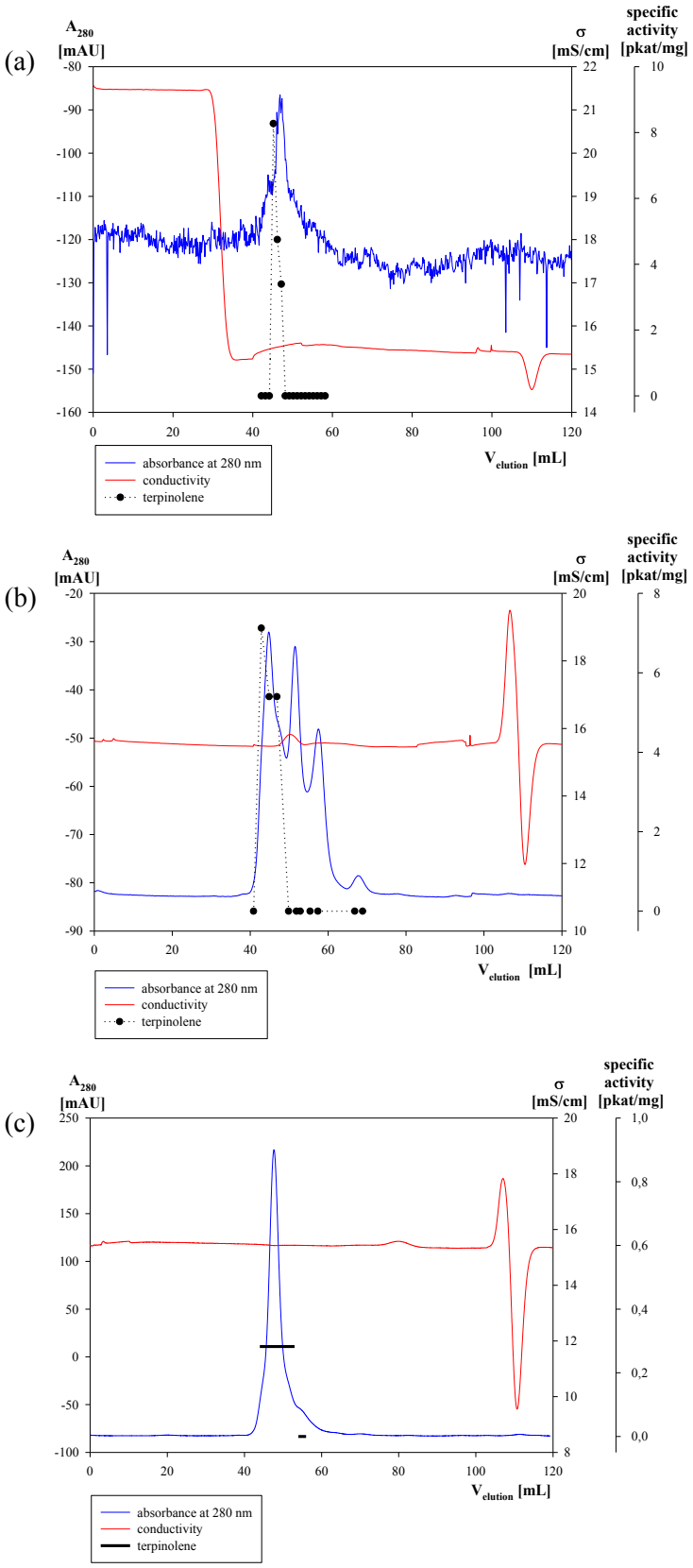

Figure 49: Chromatograms from SEC of terpinolene synthase activity purification after previous IEC. The SECs were performed with 1,89 mg protein, 6,15 mg protein, and 12,7 mg protein, respectively, in 25 mM Tris-HCl including 100 mM KCl, pH 7,5 (running buffer) at a flow rate of 0,5 mL/min. Enzyme activity reached maxima at elution volumes of 45 mL (a), 43 mL (b) and 44 mL (c) (Figure 30, Figure 32 and Figure 34, modified).

A dimerization of a 72 kDa protein may be suggested as explanation for the duplication of the molecular size of the partially purified enzyme. The molecular cause of this shift in apparent size could not be investigated in the timeframe of this thesis.

A hypothesis predicting enzyme polymerization due to increased salt concentrations during IEC was refuted by the fact that the SEC works in a desalting mode. Any polymer formation caused by high salt concentration would have been reverted during SEC. Aggregates, in contrast, could be irreversibly induced by high salt concentrations. Conformational changes and aggregation of proteins during IEC were observed before with an increase in high molecular weight proteins [Arakawa *et al.*, 2007; Gillespie *et al.*, 2012]. An aggregate formation, on the other hand, would have caused the loss of enzyme activity in the IEC fractions due to changes in the three-dimensional structure which was not the case during this study.

Instead another hypothesis can be formulated predicting the formation of multi-enzyme complexes after multiple purification steps. In the soluble extract a hypothetical enzyme complex ‘AB’ and a hypothetical single enzyme ‘C*’ might have been present. Being ‘C*’ the enzyme responsible for activity. After IEC ‘A’ could now be the single enzyme, while there is a new enzyme complex ‘BC*’. This could explain the premature elution from the SEC column of terpinolene synthase activity after a combination of IEC and SEC. The complex formation did not have a suppressing effect on enzyme activity, if anything, it enhanced the activity.

In bacterial cells multi-enzyme complexes were found to have beneficial effects for cellular processes like cellulose breakdown or promotion of cell wall synthesis [Israeli-Ruimy *et al.*, 2017; Leclercq *et al.*, 2017]. The catalytic activity of these complexes is depending on their three-dimensional organization [Fu *et al.*, 2016].

In an experiment with two IECs followed by a SEC an elution volume of 48 mL, equivalent to a molecular size of 106 kDa, was observed. Although no enzyme activity was detected in the fractions of the SEC a peak detected by UV absorbance fitting the measured protein amount was observable (Figure 50).

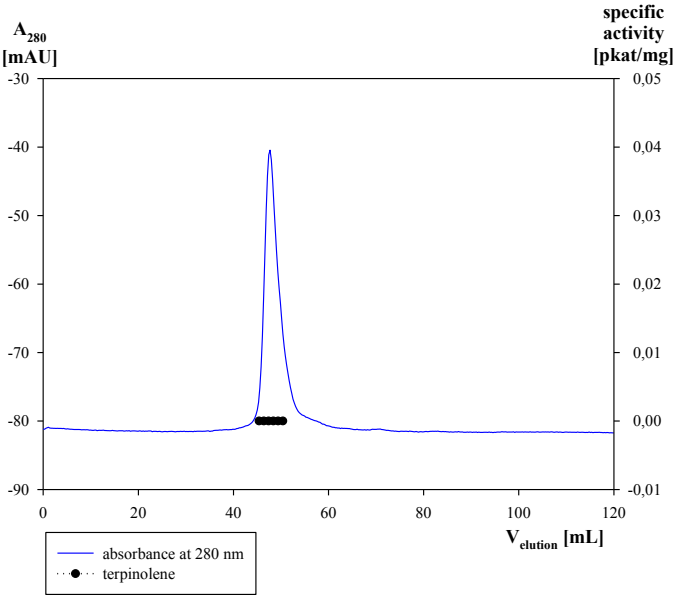

Figure 50: Chromatogram from SEC of terpinolene synthase activity purification after previous purification via two IECs. The SEC was performed with 0,93 mg protein in 25 mM Tris-HCl including 100 mM KCl, pH 7,5 (running buffer) at a flow rate of 0,5 mL/min. The peak signal showed a maximum at an elution volume of 48 mL (Figure 43, modified).

The maximum of this peak is located at an elution volume of 48 mL. This elution volume lies between the elution volumes of SEC fractions from soluble extract (53 mL) and SEC fractions from previous purification by IEC (45 mL, 43 mL and 44 mL). This might be due to a decomposition of the enzyme complexes formed during the first IEC.

The aforementioned combination of a first SEC, an IEC and a second SEC could be used to investigate formation of enzyme complexes during IEC to confirm the findings of this study. Additionally, another SEC column with a resolution capacity in a higher molecular weight range could be used. Superdex 75 has a theoretical resolution capacity ranging from 3 kDa to 70 kDa, while Superdex 200 has a theoretical resolution capacity ranging from 10 kDa to 600 kDa, both given by the manufacturer. For the first SEC the Superdex 200 might be used and for the second SEC the Superdex 75 could be applied.

4.5 Virtual SDS-PAGE gel as reference gel

To compare the purification success with different chromatographic methods, a virtual SDS-PAGE gel was generated. The fractions chosen were the ones with the highest terpinolene synthase activities. For soluble extract and pellet the extraction 10 (see Table 5) was chosen. Activities are given as specific activities in pkat/mg (Figure 51).

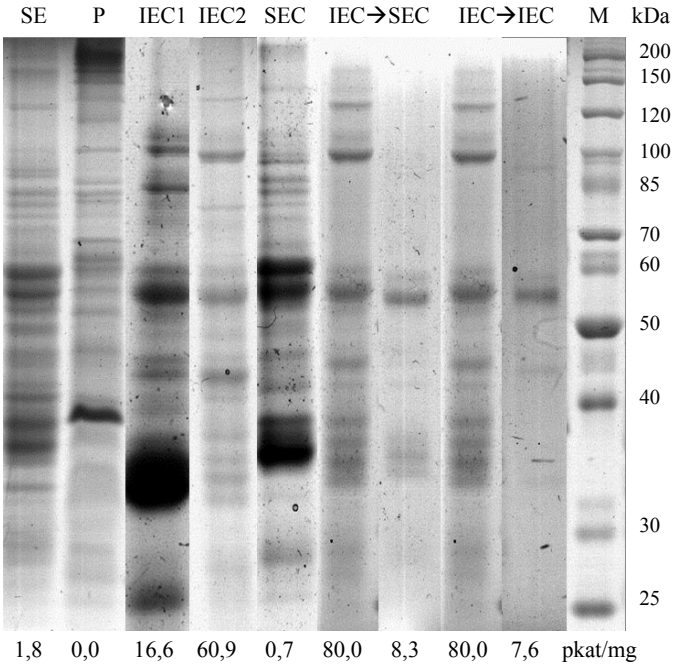

Figure 51: Virtual SDS-PAGE of most active fractions of all purification approaches. Samples were applied on polyacrylamide gels with 10 % acrylamide in the separation gel. Electrophoresis was carried out at 70 V for 3 hours. The gels were stained with Coomassie Blue staining solution. Soluble extract (SE) and pellet (P) obtained from extraction 10. IEC1: 5 CV gradient; IEC2: step gradient. At the bottom of the gel the detected terpinolene synthase activities in the fractions are given (Figure 12, Figure 17, Figure 24, Figure 31, Figure 39 and Figure 40, modified).

Protein bands at 100 kDa and 120 kDa are observable in fractions with high specific activities ranging from 60,9 to 80,0 pkat/mg, while in fractions with lower specific activities ranging from 0,7 to 7,6 pkat/mg no such bands can be observed. A protein band at 45 kDa can be seen in fractions with specific activities ranging from 16,6 to 80,0 pkat/mg. In fractions with lower enzyme activities this band is not noticeable. Furthermore, a protein band at 35 kDa is present in fractions with specific activities ranging from 8,3 to 80,0 pkat/mg. In the fraction with 8,3 pkat/mg this band is less distinct than in fractions with higher enzyme activity. These observations show the correlation between enzymatic activity and protein band intensity and presence, respectively.

Throughout all fractions the protein band at 55 kDa is observable. This band is even visible in the multiple step purification approaches shown (combination of IEC and SEC and of a weak and a strong anion exchange column). All shown chromatography fractions had a terpinolene synthase activity. No such activity was found in the pellet, reflected by a very weak protein band at 55 kDa in this protein lane. This leads to the suggestion of the protein band at 55 kDa to be the one involved in the enzyme activity of the terpinolene synthase.

The size of this denatured protein is below the size determined via SEC (72 kDa resp. 144 ± 11 kDa). During SEC the protein was still in its native form yielding a higher molecular size.

In a previous project a protein band at 55 kDa after IEC was examined by matrix-assisted laser desorption/ionization-time of flight (MALDI-ToF) (Scilipoti, S. (2016), personal communication). Methylmalonate semialdehyde dehydrogenase (acylating) with a molecular size of 54 kDa was detected. The gene for this enzyme with the protein-ID CDM23572 is not inside the genomic island (CDM25240 – CDM25302) coding for many enzymes involved in the monoterpene metabolism in *C. defragrans* as described before [Petasch *et al.*, 2014]. Instead it belongs to the CoA-dependent aldehyde dehydrogenase subfamily and catalyzes the NAD-dependent oxidation of methylmalonate semialdehyde to propionyl-CoA [Talfournier, Stines-Chaumeil, and Branlant, 2011]. An additional determination of the protein bands by MALDI-ToF could not be performed in the timeframe of this thesis. In further experiments protein bands could be investigated by MALDI-ToF to confirm the result of the previous project and gain knowledge about the genes responsible for enzyme activity.

4.6 Characterization of the novel monoterpene synthase

The characteristics of the unknown enzyme of interest were further clarified during this study. With an optimal pH range between pH 6 and pH 9 this enzyme is comparable to other known monoterpene synthases with pH optima in the same range [Brodkorb *et al.*, 2010; Fischbach *et al.*, 2000; Lewinsohn, Gijzen, and Croteau, 1992; Savage, Hatch, and Croteau, 1994]. The discovered optimal temperature of 37 °C matches previously found optimal temperatures ranging from 25 to 45 °C [Brodkorb *et al.*, 2010; Fischbach *et al.*, 2000; Lewinsohn, Gijzen, and Croteau, 1992; Ruan *et al.*, 2016]. Molecular sizes of 50 kDa and 59 kDa [Fischbach *et al.*, 2000], 63 kDa [Lewinsohn, Gijzen, and Croteau, 1992], 64 kDa [Shelton *et al.*, 2004], and 67 kDa [Savage, Hatch, and Croteau, 1994] were determined in former studies, indicating a molecular size ranging from 50 to 70 kDa for monoterpene synthases. A molecular size of 160 kDa in its native form and 40 kDa in the denatured form was found for the LDI [Brodkorb *et al.*, 2010]. During this study, a molecular size of 72 kDa for the terpinolene synthase in soluble extract and 144 ± 11 kDa for the partially purified synthase were identified, with a potential size of 55 kDa of the

denatured protein. If the denatured protein size is considered, the molecular size fits the aforementioned molecular size range for monoterpene synthases.

4.7 Improved data analysis for further experiments

A different calculation method for the integrated peak, unlike the one described, could be used. In this thesis, values between all active fractions where calculated. This led in some cases to very broad integrated peaks. If only fractions with at least 50 % of the maximal detected activity are used for the calculation, a narrower integrated peak would be formed. Table 11 is used as an example: The integrated peak of this IEC consisted of 49 fractions (F162 – F210). If only fractions with at least 50 % of the maximal activity are considered, the integrated peak would consist of only 8 fractions (F180 – F187) with 3,28 mg protein instead of 36,1 mg. The specific terpinolene synthase activity would reach a value of 52,8 pkat/mg instead of 9,61 pkat/mg which is also reflected by a difference in relative specific activity (415 x instead of 75,5 x). Thereby, a specific terpinolene synthase activity closer to the detected maximal specific activity of 60,9 pkat/mg would be calculated.

Conclusion

Gaining pharmaceutical active substances from natural sources has become of deep interest over the last years. Essential oils are known to have antibiotic effects and are widely used. The components in essential oils responsible for their beneficial effects are hydrocarbons, named monoterpenes. To understand the degradation of linalool, a monoterpene frequently used by the cosmetic industry, would allow a better understanding of the whole monoterpene metabolism and profiting from it. Enzymes responsible for certain parts of this metabolism could be multiplied to enhance the product yield during monoterpene synthesis.

In this study, the purification of a novel enzyme in *Castellaniella defragrans* 65Phen was improved by a combination of liquid chromatographic techniques. The enzyme of interest, responsible for the formation of α-terpinene and terpinolene from (R,S)-linalool, was further characterized, leading to the suggestion of more than one enzyme involved in the transformation. Few protein bands on the SDS-PAGE were observed, allowing a first assumption regarding the protein band responsible for enzyme activity.

Further identification of the enzyme is required. An analysis of the single protein bands by MALDI-ToF could be used to identify the enzyme of interest and enhance the knowledge about it and its function in the cell. This knowledge could be used to optimize the purification procedure even more. Analysis of enzyme kinetics could be performed in further studies.

Appendix

Appendix A

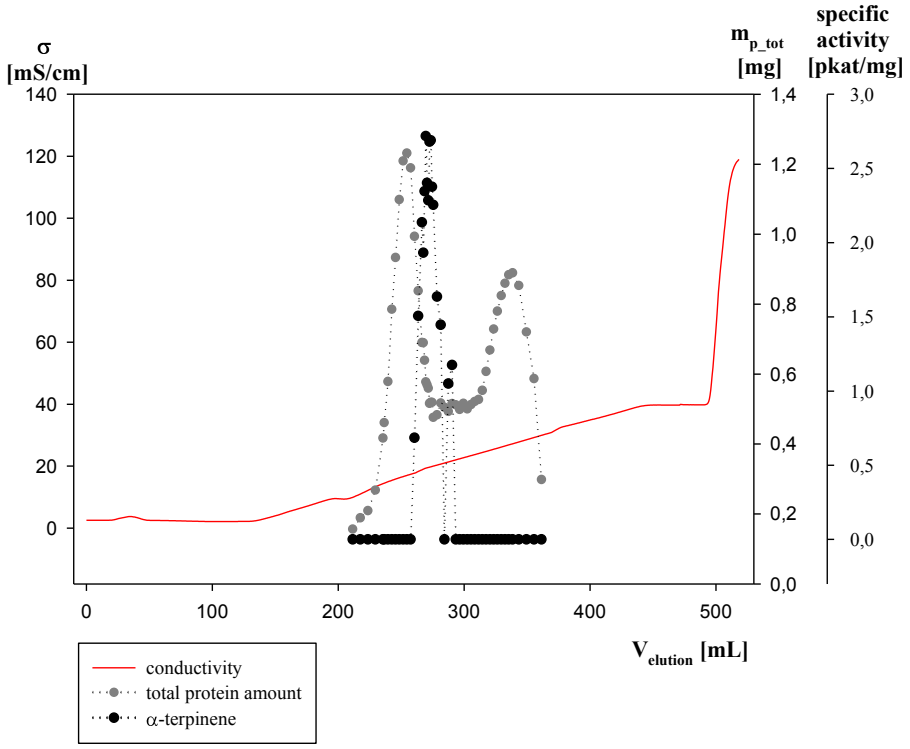

Figure 52: Protein separation and α-terpinene synthase activity on DEAE-Sepharose using a linear gradient from 0 to 300 mL KCl over 15 CV (300 mL). The IEC was performed with 205 mg protein in 25 mM Tris-HCl, pH 7,5 (binding buffer) at a flow rate of 1 mL/min. Flow rate during gradient elution: 0,3 mL/min. Due to a detector failure the absorbance at 280 nm is not shown. Red line: Inline measured conductivity. The protein amount was determined offline in triplicates. Enzyme activity was determined offline in a single test and reached a maximum of 2,72 pkat/mg.

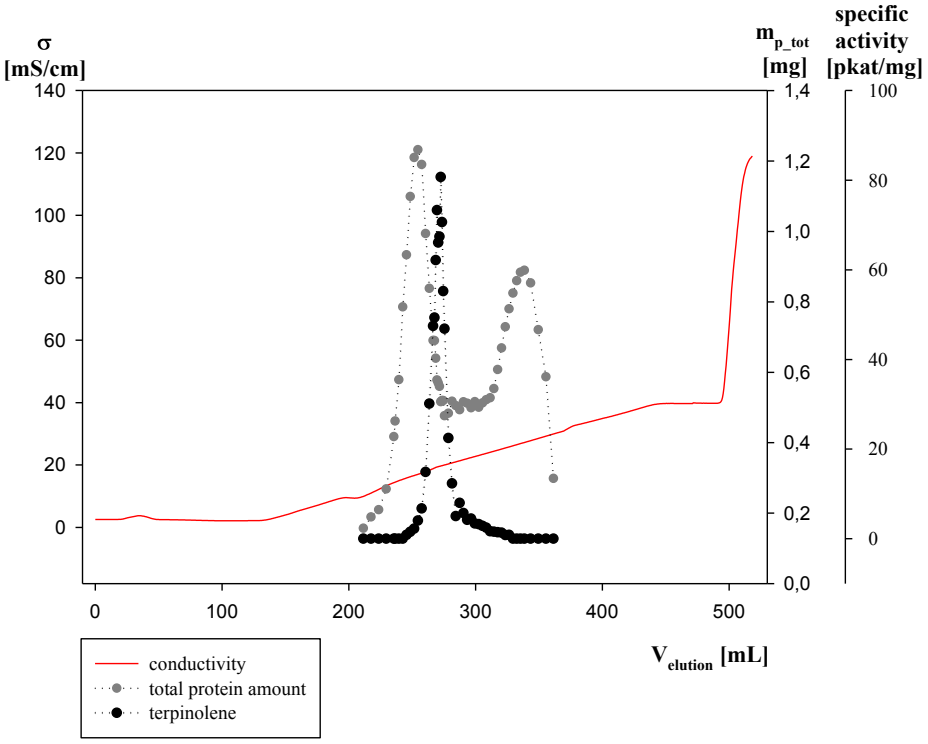

Figure 53: Protein separation and terpinolene synthase activity on DEAE-Sepharose using a linear gradient from 0 to 300 mL KCl over 15 CV (300 mL). The IEC was performed with 205 mg protein in 25 mM Tris-HCl, pH 7,5 (binding buffer) at a flow rate of 1 mL/min. Flow rate during gradient elution: 0,3 mL/min. Due to a detector failure the absorbance at 280 nm is not shown. Red line: Inline measured conductivity. The protein amount was determined offline in triplicates. Enzyme activity was determined offline in a single test and reached a maximum of 80,7 pkat/mg.

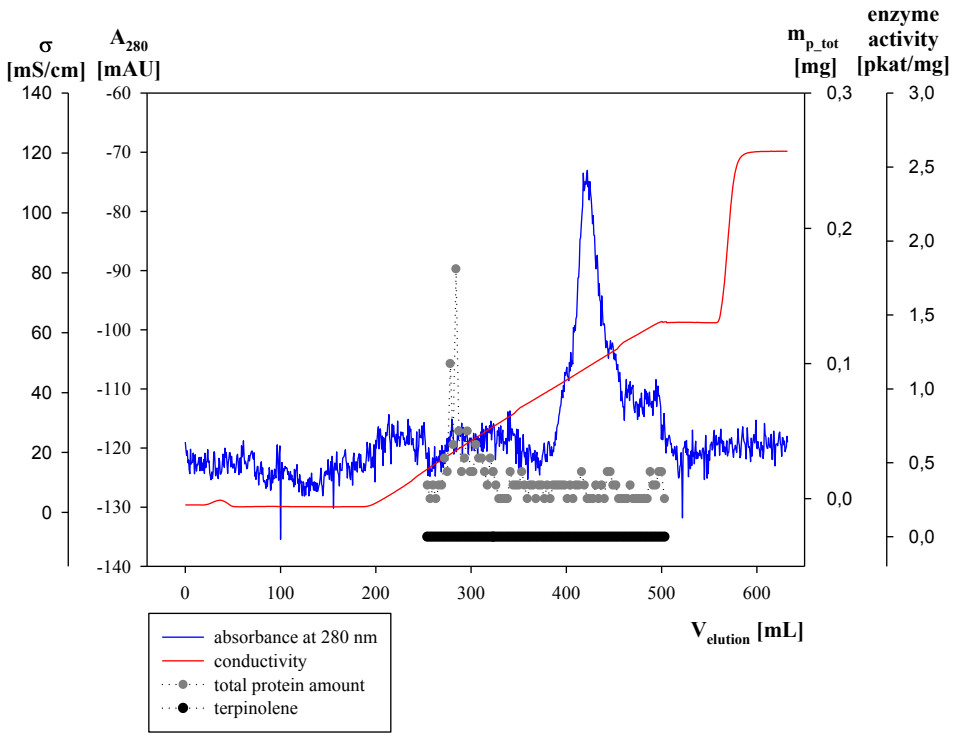

Figure 54: Protein separation and terpinolene synthase activity on DEAE-Sepharose using a linear gradient from 0 to 500 mL KCl over 15 CV (300 mL). The IEC was performed with 0,94 mg protein in 25 mM Tris-HCl, pH 8,0 (binding buffer) at a flow rate of 1 mL/min. Flow rate during gradient elution: 0,3 mL/min. Due to a failure of the UV detector the obtained absorbance signal (blue) is noisy. Red line: Inline measured conductivity. The protein amount was determined offline in triplicates. Enzyme activity was determined offline in a single test.

Appendix B

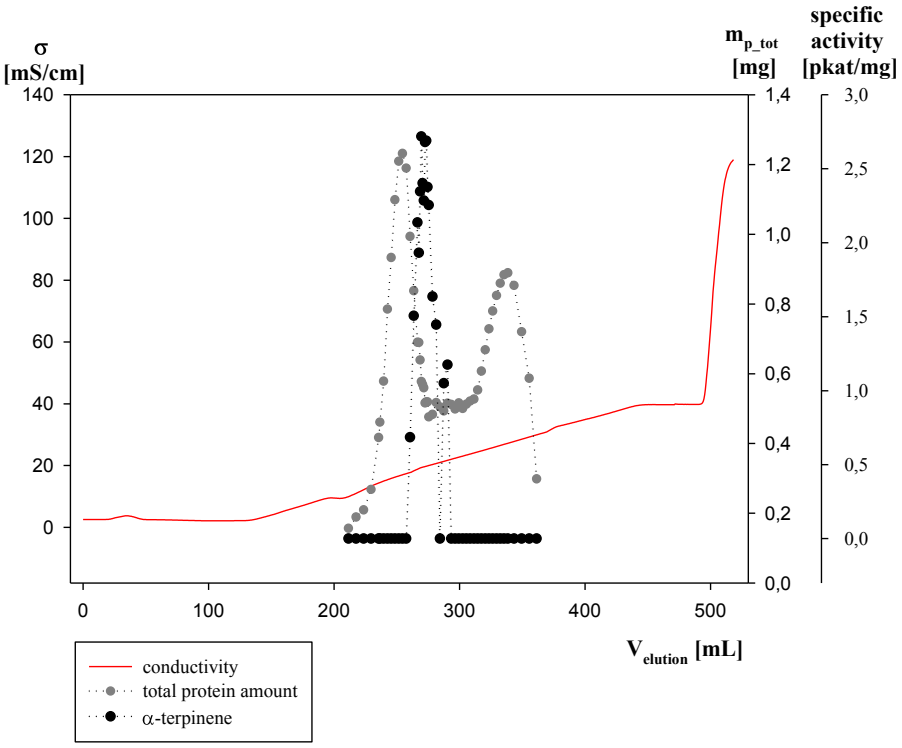

Figure 55: Protein separation and α-terpinene synthase activity on DEAE-Sepharose using a linear gradient from 0 to 300 mL KCl over 15 CV (300 mL). The IEC was performed with 205 mg protein in 25 mM Tris-HCl, pH 7,5 (binding buffer) at a flow rate of 1 mL/min. Flow rate during gradient elution: 0,3 mL/min. Due to a detector failure the absorbance at 280 nm is not shown. Red line: Inline measured conductivity. The protein amount was determined offline in triplicates. Enzyme activity was determined offline in a single test and reached a maximum of 2,72 pkat/mg.

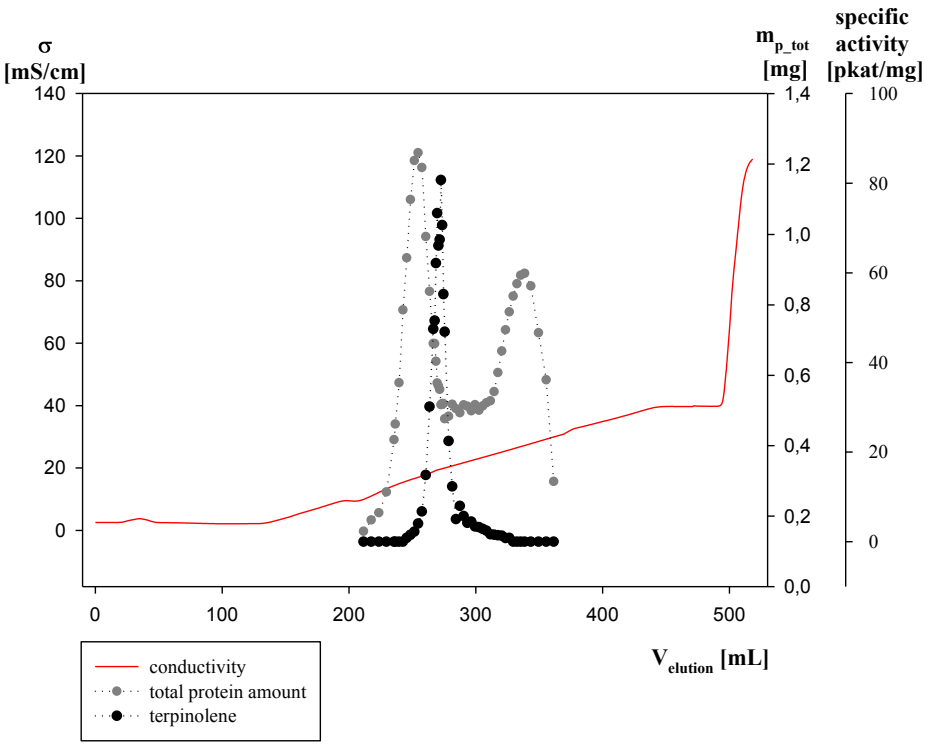

Figure 56: Protein separation and terpinolene synthase activity on DEAE-Sepharose using a linear gradient from 0 to 300 mL KCl over 15 CV (300 mL). The IEC was performed with 205 mg protein in 25 mM Tris-HCl, pH 7,5 (binding buffer) at a flow rate of 1 mL/min. Flow rate during gradient elution: 0,3 mL/min. Due to a detector failure the absorbance at 280 nm is not shown. Red line: Inline measured conductivity. The protein amount was determined offline in triplicates. Enzyme activity was determined offline in a single test and reached a maximum of 80,7 pkat/mg.

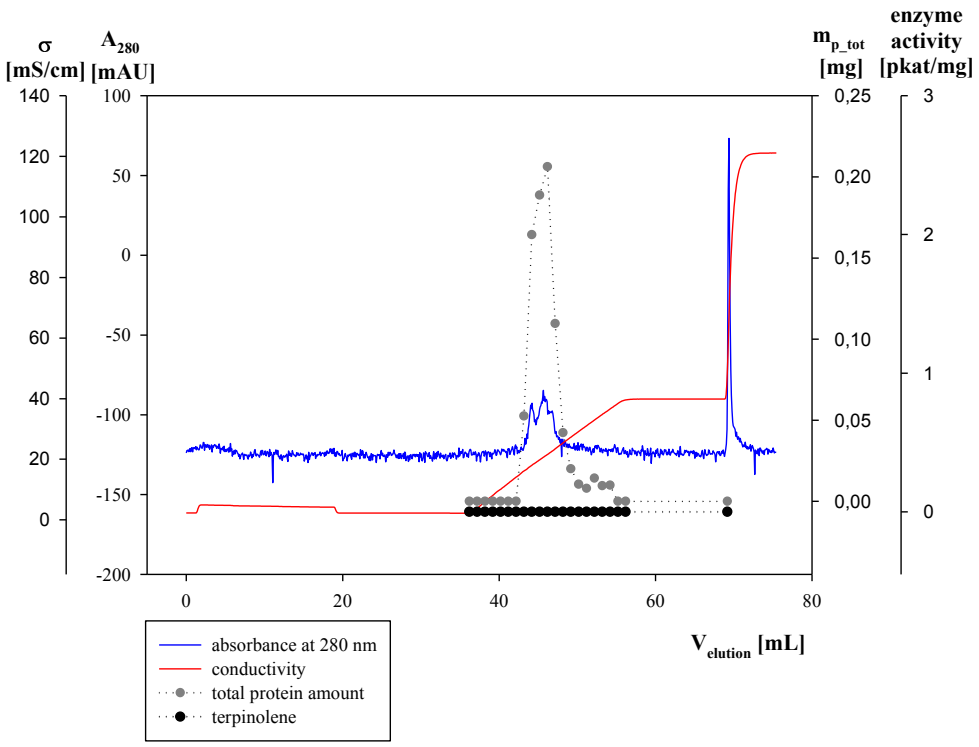

Figure 57: Protein separation and α-terpinene synthase activity on Resource-Q using a linear gradient from 0 to 300 mL KCl over 20 CV (20 mL). The IEC was performed with 1 mg protein in 25 mM Tris-HCl, pH 7,5 (binding buffer) at a flow rate of 0,5 mL/min. Flow rate during gradient elution: 1 mL/min. Due to a failure of the UV detector the obtained absorbance signal (blue) is noisy. Red line: Inline measured conductivity. The protein amount was determined offline in triplicates. Enzyme activity was determined offline in a single test.

Table 26: Purification of α-terpinene synthase activity by a multiple step purification with IEC using a weak and a strong anion exchanger from soluble extract obtained from biomass of *C. defragrans*.

c_{KCl_calc} [mM]	Purification level	Volume [mL]	Total protein [mg]	Total activity [pkat]	Specific activity [pkat/mg]	Relative specific activity	Protein yield [%]
-	Soluble Extract 9	9	205	34,8	0,17	1,0	100,0
	IEC weak						
	Pool						
135 - 139	(Fraction 269 - 273)	1,9	1,00	0,00	0,00	0,0	0,5
	IEC strong						
123	Fraction 45	1	0,16	0,00	0,00	0,0	0,1
137	Fraction 46	1	0,19	0,00	0,00	0,0	0,1
152	Fraction 47	1	0,21	0,00	0,00	0,0	0,1

Table 27: Purification of terpinolene synthase activity by a multiple step purification with IEC using a weak and a strong anion exchanger from soluble extract obtained from biomass of *C. defragrans*.

c_{KCl_calc} [mM]	Purification level	Volume [mL]	Total protein [mg]	Total activity [pkat]	Specific activity [pkat/mg]	Relative specific activity	Protein yield [%]
-	Soluble Extract 9	9	205	18,1	0,09	1,0	100,0
	IEC weak						
	Pool						
135 - 139	(Fraction 269 - 273)	1,9	1,00	17,6	17,6	200	0,5
	IEC strong						
123	Fraction 45	1	0,16	0,00	0,00	0,0	0,1
137	Fraction 46	1	0,19	0,00	0,00	0,0	0,1
152	Fraction 47	1	0,21	0,00	0,00	0,0	0,1

Bibliography

Alcalde-Rico, M., Hernando-Amado, S., Blanco, P., and Martìnez, J. L. (2016). Multidrug efflux pumps at the crossroad between antibiotic resistance and bacterial virulence. *Front Microbiol, 7*, 1483.

Alonso, W. R., Rajaonarivony, J. I. M., Gershenzon, J., and Croteau, R. (1992). Purification of 4S-limonene synthase, a monoterpene cyclase from glandular trichomes of peppermint (*Mentha x piperita*) and spearmint (*Mentha spicata*). *J Biol Chem, 267*, 7582-7587.

Andrews, R. E., Parks, L. W., and Spence, K. D. (1980). Some effects of Douglas fir terpenes on certain microorganisms. *Appl Environ Microbiol, 40*, 301-304.

Arakawa, T., Tsumoto, K., Nagase, K., and Ejima, D. (2007). The effects of arginine on protein binding and elution in hydrophobic interaction and ion-exchanger chromatography. *Protein Expr Purif, 54*, 110-116.

Bicas, J. L., Fontanille, P., Pastore, G. M., and Larroche, C. (2008). Characterization of monoterpene biotransformation in two pseudomonads. *J Appl Microbiol, 105*, 1991-2001.

Bohlmann, J., and Gershenzon, J. (2009). Old substrates for new enzymes of terpenoid biosynthesis. *Proc Natl Acad Sci U S A, 106*, 10402-10403.

Bohlmann, J., Meyer-Gauen, G., and Croteau, R. (1998). Plant terpenoid synthases: Molecular biology and phylogenetic analysis. *Proc Natl Acad Sci U S A, 95*, 4126-4133.

Boronat, A., and Rodríquez-Concepción, M. (2015). Terpenoid biosynthesis in prokaryotes. *Adv Biochem Eng Biotechnol, 148*, 3-18.

Brodkorb, D., Gottschall, M., Marmulla, R., Lüddeke, F., and Harder, J. (2010). Linalool dehydratase-isomerase, a bifunctional enzyme in the anaerobic degradation of monoterpenes. *J Biol Chem, 285*, 30436-30442.

Chen, J., and Cramer, S. M. (2007). Protein adsorption isotherm behavior in hydrophobic interaction chromatography. *J Chromatogr A, 1165*, 67-77.

Cheng, A. X., Lou, Y. G., Mao, Y. B., Lu, S., Wang, L. J., and Chen, X. Y. (2007). Plant terpenoids: Biosynthesis and ecological functions. *J Integr Plant Biol, 49*, 179-186.

Christianson, D. W. (2008). Unearthing the roots of the terpenome. *Curr Opin Chem Biol, 12*, 141-150.

Cromwell, M. E. M., Hilaro, E., and Jacobson, F. (2006). Protein aggregation and bioprocessing. *AAPS J, 8*, 572-579.

Croteau, R. (1986). Biosynthesis of cyclic monoterpenes. *ACS Symp Ser, 317*, 134-156.

Croteau, R. (1987). Biosynthesis and catabolism of monoterpenoids. *Chem Rev, 87*, 929-954.

Davis, E. M., and Croteau, R. (2000). Cyclization enzymes in the biosynthesis of monoterpenes, sesquiterpenes, and diterpenes. In F. J. Leeper & J. C. Vederas (Eds.), *Biosynthesis* (pp. 53-95). Berlin Heidelberg: Springer

Davis, E. M., Tsuji, J., Davis, G. D., Pierce, M. L., and Essenberg, M. (1996). Purification of (+)-delta-cadinene synthase, a sesquiterpene cyclase from bacteria-inoculated cotton foliar tissue. *Phytochemistry, 41*, 1047-1055.

de Souza, N. (2007). Mining for natural products. *Nat Methods, 4*, 470-471.

Diaz Carrasco, J. M., Redondo, L. M., Redondo, E. A., Dominguez, J. E., Chacana, A. P., and Fernandez Miyakawa, M. E. (2016). Use of plant extracts as an effective manner to control *Clostridium perfringens* induced necrotic enteritis in poultry. *Biomed Res Int, 2016*, 3278359.

Ebel, R. (2010). Terpenes from marine-derived fungi. *Mar Drugs, 8*, 2340-2368.

Effmert, U., Kalderás, J., Warnke, R., and Piechulla, B. (2012). Volatile mediated interactions between bacteria and fungi in the soil. *J Chem Ecol, 38*, 665-703.

Fischbach, R. J., Zimmer, I., Steinbrecher, R., Pfichner, A., and Schnitzler, J. P. (2000). Monoterpene synthase activities in leaves of *Picea abies* (L.) Karst. and *Quercus ilex* L. *Phytochemistry, 54*, 257-265.

Förster-Fromme, K., and Jendrossek, D. (2006). Identification and characterization of the acyclic terpene utilization gene cluster of *Pseudomonas citronellolis*. *FEMS Microbiol Lett, 264*, 220-225.

Foss, S., and Harder, J. (1998). *Thauera linaloolentis* sp. nov. and *Thauera terpenica* sp. nov., isolated on oxygen-containing monoterpenes (linalool, menthol, and eucalyptol) and nitrate. *Syst Appl Microbiol, 21*, 365-373.

Foss, S., Heyen, U., and Harder, J. (1998). *Alcaligenes defragrans* sp. nov., description of four strains isolated on alkenoic monoterpenes ((+)-menthene, α-pinene, 2-carene, and α-phellandrene) and nitrate. *Syst Appl Microbiol, 21*, 237-244.

Fu, J., Yang, Y. R., Dhakal, S., Zhao, Z., Liu, M., Zhang, T., Walter, N. G., and Yan, H. (2016). Assembly of multienzyme complexes on DNA nanostructures. *Nat Protoc, 11*, 2243-2273.

Gao, Y., Honzatko, R. B., and Peters, R. J. (2012). Terpenoid synthase structures: a so far incomplete view of complex catalysis. *Nat Prod Rep, 29*, 1153-1175.

Gershenzon, J., and Dudareva, N. (2007). The function of terpene natural products in the natural world. *Nat Chem Biol, 3*, 408-414.

Gillespie, R., Nguyen, T., Macneil, S., Jones, L., Crampton, S., and Vunnum, S. (2012). Cation exchanger surface-mediated denaturation of an aglycosylated immunoglobulin (IgG1). *J Chromatogr A, 1251*, 101-110.

Hansen, S. C., Stolter, C., Imholt, C., and Jacob, J. (2016). Plant secondary metabolites as rodent repellents: A systematic review. *J Chem Ecol, 42*, 970-983.

Harder, J., and Probian, C. (1995). Microbial degradation of monoterpenes in the absence of molecular oxygen. *Appl Environ Microbiol, 61*, 3804-3808.

Heddergott, C., Calvo, A. M., and Latgé, J. P. (2014). The volatome of *Aspergillus fumigatus*. *Eukaryot Cell, 13*, 1014-1025.

Heyen, U., and Harder, J. (2000). Geranic acid formation, an initial reaction of anaerobic monoterpene metabolism in denitrifying *Alcaligenes defragrans*. *Appl Environ Microbiol, 66*, 3004-3009.

Hohn, T. M., and Vanmiddlesworth, F. (1986). Purification and characterization of the sesquiterpene cyclase trichodiene synthetase from *Fusarium sporotrichioides*. *Arch Biochem Biophys, 251*, 756-761.

Höschle, B., Gnau, V., and Jendrossek, D. (2005). Methylcrotonyl-CoA and geranyl-CoA carboxylases are involved in leucine/isovalerate utilization (Liu) and acyclic terpene utilization (Atu), and are encoded by liuB/liuD and atuC/atuF, in *Pseudomonas aeruginosa*. *Microbiology, 151*, 3649-3656.

Hottman, D. A., and Li, L. (2014). Protein prenylation and synaptic plasticity: Implications for Alzheimer's disease. *Mol Neurobiol, 50*, 177-185.

Israeli-Ruimy, V., Bule, P., Jindou, S., Dassa, B., Moraïs, S., Borovok, I., Barak, Y., Slutzki, M., Hamberg, Y., Cardoso, V., Alves, V. D., Najmudin, S., White, B. A., Flint, H. J., Gilbert, H. J., Lamed, R., Fontes, C. M. G. A., and Bayer, E. A. (2017). Complexity of the *Ruminococcus flavefaciens* FD-1 cellulosome reflects an expansion of family-related protein-protein interactions. *Sci Rep, 7*, 42355.

Kämpfer, P., Denger, K., Cook, A. M., Lee, S. T., Jäckel, U., Denner, E. B., and Busse, H. J. (2006). *Castellaniella* gen. nov., to accommodate the phylogenetic lineage of *Alcaligenes defragrans*, and proposal of *Castellaniella defragrans* gen. nov., comb. nov. and *Castellaniella denitrificans* sp. nov. *Int J Syst Evol Microbiol, 56*, 815-819.

Kesselmeier, J., and Staudt, M. (1999). Biogenic volatile organic compounds (VOC): An overview on emission, physiology and ecology. *J Atmos Chem, 33*, 23-88.

Kirby, J., and Keasling, J. D. (2009). Biosynthesis of plant isoprenoids: Perspectives for microbial engineering. *Annu Rev Plant Biol, 60*, 335-355.

Koehn, F. E., and Carter, G. T. (2005). The evolving role of natural products in drug discovery. *Nat Rev Drug Discov, 4*, 206-220.

Kurien, B. T., and Scofield, R. H. (2012). Common artifacts and mistakes made in electrophoresis. In B. T. Kurien & R. H. Scofield (Eds.), *Protein electrophoresis - methods and protocols* (pp. 633-640). New York: Springer Science + Business Media.

Leclercq, S., Derouaux, A., Olatunji, S., Fraipont, C., Egan, A. J. F., Vollmer, W., Breukink, E., and Terrak, M. (2017). Interplay between penicillin-binding proteins and SEDS proteins promotes bacterial cell wall synthesis. *Sci Rep, 7*, 43306.

Lesburg, C. A., Zhai, G., Cane, D. E., and Christianson, D. W. (1997). Crystal structure of pentalene synthase: Mechanistic insights on terpenoid cyclizytion reactions in biology. *Science, 277*, 1820-1824.

Lewinsohn, E., Gijzen, M., and Croteau, R. (1992). Wound-inducible pinene cyclase from grand fir: Purification, characterization, and renaturation after SDS-PAGE. *Arch Biochem Biophys, 293*, 167-173.

Li, R., Chou, E. K. W., Himmelberger, J. A., Litwin, K. M., Harris, G. G., Cane, D. E., and Christianson, D. W. (2014). Reprogramming the chemodiversity of terpenoid cyclization by remolding the active site contour of epi-isozizaene synthase. *Biochemistry, 53*, 1155-1168.

Livshts, M. A., Khomyakova, E., Evtushenko, E. G., Lazarev, V. N., Kulemin, N. A., Semina, S. E., Generozov, E. V., and Govorun, V. M. (2015). Isolation of exosomes by differential centrifugation: Theoretical analysis of a commonly used protocol. *Sci Rep, 5*, 1731910.

Lüddeke, F., Dikfidan, A., and Harder, J. (2012). Physiology of deletion mutants in the anaerobic beta-myrcene degradation pathway in *Castellaniella defragrans*. *BMC Microbiol, 12*, 192.

Lüddeke, F., Wülfing, A., Timke, M., Germer, F., Weber, J., Dikfidan, A., Rahnfeld, T., Linder, D., Meyerdierks, A., and Harder, J. (2012). Geraniol and geranial dehydrogenases induced in anaerobic monoterpene degradation by *Castellaniella defragrans*. *Appl Environ Microbiol, 78*, 2128-2136.

Marmulla, R. (2015). *The anaerobic linalool metabolism in the betaproteobacteria Castellaniella defragrans 65Phen and Thauera linaloolentis 47Lol.* (PhD Thesis), Universität Bremen, Bremen.

Marmulla, R., Šafarić, B., Markert, S., Schweder, T., and Harder, J. (2016). Linalool isomerase, a membrane-anchored enzyme in the anaerobic monoterpene degradation in *Thauera linaloolentis* 47Lol. *BMC Biochem, 17*, 6.

Melo, A. D. B., Amaral, A. F., Schaefer, G., Luciano, F. B., de Andrade, C., Costa, L. B., and Rostagno, M. H. (2015). Antimicrobial effect against different bacterial strains and bacterial adaptation to essential oils used as feed additives. *Can J Vet Res, 79*, 285-289.

Papadopoulos, C. J., Carson, C. F., Chang, B. J., and Riley, T. V. (2008). Role of the MexAB-OprM efflux pump of *Pseudomonas aeruginosa* in tolerance to tea tree (*Melaleuca alternifolia*) oil and its monoterpene components terpinen-4-ol, 1,8-cineole, and alpha-terpineol. *Appl Environ Microbiol, 74*, 1932-1935.

Peñuelas, J., Rutishauser, T., and Filella, I. (2009). Phenology feedbacks on climate change. *Science, 324*, 887-888.

Peñuelas, J., and Staudt, M. (2010). BVOCs and global change. *Trends Plant Sci, 15*, 133-144.

Petasch, J., Disch, E. M., Markert, S., Becher, D., Schweder, T., Hüttel, B., Reinhardt, R., and Harder, J. (2014). The oxygen-independent metabolism of cyclic monoterpenes in *Castellaniella defragrans* 65Phen. *BMC Microbiol, 14*, 164.

Pichersky, E., Noel, J. P., and Dudareva, N. (2006). Biosynthesis of plant volatiles: Nature's diversity and ingenuity. *Science, 311*, 808-811.

Rohmer, M., Knani, M., Simonin, P., Sutter, B., and Sahm, H. (1993). Isoprenoid biosynthesis in bacteria: A novel pathway for the early steps leading to isopentenyl diphosphate. *Biochem J, 295*, 517-524.

Ruan, J. X., Li, J. X., Fang, X., Wang, L. J., Hu, W. L., Chen, X. Y., and Yang, C. Q. (2016). Isolation and characterization of three new monoterpene synthases from *Artemisia annua*. *Front Plant Sci, 7*, 638.

Sangari, F. J., Pérez-Gil, J., Carretero-Paulet, L., García-Lobo, J. M., and Rodríquez-Concepción, M. (2010). A new family of enzymes catalyzing the first committed step of the methylerythritol 4-phosphate (MEP) pathway for isoprenoid biosynthesis in bacteria. *Proc Natl Acad Sci U S A, 107*, 14081-14086.

Savage, T. J., Hatch, M. W., and Croteau, R. (1994). Monoterpene synthases of *Pinus contorta* and related conifers. A new class of terpenoid cyclase. *J Biol Chem, 269*, 4012-4020.

Schilmiller, A. L., Schauvinhold, I., Larson, M., Xu, R., Charbonneau, A. L., Schmidt, A., Wilkerson, C., Last, R. L., and Pichersky, E. (2009). Monoterpenes in the glandular trichomes of tomato are synthesized from a neryl diphosphate precursor rather than geranyl diphosphate. *Proc Natl Acad Sci U S A, 106*, 10865-10870.

Scilipoti, S. (2016). *Characterization of a novel linalool-metabolizing enzyme in Castellaniella defragrans 65 Phen.* (MSc Thesis), University of Trieste.

Seubert, W. (1960). Degradation of isoprenoid compounds by microorganisms I. Isolation and characterization of an isoprenoid-degrading bacterium, *Pseudomonas citronellolis* n. sp. *J Bacteriol, 79*, 426-434.

Shelton, D., Zabaras, D., Chohan, S., Wyllie, S. G., Baverstock, P., Leach, D., and Henry, R. (2004). Isolation and partial characterisation of a putative monoterpene synthase from *Melaleuca alternifolia*. *Plant Phys Biochem, 42*, 875-882.

Srividya, N., Davis, E. M., Croteau, R. B., and Lange, B. M. (2015). Functional analysis of (4S)-limonene synthase mutants reveals determinant of catalytic outcome in a model monoterpene synthase. *Proc Natl Acad Sci U S A, 112*, 3332-3337.

Switzer, R. C. I., Merril, C. R., and Shifrin, S. (1979). A highly sensitive silver stain for detecting proteins and peptides in polyacrylamide gels. *Anal Biochem, 98*, 231-237.

Talfournier, F., Stines-Chaumeil, C., and Branlant, G. (2011). Methylmalonate-semialdehyde dehydrogenase from *Bacillus subtilis*: Substrate specificity and coenzyme a binding. *J Biol Chem, 286*, 21971-21981.

Theoduloz, C., Delporte, C., Valenzuela-Barra, G., Silva, X., Cádiz, S., Bustamante, F., Pertino, M. W., and Schmeda-Hirschmann, G. (2015). Topical anti-

inflammatory activity of new hybrid molecules of terpenes and synthetic drugs. *Molecules, 20*, 11219-11235.

Trombetta, D., Castelli, F., Sarpietro, M. G., Venuti, V., Cristani, M., Daniele, C., Saija, A., Mazzanti, G., and Bisignano, G. (2005). Mechanisms of antibacterial action of three monoterpenes. *Antimicrob Agents Chemother, 49*, 2474-2478.

Turina, A. V., Nolan, M. V., Zygadlo, J. A., and Perillo, M. A. (2006). Natural terpenes: Self-assembly and membrane partitioning. *Biophys Chem, 122*, 101-113.

Uma, K., Huang, X., and Kumar, B. A. (2017). Antifungal effect of plant extract and essential oil. *Chin J Integr Med, 23*, 233-239.

van der Werf, M. J., Swarts, H. J., and de Bont, J. A. M. (1999). *Rhodococcus erythropolis* DCL14 contains a novel degradation pathway for limonene. *Appl Environ Microbiol, 65*, 2092-2102.

Wang, M., and Casey, P. J. (2016). Protein prenylation: Unique fats make their mark on biology. *Nat Rev Mol Cell Biol, 17*, 110-122.

Weidenweber, S., Marmulla, R., Ermler, U., and Harder, J. (2016). X-ray structure of linalool dehydratase/isomerase from *Castellaniella defragrans* reveals enzymatic alkene synthesis. *FEBS Lett, 590*, 1375-1383.

Yin, J., Straight, P. D., Hrvatin, S., Dorrestein, P. C., Bumpus, S. B., Jao, C., Kelleher, N. L., Kolter, R., and Walsh, C. T. (2007). Genome-wide high-throughput mining of natural-product biosynthetic gene clusters by phage display. *Chem Biol, 14*, 303-312.

Yoo, S. K., and Day, D. F. (2002). Bacterial metabolism of alpha- and beta-pinene and related monoterpenes by *Pseudomonas* sp. strain PIN. *Proc Biochem, 37*, 739-745.

Zengin, H., and Baysal, A. H. (2014). Antibacterial and antioxidant activity of essential oil terpenes against pathogenic and spoilage-forming bacteria and cell structure-activity relationships evaluated by SEM microscopy. *Molecules, 19*, 17773-17798.

Acknowledgements

After 10 cell disintegrations, 16 SDS-PAGEs, 22 chromatographies, 688 enzyme activity assays and roughly 1782 Bradford protein assays, I want to thank all persons supporting me during this time.

First, I would like to express my gratitude to Prof. Dr. Jens Harder for the opportunity to write my master thesis in the department for microbiology at the Max-Planck-Institute for Marine Microbiology. I really appreciate the guidance and useful critiques during my work and during the writing of my thesis.

I would also like to thank Prof. Dr. Oliver Ullrich, for his advice and for being my first referee.

My grateful thanks are also extended to Edinson Puentes, for explaining me everything in the lab, and for always having a friendly ear for all my problems and findings throughout the work.

I thank all the technicians in the laboratory, especially Christina Probian, for the help in the laboratory and the briefing on the GC. Although the radio station sometimes was repetitive, it was really fun working in the laboratory.

Last but not least I would like to thank friends and family for always supporting and encouraging me during my study.

Eidesstattliche Erklärung

Hiermit versichere ich, dass ich die vorliegende Master Thesis mit dem Titel „Characterization of a terpene synthase activity in *Castellaniella defragrans*“ ohne fremde Hilfe selbstständig verfasst und nur die angegebenen Quellen und Hilfsmittel verwendet habe. Wörtlich oder dem Sinn nach aus anderen Werken entnommene Stellen sind unter Angabe der Quellen kenntlich gemacht.

Bremen, 31.03.2017 _____

(Elisabeth Engler-Hüsch)